AD NUMBER

AD823515

LIMITATION CHANGES

TO:

Approved for public release; distribution is unlimited.

FROM:

**Distribution authorized to U.S. Gov't. agencies and their contractors;
Administrative/Operational Use; OCT 1967. Other requests shall be referred to Air Force Aero Propulsion Lab., Wright-Patterson AFB, OH 45433.**

AUTHORITY

AFAPL ltr 12 Apr 1972

AFAPL-TR-67-141

TRANSIENT HEAT TRANSFER MEASUREMENT WITH THIN-FILM RESISTANCE THERMOMETERS -- DATA REDUCTION TECHNIQUES

Leonard Bogdan
Cornell Aeronautical Laboratory, Inc.

Technical Report AFAPL-TR-67-141

October 1967

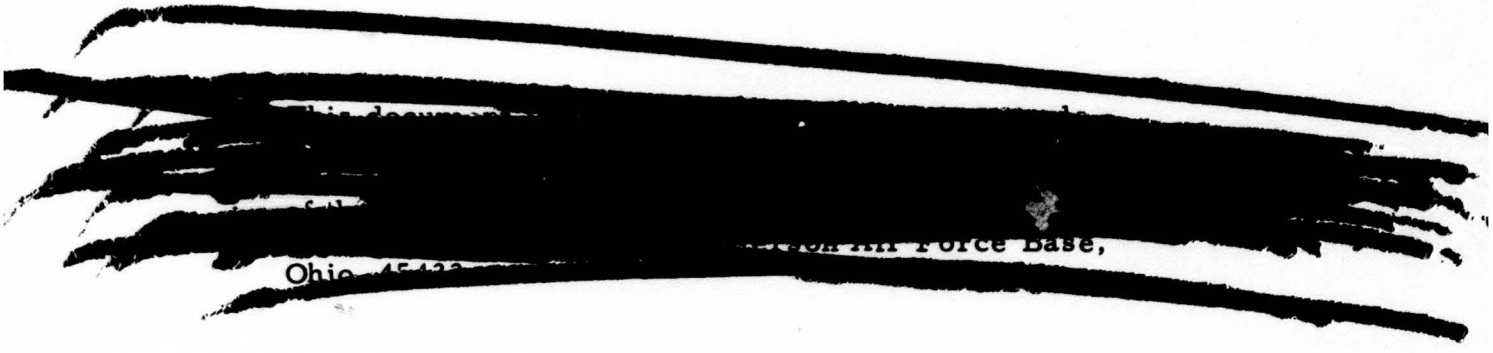

Air Force Aero Propulsion Laboratory
Research and Technology Division
Air Force Systems Command
Wright-Patterson Air Force Base, Ohio

NOTICES

[redacted] specifications, or other data are [redacted] for any purpose [redacted] with a definitely related Government procure- [redacted] have [redacted] formulated by implication or otherwise as in any [redacted] manufacture [redacted] or conveying [redacted] information [redacted] [redacted] transmittal to foreign [redacted] with approval of the Air Force Aero Propulsion [redacted] Air Force Base, Ohio 45433.

Information in this report is embargoed under the U. S. Export Control Act of 1949, administered by the Department of Commerce. This report may be released by departments of agencies of the U. S. Government to departments or agencies of foreign governments with which the United States has defense treaty commitments. Private individuals of firms must comply with Department of Commerce export control regulations.

Copies of this report should not be returned to the Research and Technology Division unless return is required by security considerations, contractual obligations, or notice on a specific document.

AF-WP-O-Feb 65 1500

TRANSIENT HEAT TRANSFER MEASUREMENT WITH THIN-FILM RESISTANCE THERMOMETERS -- DATA REDUCTION TECHNIQUES

Leonard Bogdan

FOREWORD

This report was prepared by Cornell Aeronautical Laboratory, Inc., Buffalo, New York under USAF Contract No. AF 33(615)-67-C-1144, Project No. 651-E. The work was administered under the direction of the Air Force Aero Propulsion Laboratory, Research and Technology Division, Mr. Harold F. Chambers, Jr., Contract Monitor.

This is the project final technical report that describes and summarizes studies conducted during the period from April 1967 through September 1967 on analog and digital data reduction techniques for heat transfer measurements made with thin-film resistance thermometers. A draft of this report, identified by the contractor as Report No. AE-2385-Y-2, was submitted on 1 October 1967.

This effort was performed jointly by the Hypersonic Facilities Department, the Computer Services Department, and the Avionics Department of Cornell Aeronautical Laboratory (CAL). Acknowledgement is made of the major technical contributions of the following individuals: V. V. Abrahamian, analog computer (COMCOR) studies, W. D. Fryer, analog computer studies and digital program development, D. H. Bock, P. F. Heggs, and S. A. R. Ayyar, analog circuit development.

Publication of this report does not constitute Air Force approval of the report's findings or conclusions. It is published only for the exchange and stimulation of ideas.

ABSTRACT

An account is presented of experimental studies of techniques of data reduction required to convert measurements obtained with thin-film resistance thermometers to incident heating rates. Emphasis is on development of practical data reduction techniques accommodating nonspecific gage surface temperature histories as well as temperature excursions sufficiently large to necessitate correction for variable thermal properties of the gage.

Analog computer solutions were obtained for a range of surface temperature functions representative of phenomena observed in actual shock tunnel operations. The mathematical formulation used in the analog studies was adapted to the development of an economical and general digital data reduction program. A description is given of the operation and design details of a compensated analog circuit which operates directly on the electrical output of the thin-film gage to provide an output signal proportional to the true heating rate.

TABLE OF CONTENTS

SECTION I

INTRODUCTION

The thin-film resistance thermometer, comprised of a platinum alloy element on a Pyrex substrate, has been used extensively for measurements of heat transfer in short-duration hypersonic test facilities because of its simplicity of principle and construction as well as very rapid response. Since the output signal from the gage is a measure of the substrate surface temperature rise, rather than the incident heat transfer rate, signal processing is required to obtain the desired parameter. By application of classical solid conduction theory, surface temperature-time data may be transformed into the incident heat flux provided the electrical and the thermal properties of the gage are known.

For modest heating rates that result in a substrate surface temperature increase of the order of 100°F or less during the test period, the electrical characteristic of the thermometer may be taken as a linear function of temperature and the substrate thermal properties assumed invariant. For these particular circumstances, both analog and digital techniques for data reduction have long been available[1, 2*] since a closed form mathematical solution to the problem exists. On the other hand, for substrate surface temperature excursions up to 1000°F, the upper practical limit of the thin-film gage, the electrical characteristic of the resistance thermometer is highly nonlinear and the temperature variation of the substrate thermal properties results in a nonlinear form of the heat diffusion equation for which no closed form mathematical solution exists. Data reduction techniques in this regime (high heating rates) are not as well defined.

This report discusses studies directed toward the formulation of digital and analog techniques for the conversion of thin-film resistance thermometer data to heat transfer rate with emphasis on high heating rates and nonconstant heat flux conditions. Specifically, the program consisted of three distinct efforts: (1) analog computer solutions of a variety of temperature histories which included the study of such factors as noise, tunnel starting phenomena, and gage abrasion; (2) development of a practical digital computer program for data reduction for nonspecific temperature histories (and amplitudes); and, finally, (3) formulation of a small, compact electronic analog circuit suitable for general data conversion applications.

The technology related to the fabrication and application of the thin-film heat transfer gage has been presented in an earlier interim project report[3]. Consequently only a brief mention is made in the next section of the underlying principles of the gage. These comments are then followed by a short discussion of the electrical and thermal characteristics of the gage together with numerical data. The three parts of the program are then presented and the report is concluded with a summary.

---

*Superscripts denote references.

SECTION II

SURFACE THERMOMETRY AND DATA REDUCTION

The thin-film heat transfer gage is a device that provides a measurement of the surface temperature of a substrate which is characterized as semi-infinite, homogeneous, and isotropic. By application of classical solid conduction theory[1,4], surface temperature-time data may be transformed into the incident heat transfer rate when the substrate thermal properties are known. To achieve a very rapid response of the sensor, and to simplify the data reduction procedures, the thickness of the thin-film resistance thermometer is made sufficiently small that its presence on the substrate has a negligible effect on the substrate surface temperature. The characteristic diffusion time for a metallic film about four microinches thick is approximately a microsecond; hence for practical purposes, the film senses the instantaneous substrate surface temperature.

An insulator material, in both a thermal and electrical sense, is used as the substrate, functioning mechanically as a support for the resistance film and thermally as a heat sink. Sensitivity in the measurement of very low heat transfer rates is enhanced by the use of a substrate with poor thermal conductivity. For practical shock tunnel applications, #7740 Pyrex is used widely as a gage substrate so that even in small thicknesses (say 0.04 to 0.06 inch) it represents a semi-infinite heat sink because of the small depth of heat penetration.

The transient one-dimensional heat conduction problem for a semi-infinite slab of material with heat flux normal to the surface is illustrated by the following sketch.

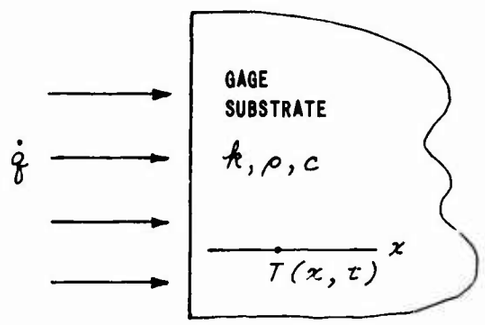

$\dot{q}$ = heat transfer rate
k = thermal conductivity
ρ = density
c = specific heat
T = temperature
t = time

For conditions of constant substrate properties, the thermal diffusion equation is

$$\frac{\partial T(x,t)}{\partial t} = \frac{k}{\rho c} \frac{\partial^2 T(x,t)}{\partial x^2} \tag{1}$$

with boundary conditions

$$T(x,0) = 0 \quad x \geq 0$$

$$\dot{q}(0,t) = -\frac{k\partial t}{\partial x} \quad , t > 0$$

$$T(x,t) = 0 \, , \; x \to \infty \, , \; t \geq 0$$

One form of solution to Eq. (1), the derivation of which is given in detail in the literature on thin-film gages[1], is given below

$$\dot{q}(0,t) = \frac{1}{2}\left(\frac{\pi\rho ck}{t}\right)^{\frac{1}{2}} \left[T(t) + \frac{1}{\pi}\int \frac{\lambda^{\frac{1}{2}} T(t) - t^{\frac{1}{2}} T(\lambda)}{(t-\lambda)^{3/2}} \, d\lambda \right] \tag{2}$$

where T(t) is the substrate surface temperature and λ is a dummy variable of integration. This form of the equation is readily adaptable for evaluation by a digital computer. For the special situation when the incident heat transfer rate is constant, Eq. (2) reduces to the following form.

$$\dot{q}(0,t) = \frac{(\pi\rho ck)^{\frac{1}{2}} T(t)}{2t^{\frac{1}{2}}} \tag{3}$$

The increase in surface temperature occurs in proportion to the square root of time and the recorded gage output signals consequently are of parabolic form.

A parabolic surface-temperature function has been assumed in formulating Eq. (2). As the temperature function deviates from this form, results obtained from Eq. (2) become increasingly less accurate[4]. A perfectly general expression, which does not involve initial assumptions about the form of the temperature function, is given in Ref. 4.

$$\dot{q}_n(t) = \frac{2(\rho ck)^{\frac{1}{2}}}{\pi^{\frac{1}{2}}} \left[\left\{ \sum_{i=1}^{n-1} \frac{T(t_i) - T(t_{i-1})}{(t_n - t_i)^{\frac{1}{2}} + (t_n - t_{i-1})^{\frac{1}{2}}} \right\} + \frac{T_n - T_{n-1}}{(t_n - t_{n-1})^{\frac{1}{2}}} \right] \tag{4}$$

In deriving Eq. (4) however, the temperature function is approximated by a piecewise linear function so that the accuracy of the result obtained is only limited by the degree to which the actual function is approximated by this means. Accuracy is improved therefore by choosing n sufficiently large to insure a satisfactory approximation to the true temperature function. Equation (4) is also easily programmed for digital computer calculations.

On the other hand, analog techniques have been developed for data reduction by taking advantage of the fact that differential equations which describe the one-dimensional heat flux into a semi-infinite solid are identical with those that apply to the current flow in a distributed resistance-capacitance line. A variety of simple, passive analog circuits, which operate in real time, have been developed for converting thin-film heat transfer gage signals directly into signals proportional to heat flux. One particular type, described in Ref. 2, has been used extensively at CAL. Except for the need to match the frequency range of the analog circuit to the Fourier frequency components

of the temperature function, there are no assumptions or restrictions concerning the nature of the temperature function.

For test conditions at which the substrate thermal properties cannot be taken as constant, Eq. (1) must be recast in the following form

$$\rho c(T) \frac{\partial T}{\partial t} = \frac{\partial}{\partial x} \left[k(T) \frac{\partial T}{\partial x} \right] \tag{5}$$

which has no closed form analytical solution. Numerical techniques may be used to evaluate Eq. (5) in terms of the incident heat flux $\dot{q}(t)$ which produces the measured surface temperature T(t). The specific method which was used on this project to obtain both the analog computer and the digital computer solutions to Eq. (5) is described in detail in sections IV and V of this report.

Hartunian and Varwig[5] have solved Eq. (5) by making use of a transformed variable, $\phi = \int_0^T k \, dT$ and linearized forms for the transformed variable and the thermal diffusivity. In essence, a transformed surface temperature is obtained which when used with the linear digital and analog data reduction techniques described above will yield the true incident heat flux. A detailed account of this procedure, which was used in computing design information for the electronic analog circuit, is included in Appendix C of this report.

Finally, note should be made of the work of Schmitz[6] in the development of a nonlinear analog network to directly compensate for the changes in substrate properties. The circuit proved to be too complex for practical use and was further restricted by an ability to compensate for changes in but one of the substrate parameters (specific heat).

The purpose of the preceding discussion has been to describe, in general terms, the various methods used in the computation of heat flux from thin-film heat transfer gage measurements of surface temperatures. It is apparent that preceding this investigation relatively little emphasis has been placed on solutions to the nonlinear heat diffusion equation (Eq. 5). This consideration led to the present study of economical methods of analog and digital data reduction for the nonlinear heat conduction situation.

SECTION III

ELECTRICAL AND THERMAL CHARACTERISTICS OF THE THIN-FILM RESISTANCE THERMOMETER

Two distinct operations must be performed on the output signal of the thin-film resistance thermometer; first, a correction must be made for the nonlinear resistance-temperature function of the resistance element (to convert the measured surface temperature to a true surface temperature) and second, the variation of the gage thermal parameters with temperature must be accommodated in the data analysis.

Measurements of the electrical and thermal characteristics of the thin-film resistance thermometer in the range from room temperature of 1000°F have been made at CAL[7]. These tests were performed on gages which used Hanovia Bright Platinum 05-X solution for the resistance thermometer and #7740 Pyrex as the substrate.

The resistance-temperature characteristic of the film is the quadratic function

$$\frac{\Delta R}{K_{70}} = (T-70) - 1.295 \times 10^{-4}(T-70)^2 = T_m \qquad (6)$$

ΔR = change in gage resistance
K_{70} = slope of the resistance function (dR/dT) at 70°F
T = actual temperature
T_m = measured gage temperature change*

Table I provides a quantitative tabulation of the magnitude of the correction required to the temperature change as measured by the gage. Corrections are of the order of +15% at 1000°F.

The temperature variation of the substrate thermal properties was determined by an electrical pulsing technique[8] that provided a constant flux into the resistance thermometer. Using Eq. (3), the value of (ρ ck) as a function of temperature was obtained. However, as shown in Eq. (5), the parameters required are ρ c(T) and k(T) rather than (ρ ck) (T). Handbook data for ρ c(T) for #7740 Pyrex were used and k(T) was computed from the experimental data**. Table II lists the values for ρ c and k that were exclusively employed in all of the studies included in this report.

---

* Measured gage temperature change is that obtained by assuming a linear resistance change with temperature and using K_{70} as the slope of the function.

** Whereas published data for ρ c(T) are in excellent agreement, wide disagreement exists on measurements of k(T) (see Ref. 9, for example).

SECTION IV

ANALOG COMPUTER STUDIES

1. OBJECTIVES

Analog computers are uniquely appropriate to the solution of partial differential equations and offer advantages of economy and flexibility especially when the effects of variations in parameters are to be explored. Accordingly, a limited analog computer study was conducted at CAL several years ago using the computing equipment available at that time*. The purpose of that study was to ascertain the magnitudes of the corrections required to measure heating rates as the result of substrate property changes with temperature. Accuracy limitations of the analog equipment precluded any extensive investigations.

With improved analog computer hardware now available at CAL, it was believed the project objectives aimed at developing performance criteria for computer programs and analog network designs for conditions of nonconstant heating rates could be furthered by solving the nonlinear, one-dimensional heat diffusion equation on these facilities. A variety of temperature histories would be used as inputs to which would be added such modifying factors as tunnel starting phenomena, random noise, and sinusoidal modulation. In all cases the interest was in the influence of those disturbances on the heat flux history. Input variables were limited to a real life test time of 0.010 second and a maximum temperature change of 1000°F.

2. GENERAL MATHEMATICAL FORMULATION

The nonlinear diffusion equation for one-dimensional heat conduction in a homogeneous and isotropic slab of material of thickness ℓ is given below.

$$\frac{\partial T}{\partial t} = \frac{1}{\rho c(T)} \frac{\partial}{\partial x}\left(k(T)\frac{\partial T}{\partial x}\right) \tag{7}$$

T	=	temperature
t	=	time
x	=	depth into slab (measured normal to surface)
ρ	=	density of slab
c	=	specific heat of slab
k	=	thermal conductivity of slab

Assumed boundary conditions are as follows:

$T = T(x, t)$
$T(0, t) \equiv T(t)$ (forcing function)
$T(0, 0) \equiv 70°F$ (assumed initial
$T(\ell, t) \equiv 70°F$ temperature)

*The results of this effort have not been published.

The last relation above indicates that the slab is sufficiently thick (semi-infinite) that the rear surface temperature remains constant for the duration of the test event.

For computational purposes, Eq. (7) is recast into a different but equivalent form. If we let $\dot{q}$ represent the heating rate (in general $\dot{q} = \dot{q}(x, t)$), then by definition

$$\dot{q} = - \frac{k \partial T}{\partial x} \tag{8}$$

By substitution, Eq. (9) is obtained*.

$$\frac{\partial T}{\partial x} = - \frac{1}{\rho c} \frac{\partial \dot{q}}{\partial x} \tag{9}$$

This partial differential equation may be approximated with a finite set of ordinary differential equations developed by quantizing the space variable, x, into n + 2 values: $x_0, x_1, \ldots x_n, x_{n+1}$. The front surface of the slab would be denoted by x_0 and the rear surface by x_{n+1} while $x_1, x_2, \ldots x_n$ would correspond to spatial locations within the slab at which T and $\dot{q}$ are not known (not specified by boundary conditions).

To illustrate the concept used in formulating the set of approximate equations, consider first the case of using a uniform spacing in the slab depth x. Let x take the values o, h, 2h, 3h, ... (n + 1)h with n odd and, as a matter of choice, let the value of $\dot{q}$ be calculated at the odd multiples of h and T values be calculated at even values of h. The figure below illustrates this concept.

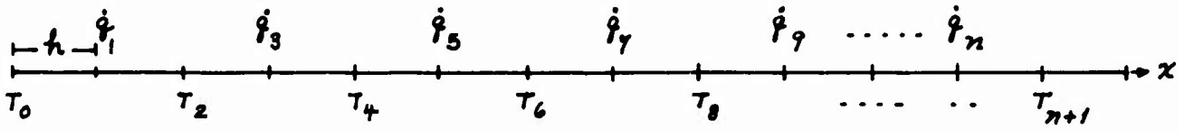

T_0 and T_{n+1} are specified boundary conditions

Thus the equation

$$\dot{q}_1 = - \left[k_1(T) \frac{\partial T}{\partial x} \right]_{x = x_1}$$

may be approximated as

$$\dot{q}_1 = - k_1 \frac{T_2 - T_0}{2h}$$

where $k_1 \equiv k(T_1)$**.

---

* This substitution has made use of the linear form of Eq. (7).

** k_1 must be evaluated in terms of T_0 and T_2 since T values are not defined for an odd subscript. In actual practice k_1 was taken as the value of k at $\frac{T_0 + T_2}{2}$.

The companion equation for T

$$\left[\frac{\partial T}{\partial t}\right]_{x=x_2} = \left[-\frac{1}{\rho c}\ \frac{\partial \dot{q}}{\partial x}\right]_{x=x_2}$$

may be approximated analogously as

$$\frac{dT_2}{dt} = -\frac{1}{\rho c_2}\left(\frac{\dot{q}_3 - \dot{q}_1}{2h}\right)$$

where $T_2 = T_2(t) \equiv T(x_2, t)$

$\rho c_2 = \rho c(t)]_{x=x_2} = \rho c(T_2)$

By this procedure, the following set of equations is generated.

$$\dot{q}_n = -k_n \frac{T_{n+1} - T_{n-1}}{2h},\quad n = 1, 3, 5 \ldots \tag{10a}$$

$$\frac{dT_n}{dt} = -\frac{1}{\rho c_n}\ \frac{\dot{q}_{n+1} - \dot{q}_{n-1}}{2h},\quad n = 2, 4, 6 \ldots \tag{10b}$$

Thus with T_o and T_{n+1} known and T_2, $T_4 \ldots T_{n-1}$ the unknown dependent variables (with the "$\dot{q}$'s" algebraically related), Eq. (10a) and (10b) represent a set of $\frac{n-1}{2}$ simultaneous differential equations. These equations are quadratically correct in the sense that if (for a fixed t) T (x, t) varies at most quadratically in x, Eq. (10b) is exact. Equation (10a) and (10b) may be regarded as the results obtained when correction terms proportional to h^3, h^4, etc. are dropped (the validity of this procedure is dependent on h being made sufficiently small).

The result desired from the solution of Eq. (10a) and (10b) is the surface heat transfer rate, $\dot{q}_o \equiv \dot{q}(0, t)$ whereas the direct results obtained provide $\dot{q}_1$, $\dot{q}_3$, etc. at interior planes. If h is small, the assumption may be made that $\dot{q}_1 = \dot{q}_o$. An appreciable increase in accuracy is easily achieved however by appropriate extrapolation to the surface heating rate.

An analysis of the errors can be made by assuming $\dot{q}_1 = \dot{q}_o$. Taking the linear diffusion equation, the following well-known relation is obtained as a solution.

$$T(x,t) = \dot{q}_o \frac{Kt}{k}\left[\frac{2}{\sqrt{\pi}}\, e^{-\frac{x^2}{4Kt}} - \frac{x}{\sqrt{Kt}}\ erfc\ \frac{x}{2\sqrt{Kt}}\right] \tag{11}$$

K = thermal diffusivity = $k/\rho c$

Differentiating Eq. (11) yields the following relation for the temperature gradient and hence heating rate[10].

$$k \frac{\partial T(x,t)}{\partial x} = \dot{q}(x,t) = \dot{q}_o \operatorname{erfc} \frac{x}{2\sqrt{\kappa t}} \tag{12}$$

At a fixed t, Eq. (12) is nearly linear in x for small values of x.

$$\dot{q}(x,t) = \dot{q}_o \left\{ 1 - \frac{x}{\sqrt{\kappa t}} + O(x^3) \right\} \tag{13}$$

Thus a linear extrapolation formula is reasonable for the case of the linear diffusion equation and by inference for the nonlinear case as well since the thermal substrate properties are smoothly changing functions of T. A much better estimate than $\dot{q}_1$ by itself is obtained by use of Eq. (14).

$$\dot{q}_o = \frac{3\dot{q}_1 - \dot{q}_2}{2} \tag{14}$$

While Eq. (10a) and (10b) are conceptually simple, the use of uniform spacing in x over the entire thickness of the slab is not practical. To achieve accuracy, the spacing h would have to be very small so that the temperature variation over h is also small. Since most of the temperature variation occurs very near the front surface (in materials of relatively low thermal diffusivity like Pyrex), a value of h of the order of 5 microinches would be implied. Thus, for slabs fulfilling semi-infinite depth requirements in shock tunnel applications, several thousand differential equations would be required. Of this large total, relatively few would have physical significance.

Two equally logical modifications are available to avoid the problems associated with a uniform spacing in x. One approach is to use nonuniform x spacing (requiring replacement of Eq. (10a) and (10b) with more complicated expressions) while the other involves a change of variable, e.g., $x = \gamma z^2$ or $x = \gamma z^3$, etc. with uniform spacing in the new variable. The latter approach was considered most expedient and therefore adopted.

3. SPECIFIC DETAILS OF ANALOG SIMULATION

The earlier (unreported) analog computer studies had made use of the transformation $x = \gamma z^3$ (γ = constant) which was chosen somewhat arbitrarily. A review was made accordingly at this time to determine the appropriateness of this transformation.

As stated previously, near the front surface of the slab (which is the region of most significance), $\dot{q}$ is nearly linear in x so that it would be cubic in z ($\dot{q} \sim a_o + a_i x \sim a_o + a_1 z^3$). The simpler forms of difference equations, analogous to Eq. (10a), however are not accurate for cubic terms but only accurate for terms through quadratic. For this reason the cubic transformation is not mathematically sound and, in effect, over-emphasizes the distortion in the space coordinate. This effect has also more than mathematical implications. Rather severe scale factor and accuracy problems are encountered in analog computer implementation. In effect, very small voltages are formed by the difference in two large (nearly equal) voltages. These low signal levels

also result in unfavorable signal-to-noise ratios. Consequently, a transformation nearly linear for small x, and at most quadratic, is desirable.

The $x = \gamma z^2$ ($\gamma = 2.5 \times 10^{-6}$) transformation was chosen for analog computation and very satisfactory locations of internal planes were thereby achieved. High resolution near the surface was realized simultaneously with adequate coverage of the deeper internal regions. Furthermore, the transformation satisfies the "quadratic" requirement of simple difference approximations to derivatives. Locations and designations of the planes defined by this transformation are tabulated below.

Temperature and Heating Rate Plane
Locations in Actual and Transformed Spatial Coordinates

x microfeet	z microfeet	Plane T = temperature $\dot{q}$ = heating rate
0	0	T_o, $\dot{q}_o$
2.5	1	$\dot{q}_1$
10.0	2	T_2
22.5	3	$\dot{q}_3$
40.0	4	T_4
62.5	5	$\dot{q}_5$
90.0	6	T_6
122.5	7	$\dot{q}_7$
160.0	8	T_8
202.5	9	$\dot{q}_9$
250.0	10	T_{10}
360.0	12	$\dot{q}_{12}$
490.0	14	T_{14}
902.5	19	$\dot{q}_{19}$
1440.0	24	T_{24}

Regardless of the change in variable, it is recognized that extrapolation to heat transfer rate at the surface, $\dot{q}_o$, must be based on linearity in x, not linearity in the artificial variable z. Thus

$$x = 2.5 \times 10^{-6} z^2 \text{ feet} = 2.5 z^2 \text{ microfeet}$$

so that computer implementation produced voltages corresponding to

$$\dot{q}_1 \equiv \dot{q} \text{ (evaluated at } z = 1) = \dot{q} \text{ (evaluated at } x = 2.5)$$

and

$$\dot{q}_3 \equiv \dot{q} \text{ (evaluated at } z = 3) = \dot{q} \text{ (evaluated at } x = 22.5).$$

Thus to obtain $\dot{q}_o$ ($x = 0$, $z = 0$), the correct relationship* is

*Note that the value of $\dot{q}_1$ is evaluated at a point physically 9 times closer to the surface than is $\dot{q}_3$, hence the 9:1 relative weighting.

$$\dot{q}_0 = \frac{9\dot{q}_1 - \dot{q}_3}{8}$$

and <u>not</u>

$$\dot{q}_0 = \frac{3\dot{q}_1 - \dot{q}_3}{2}$$

A listing of the set of linear difference equations and the ordinary differential equations actually used is given below. A tabulation of the values used for k(T) and $\rho c(T)$ is shown in Table II.

Difference Equations for $\dot{q}$*

$$\dot{q}_0 = 1/8\,(9\dot{q}_1 - \dot{q}_3)$$

$$\dot{q}_1 = \frac{-k_1}{2\gamma g_1}\,\frac{T_2 - T_0}{2} = -\frac{1}{10 \times 10^{-6}}\,k_1 (T_2 - T_0)$$

$$\dot{q}_3 = \frac{-k_3}{2\gamma g_3}\,\frac{T_4 - T_2}{2} = -\frac{1}{30 \times 10^{-6}}\,k_3 (T_4 - T_2)$$

$$\dot{q}_5 = \frac{-k_5}{2\gamma g_5}\,\frac{T_6 - T_4}{2} = -\frac{1}{50 \times 10^{-6}}\,k_5 (T_6 - T_4)$$

$$\dot{q}_7 = \frac{-k_7}{2\gamma g_7}\,\frac{T_8 - T_6}{2} = -\frac{1}{70 \times 10^{-6}}\,k_7 (T_8 - T_6)$$

$$\dot{q}_9 = \frac{-k_9}{2\gamma g_9}\,\frac{T_{10} - T_8}{2} = -\frac{1}{90 \times 10^{-6}}\,k_9 (T_{10} - T_8)$$

$$\dot{q}_{12} = \frac{-k_{12}}{2\gamma g_{12}}\,\frac{T_{14} - T_{10}}{4} = -\frac{1}{240 \times 10^{-6}}\,k_{12} (T_{14} - T_{10})$$

$$\dot{q}_{19} = \frac{-k_{19}}{2\gamma g_{19}}\,\frac{T_{24} - T_{14}}{10} = -\frac{1}{950 \times 10^{-6}}\,k_{19} (T_{24} - T_{14})$$

$$k_1 = \frac{k(T_2) + k(T_0)}{2};\quad k_3 = \frac{k(T_4) + k(T_2)}{2};\quad \cdots\quad k_{19} = \frac{k(T_{24}) + k(T_{14})}{2}$$

*See Eq. (10a).

Differential Equations for T*
T_o: the input function

$$\frac{dT_2}{d\tau} = -\frac{\alpha}{C_2}\frac{1}{2\gamma g_2}\frac{\dot{q}_3-\dot{q}_1}{2} = -\frac{100}{2}\frac{\dot{q}_3-\dot{q}_1}{C_2}$$

$$\frac{dT_4}{d\tau} = -\frac{\alpha}{C_4}\frac{1}{2\gamma g_4}\frac{\dot{q}_5-\dot{q}_3}{2} = -\frac{100}{2}\frac{\dot{q}_5-\dot{q}_3}{C_4}$$

$$\frac{dT_6}{d\tau} = -\frac{\alpha}{C_6}\frac{1}{2\gamma g_6}\frac{\dot{q}_7-\dot{q}_5}{2} = -\frac{100}{6}\frac{\dot{q}_7-\dot{q}_5}{C_6}$$

$$\frac{dT_8}{d\tau} = -\frac{\alpha}{C_8}\frac{1}{2\gamma g_8}\frac{\dot{q}_9-\dot{q}_7}{2} = -\frac{100}{8}\frac{\dot{q}_9-\dot{q}_7}{C_8}$$

$$\frac{dT_{10}}{d\tau} = -\frac{\alpha}{C_{10}}\frac{1}{2\gamma g_{10}}\left\{0.8\frac{\dot{q}_{12}-q_9}{3}+0.2\frac{\dot{q}_9-\dot{q}_7}{2}\right\} = -\frac{100}{5}\left\{0.8\frac{\dot{q}_{12}-\dot{q}_9}{3}+0.2\frac{\dot{q}_9-\dot{q}_7}{2}\Big/C_{10}\right\}$$

$$\frac{dT_{14}}{d\tau} = -\frac{\alpha}{C_{14}}\frac{1}{2\gamma g_{14}}\frac{\dot{q}_{19}-\dot{q}_9}{10} = -\frac{20}{14}\frac{\dot{q}_{19}-\dot{q}_9}{C_{14}}$$

T_{24} = 70 by hypothesis
C^{24} = ρc
t = $\alpha\tau$; $\alpha = 10^{-3}$ (change from real time to computer time)

4. TEST PROGRAM AND RESULTS

A total of 46 test runs was made during the program. In general, the input temperature rise** was permitted to reach a maximum value of 1000°F in 10 msec to explore the full effects of the variation in substrate thermal

* See Eq. (10b).

**It was not considered important to the results of this study that the correction of nonlinearity of the resistance characteristic of the thermometer be included in the program. Accordingly, the input temperature to the analog computer was taken as the actual (or true) surface temperature.

properties. Except in special situations where the ease of discerning the effects of changes in the input function would have been compromised, each set of test conditions was used to generate two heat transfer rate histories: one with the substrate properties constant and the other with the properties variable with temperature.

Data were recorded on a single channel x-y plotter and comprised the temperature input signal and the corresponding heating rate. The resultant plots are shown labeled as Run #1 through Run #46 and are included as part of Appendix A. Each record includes a brief tabulation of the test conditions imposed. To an extent, these records are self-explanatory; however, pertinent details, comments, and observations applicable to each record are included in Appendix A.

These records quantitatively demonstrate the effects of such factors as variable substrate properties, electronic filtering, noise (random and sinusoidal), simulated tunnel starting phenomena, and gage abrasion on the derived heat transfer rate. Basically the fundamental input has been a parabolic function with lesser emphasis given to ramp and step-type inputs as well.

For large incremental temperature changes, neglect of the temperature dependent thermal properties of the substrate (#7740 Pyrex) results in heat transfer rates that are too low by as much as 15%. Tunnel starting phenomena that are of an impulsive nature (very short in time extent) cause only a transient disturbance in the heating rate and the disturbance dies out very rapidly. Other phenomena, as exemplified by gage abrasion, that result in step-type inputs (that is of long time duration)* also result in a large transient disturbance in heating rate. This type disturbance however decays as $t^{-1/2}$ and hence has a long persistence and results in erroneous data if the $\dot{q}$ attributable to this type input is indeed spurious and not desired in the final result. Electronic filtering of the temperature signal, often employed in practice, is very effective in reducing excessive amplitude excursions in $\dot{q}$ resulting from noise and step disturbances in the temperature signal. Filtering however is not at all effective in suppressing the long term ($t^{-1/2}$) contributions of step inputs to the net $\dot{q}$. The relative effect of step inputs on $\dot{q}$ depends on the relative amplitudes of the fundamental signal (say a parabola) and the spurious (assumed) step. For approximately equal amplitudes, the $\dot{q}$ component corresponding to the step signal maybe as much as a factor of 2 larger than the component of $\dot{q}$ corresponding to the parabola (see Run #34).

The results of these analog studies highlight the dichotomy of the problem of heat transfer data reduction. First is the necessity of correctly translating the temperature data into heat flux data and second is the extraction of the desired component of the resultant heat flux which may be a composite of two or more components.

---

*Despite the fact that the impact of a particle on a gage is a transient of very brief duration in a physical sense, the electrical effect is of long duration since a step-type increase in gage signal occurs and persists throughout the test event.

In the situation where gage abrasion exists, it is obvious that the gage output signal does not represent the surface temperature history since the signal, in part, represents resistance changes caused by mechanical effects rather than thermal effects. Thus erroneous heat flux data may be obtained despite the fact that the data reduction procedures have been properly executed. As illustrated by the data of Appendix A, the $t^{-1/2}$ decay characteristic of the heat flux corresponding to a step temperature change ensures the fact that this spurious signal will persist throughout the length of the typical shock tunnel test. Where serious abrasion exists, the only recourse is to record the gage output signal and to reconstruct the actual temperature signal by subtracting from the gage signal the components attributable to abrasion (these instances are usually manifested as sharp, vertical discontinuities in the signal). The reconstructed temperature signal is then used in computing the heat transfer rate.

Whereas the effects of abrasion are well understood, the extent to which heat flux data, as computed for the steady flow portion of the test, reflect effects possibly associated with tunnel starting phenomena is not well known. If these effects are of an impulsive character, their disturbance of the heat flux signal will be a short-lived transient of small concern. On the other hand, should the flow be such to create a sharp increase in gage temperature which then is subsequently further increased relative to that level in response to the subsequent steady flow heat flux, then heat flux record interpretation would be a problem (see Run #15, Appendix A). It would be a problem in the sense that although the computed heat flux would in fact be that actually experienced by the gage (or model), only that part of the heat flux (and surface temperature rise) resulting from the steady flow portion of the test is really being sought.

The seriousness of the problems cited above is directly related to the relative magnitudes of the spurious effects compared with the steady state phenomena being measured. There is a body of experimental data which suggests that for some types of test conditions, measured heat flux data may be drastically affected by some unexplained circumstance. In such situations heating rates are much higher than expected and have a characteristic time function that suggests that tunnel starting conditions are involved. Additional studies are needed to resolve these particular problems.

SECTION V

DEVELOPMENT OF A DIGITAL COMPUTER PROGRAM

1. OBJECTIVES

The object of this portion of the project was to develop an economically practical digital computer program for solving the nonlinear heat conduction problem. Specifically, the program was to be designed for the routine conversion of the data measured with thin-film resistance thermometers into heating rates. A perfectly flexible program was desired that would combine a short running time, freedom from any restrictions on the functional form of the input data (gage surface temperature histories), and a high accuracy. Output data from this program were also to serve as the standard for evaluation of the operational performance of the compensated analog network (see Section VI).

A further requirement of the project was the placing of the digital data reduction program on an operational basis on the IBM 7094 system at WPAFB. The CAL Computing Center currently employs an IBM System 360/65 Model H and the program was initially written for, and evaluated on, this particular system.

2. MATHEMATICAL BASIS

Based on the successful experiences with the methods employed in solving the nonlinear diffusion equation on the analog computer, it was decided to adapt the identical methematical approach to the development of a digital program for data reduction. Advantage was taken of certain unique capabilities of a digital computer to improve the accuracy of the computed data. Because of the fact that an appreciable amount of the mathematics parallels that of Section IV-2 and since the specific details are included in Appendix B, this discussion will be very general and will emphasize the unique aspects of the digital formulation as contrasted to the analog formulation.

As in the analog computer application, the substrate was divided into a series of slabs by planes oriented parallel to the surface plane. If we designate the surface as the zero plane, then again the even-numbered planes (including zero) represent the temperature planes while the intermediate (odd-numbered planes) represent the heat flow planes. A set of equations may then be written for each of these planes; heat flow being expressed in terms of a first order difference formula in temperature (Eq. 10a) and the time derivative of temperature as a first order difference formula in heat flow (Eq. 10b). A simple Runge-Kutta integration scheme was adopted to solve this set of equations since in the present circumstance the time variable must be quantized in addition to the spatial coordinate x (depth into the substrate).

Whereas the required nonlinear spacing of the planes followed a quadratic function ($x = az^2$) in the analog studies, considerably more freedom in selecting the transformation function was now possible. Accordingly a polynomial transformation ($x = a_1 z + a_2 z^2 + a_3 z^3$) was employed together with a larger

total number of planes (twenty temperature planes compared with eight in the analog program). The accuracy of the program improves with an increasing number of planes. Attention is called to the selection of the exact form of the transformation which is purely arbitrary. Despite the arbitrariness entering this selection, the essential facts are that the desired linearity of spacing near the surface (see Section IV-3) is achieved and yet the entire significant depth of the slab is covered with a reasonably small number of planes.

A change of time variable was also introduced to avoid a singularity near the substrate surface. This singularity is associated with the necessity to evaluate the time derivative of temperature (Eq. 10b) which goes to infinity at time equal zero for a parabolic temperature history. A transformation of the form $t = \tau (1 - e^{-\beta\tau})$ was made so that $t \simeq \beta\tau^2$ for small values of $\beta\tau$ and $t \simeq \tau$ for large $\beta\tau$.

The digital program also includes a routine for correcting the gage measured temperature to actual surface temperature (Eq. 6).

A more detailed description of the digital program formulation is given in Appendix B together with a listing of the program in Fortran IV language.

3. RESULTS

Proper operation of the digital computer program was ascertained by the use of input data functions whose solutions could be hand calculated with ease and accuracy. Thus surface temperature histories of parabolic form were employed since these correspond to a constant level of incident heat flux if the gage properties are held constant. Adequacy of the planar spacing and the stability of the computer program is easily verified by this process. In computation techniques of this type where time and spatial parameters are quantized, instability may result when the relative sizes of the increments selected do not satisfy stability criteria.

When program operation had been properly verified, a series of parabolic temperature functions, of various amplitudes, was used as a trial problem. Solutions were obtained both for the case of constant gage properties and for the case of temperature dependent gage properties. Some of these results are summarized in Table III which tabulates the surface heat flux data for the two cases as a function of time. As in the analog studies, it is obvious that most of the effects of changing properties are experienced in the first few milliseconds since, for a parabolic function, the most rapid change in temperature also occurs in that time interval. That the corrections may be of significant proportions is illustrated below (data taken from Table III).

Time sec.	Uncorrected Heat Flux Btu/ft^{2}sec	Corrected Heat Flux Btu/ft^{2}sec	% Correction
.005	200.0	222.07	11.0
.010	200.0	231.08	15.5
.005	400.0	484.57	21.1
.010	400.0	512.74	28.2
.005	600.0	777.81	29.6
.010	600.0	847.79	41.3

The data reduction program, as presently constituted (see listing in Appendix B), is designed to provide a high accuracy of computation by virtue of the large number of temperature and heat flow planes that are employed. As demonstrated by the analog computer studies, wherein less than one half of this number of planes were successfully employed, a smaller number of planes could be used if lesser accuracy were desired in exchange for a shorter computing time.

The computer program also has application to the general study of non-linear heat conduction in materials since it evaluates the temperature history and the heat flux history at many planes within the body of the material. In its present form however, the only data printed out are: surface temperature in °F (the input) and surface heat flux in Btu/ft^2sec (the output) for a period of 10 msec at 0.05 msec intervals.

The computer program, in card deck form, has been delivered to AFAPL and some identical preliminary trial problems have been run on both the IBM 7094 system at WPAFB and the CAL IBM 360 Model 65 system at CAL. A very small discrepancy in the first and second decimal positions of the computed heating rate data has been noted between the two computers. At the writing of this report the basis for this discrepancy has not been positively identified although it is thought to be associated with lesser precision of the CAL computer which uses fewer bits per word.

SECTION VI

DEVELOPMENT OF A COMPENSATED ANALOG CIRCUIT

1. BACKGROUND AND OBJECTIVES

Desirable in most experimental endeavors, but especially important and critical in hypersonic shock tunnel testing, is immediate access to the results of measurements of the test parameter. Since the output signal of the thin-film heat transfer gage is a surface temperature, the common practice in earlier years involved manual tabulation of temperature-time data from an oscilloscope photograph of the gage signal. These data were subsequently transferred to punched cards and processed on a digital computer to obtain the heat transfer rate. This procedure was very time consuming and uneconomical. Despite the current availability of instrumentation capable of directly converting the gage output signal into a computer compatible format, the time interval between test and the availability of the test results is still often unsatisfactory.

Because they provide a direct, on-the-spot conversion of the heat transfer gage output signal into a signal proportional to heat flux, analog networks have found a wide acceptance in shock tunnel testing. The principal drawback of the simple, passive analog network is that it neither can compensate for the nonlinearity of the gage resistance-temperature function nor the effects of changing substrate thermal properties. Despite development of several compensated electronic analog circuits[6, 11, 12], little practical use appears to have resulted. Practice at CAL has been to employ the simple linear networks and (where appropriate) to manually apply corrections to the measured heating rate. The applicable corrections, derived from digital computer solutions for parabolic type temperature histories, are applied as functions of time and measured heat flux.

In these less than satisfactory circumstances, a need would seem to exist for an economical, reliable and compact compensated analog network that could be used in each thin-film thermometer channel to provide a direct output of the true heat transfer rate. Development of a circuit design aimed at achieving these objectives was therefore undertaken.

2. CORRECTION FUNCTIONS

As described in Section III, two distinct and separate operations are needed on the output signal from a thin-film heat transfer gage if the true heat flux is to be computed. These operations include the corrections for the nonlinear resistance-temperature function of the resistance element as well as the changes in substrate properties.

The functional form of the resistance nonlinearity is given in Eq. (6) and, in tabular form, in Table I. A mathematical relationship, based on gage output voltage and appropriate to circuit design considerations, is derived in Appendix C and given below.

$$\theta_w = 0.386 \times 10^{-4} - \sqrt{0.149 \times 10^{8} - 0.0771 \times 10^{8}\, u_g / u_{g_o}} \qquad (15)$$

θ_w = temperature rise, °F
u_g = gage voltage rise
v_{g_o} = initial gage voltage

To derive a compensation function for the changes in substrate properties with temperature, the mathematical techniques of Hartunian and Varwig[5] were employed. A solution to the nonlinear diffusion equation is obtained as a transformed temperature rise expressed in terms of the true surface temperature rise. The transformed temperature represents the temperature that would have been experienced by the substrate had its properties remained constant. Thus the availability of the transformed temperature permits the use of the simple, stable, reliable passive analog network to obtain the true heat transfer rate.

The expression for the transformed temperature, ϕ_w, based on the thermal property data of Table II is derived in Appendix C.

$$\phi_w = \theta_w [1 + .0001882 (5/9) \theta_w] \quad (16)$$

Equations (15) and (16) specify the operations required on the gage output signal and form the basis for the design of the function generator of the electronic circuit.

3. CIRCUIT DESCRIPTION

The nonlinear operations (Eqs. 15 and 16) used to convert the gage output signal to an analog of the transformed temperature may be combined into a single function and hence accommodated by a single circuit. A diode-type function generator was selected for this purpose and is shown as network No. 1 in Fig. 1 which is a schematic of the entire circuit. Figure 2 is a simplified schematic diagram and will be useful in graphically illustrating the following verbal description of the circuit operation.

In this schematic (Fig. 2) it is presumed that the gage signal rises from a zero level and that diodes are ideal conductors in the forward direction and perfect open circuits in the reverse direction. Voltage limits are also ignored. A 30-milliampere current source produces a potential difference of 3 volts across a 100-ohm gage at room temperature. With heat flux applied to the gage, its resistance increases and the voltage at the input of amplifier I sweeps positively reaching approximately +3 volts at a gage temperature of 1000°F above room temperature. The amplifier output, five times as large as the input, sweeps negatively by 15 volts and is applied to amplifier II by R_1. As this voltage becomes increasingly negative, the diodes that are attached to the voltage divider string at the output of amplifier I begin to conduct at intervals of one volt and shunt R_1 with the resistors in series with their anodes. Current flow through these resistances into the summing junction (J_2) of the second amplifier increases in a nonlinear fashion with the output voltage of amplifier I. The output of amplifier II, proportional to this current, will vary nonlinearly as shown in the inset graph in Fig. 2.

Series resistances in the diode network are selected to generate the composite compensation function obtained by eliminating θ_w between Eqs. (15) and (16) and expressing ϕ_w in terms of u_g / v_{g_o}. Whereas it is possible to

calculate exactly the various resistances needed for this purpose, minor variations in diode properties require corrections of a few percent. Therefore, it is realistic to calculate only the approximate values of the resistances and adjust each resistor, one at a time, to fit the desired function precisely. Adjustment is simplified when the diodes come into conduction at intervals of more than one-half volt; however, the accuracy of curve fitting is poorer the fewer the diodes. In the present application, a network of six diodes at one-half volt intervals proved less satisfactory than one with fifteen diodes operating at one volt intervals. This latter network, schematically shown in Fig. 3, required a larger voltage swing from the amplifier.

By actual trial, only thirteen biased diodes were required to generate the required compensation function since two of the diode series resistances were determined to assume infinite values (i.e., the respective diodes need to be open circuit). Bias voltage applied to the entire function generator is adjustable by means of the trimming potentiometer shown in Fig. 3.

The diode function generator provides the proper compensation to gage measured temperature changes, T_m^*, up to a maximum of 1000°F which temperature rise is taken to correspond to a 3-volt signal output from the heat transfer gage. As a result of the 5X gain of amplifier I, the function generator experiences a 15-volt signal in response to a 3-volt signal from the gage. In the manner described earlier, the function generator augments the applied signal in a nonlinear fashion with increasing signal amplitude. The input-output relationship is qualitatively shown in the inset graph on Fig. 2.

Calibration of the function generator may be accomplished statically by simulating the gage output signal (μ_g) in discrete steps in the range from 0 to 3 volts and measuring the output signal ϕ_ω. The required functional relationship between μ_g and ϕ_ω is given by Eqs. (15) and (16). A linear time dependent signal (a ramp) may be used if a dynamic check is preferred. In either case, the $\mu_g - \phi_\omega$ function will have the form shown in the inset graph of Fig. 2.

The output voltage range of the amplifier should be as large as practically possible to improve the accuracy of curve fitting and to improve the signal-to-noise ratio. Analog computer amplifiers normally possess a nearly symmetrical range of output about zero volts. It is therefore advisable to bias the amplifiers so that the full voltage range can be used with an input signal that is always of one sign. A number of resistors shown in Fig. 1, but not in Fig. 2, serve this purpose.

Two diodes at the output of amplifier I introduce a distortion into the voltage applied to the diode network which essentially cancels the nonideal logarithmic characteristic of the network diodes. A direct feed from the end of the feedback resistor of amplifier I to the input of amplifier II assures that this distortion is not applied to the linear component of the system response (that is to signals corresponding to such small temperature rises that no corrections are required).

The network connected between amplifiers II and III has a transfer function of the form $\sqrt{s}$. This network has the form of alternate series resistors and shunt capacitances (see Fig. 4) and is a variant of the standard so-

called analog $\dot{q}$ network[2]. Resistor-capacitor values may be computed by a process involving continued polynomial fractions. In practice, an algorithm due to Routh[15] is especially useful since it is more suitable to machine computation. A Fortran program for calculating the network components for a desired frequency range is given in Appendix D. The measured response of the network of Fig. 4 approximated a $\sqrt{s}$ function from 5 Hz to 40 kHz to better than 10%. This frequency range is adequately large to cover a range of test durations extending from about 2 msec to 10 msec.

Amplifier III isolates the analog network from loading effects of external circuitry and provides a voltage gain to compensate for the insertion loss of the network.

A breadboard model of the complete compensated analog circuit is shown in Fig. 5. A large fraction of the bulk of the components is seen to be associated with the capacitors of the analog network. The operational amplifiers are of the integrated circuit type; very compact and very inexpensive.

For convenience in calibrating the compensated analog network, parabolic type waveforms were applied as simulated signals from the heat transfer gage to the circuit to test its operation. With the function generator disabled, the circuit produced a step output for a parabolic input signal, as is proper. With the diode circuit activated, and with sufficiently large amplitude input signals, the output signal, corresponding to heat flux, had the rising-step waveform as shown in Run #2 of Appendix A. A parabolic signal, corresponding to a gage-measured temperature rise of 1000°F in 10 msec (the maximum design condition), was applied as a real-time signal to the compensated analog network. The input signal and the circuit output signal were recorded photographically from an oscilloscope display. The input signal was manually digitized into a temperature-time tabulation. These data were then converted to heat flux by the digital computer program. Heat flux data scaled from analog circuit output signal agreed with the computed data to within a few percent. Although time did not permit extensive testing of the circuit using a variety of input waveforms, the bandwidth of the circuit is sufficiently broad that all but extremely large temperature gradients should be correctly translated into a correct heat flux.

Several observations on the compensated circuit are pertinent here. First is the need for the diode function network to produce a smooth curve, that is the transition of conduction from one diode to the next must be carefully blended. Any perturbations in the function generator characteristic will become painfully obvious after the differentiating action of the analog network (see Appendix A, comment on Run #1). This problem was initially encountered but it is tractable. Second is the fact that two minor modifications would be required to the circuit of Fig. 1 to adapt it to practical use.

For proper circuit operation, the initial voltage drop across the gage must be nulled at the input to amplifier I and the voltage input to the diode network must bear a constant relationship to the gage temperature rise. Since the initial gage resistence and the gage calibration constant (change in gage resistance for a unit change in temperature) vary from gage to gage, calibrated controls can be installed to vary gage current and the gain of amplifier I to make these corrections. Signal-to-noise ratio at low heating rates would be improved by a range switch. A convenient arrangement would use full-scale output corresponding to 10, 100, or 1000 Btu/ft^{2}sec with the diode function generator inactivated for the lower two scales.

SECTION VII

SUMMARY

Experimental studies were conducted to develop economically practical methods of computing incident heat flux from thin-film resistance thermometer measurements made at hypersonic shock tunnel conditions that include very high heating rates and that result in nonspecific surface temperature histories from the gage. Both digital and analog techniques that are consistent with these requirements were developed. In both methods, compensation is made for thermal effects on the temperature coefficient of resistance of the thin-film element as well as on the materials properties of the substrate.

The digital program accepts quantized temperature-time data and provides a highly accurate solution for the surface heat flux history as a tabular printout. This program was written in Fortran IV language and made operational on both the IBM 7094 and IBM 360/65 Model H systems. Since this program also evaluates temperature and heat flux at many planes within the substrate, it is directly useful in general studies of heat conduction in materials of nonconstant thermal properties at nonconstant heat flux.

Design, synthesis, and evaluation of a compensated analog network was achieved. This compact, solid-state electronic circuit operates directly, in real time, on the electrical output signal from the thin-film resistance thermometer to produce an electrical output signal proportional to the true heat flux. The circuit is simple in design, stable, and easy to use. Cost and size of the actual components is such that use of individual units in each heat transfer gage channel (on model tests) is economically feasible.

Using the CAL analog computer facility (COMCOR), the heat flux data corresponding to a variety input temperature-time functions was obtained. Generally, two solutions for each case were obtained, one for constant substrate properties and one with variable substrate properties, to illustrate the effects of these variables. In addition, these fundamental input functions were also modified to include tunnel starting phenomena, random noise, and sinusoidal modulation. The tests showed that measurement of the true heating rate in the steady flow portion of a shock tunnel test may transcend the problem of proper data reduction. Cases were illustrated where the initial transient portion of the temperature record could seriously affect the heating rate even at times in excess of the run duration of the typical shock tunnel because of the very long persistence (slow decay) of the transient effects. It is recommended that detailed studies be made of tunnel starting phenomena and initial (presteady) flow conditions to establish whether these factors do indeed confound the heat flux measurement made in the steady flow portions of the test.

SECTION VIII

REFERENCES

1. Vidal, R. J., "Model Instrumentation Techniques for Heat Transfer and Force Measurement in a Hypersonic Shock Tunnel," Cornell Aeronautical Laboratory Report AD-917-A-1; also WADC TN 56-315, AD 97238, February 1956.

2. Skinner, G. T., "Analog Network to Convert Surface Temperature to Heat Flux," Cornell Aeronautical Laboratory Report No. CAL-100, February 1960.

3. Bogdan, L. and Garberoglio, J. E., "Transient Heat Transfer Measurement with Thin-Film Resistance Thermometers--Fabrication and Application Technology," Technical Report AFAPL-TR-67-72, June 1967.

4. Cook, W. J. and Felderman, E. J., "Reduction of Data from Thin-Film Heat-Transfer Gages: A Concise Numerical Technique," AIAA Journal, Vol. 4, No. 3, March 1966.

5. Hartunian, R. A. and Varwig, R. L., "A Correction to the Thin-Film Heat Transfer Measurements," Aerospace Corporation Report TDR594 (1217-01) TN-2, May 1961.

6. Schmitz, L. S., "Nonlinear Analog Network to Convert Surface Temperature to Heat Flux," CAL Report No. 130, June 1963.

7. Bogdan, L., "Thermal and Electrical Properties of Thin-Film Resistance Gages Used for Heat Transfer Measurement," AIAA Journal, Vol. 1, No. 9, September 1963.

8. Skinner, G. T., "A New Method of Calibrating Thin-Film Backing Materials," CAL Report 105, June 1962.

9. Shand, E. B., Glass Engineering Handbook, McGraw Hill, 2nd Ed., 1958.

10. Handbook of Mathematical Functions, National Bureau of Standards, AMS-55, June 1964.

11. Walenta, Z. A., "Analogue Networks for High Heat-Transfer Rate Measurements," UTIAS Technical Note No. 84, November 1964.

12. Reece, J. W. and Hale, R. W., "Compensation for Nonlinear Effects Due to High Heat Flux in Thin-Film Thermometry," Therm Advanced Research, Inc., TAR-TR 6601, June 1966.

13. Bogdan, L., "High Temperature, Thin Film Resistance Thermometers for Heat Transfer Measurement," NASA CR-26, April 1964.

REFERENCES (CONTD)

14. Reece, J. W., "Temperature Dependent Materials Properties and Theory for their Compensation," Therm Advanced Research, Inc. TAR-RM 6501, October 1965.

15. Fryer, W. D., "Applications of Routh's Algorithm to Network Theory Problems," I.R.E. Trans. on Circuit Theory, Vol. CT-6, No. 2, June 1959.

TABLE I

A Comparison of Actual Temperature Rise and Gage-Measured Temperature Change (Relative to 70°F)

Measured Temperature Change, °F	Actual Temperature Change*, °F
0	0
29.9	30
127.8	130
223.1	230
315.8	330
406.0	430
493.5	530
578.4	630
660.9	730
740.7	830
817.9	930
892.5	1030

TABLE II

Thermal Properties of #7740 Pyrex as a Function of Temperature

Temperature °F	c** Btu $°F^{-1}$ ft^{-3}	k Btu sec^{-1} ft^{-1} $°F^{-1}$
70	25.03	2.17×10^{-4}
122	26.60	2.19
212	29.20	2.20
392	33.15	2.22
572	36.25	2.17
752	38.37	2.12
932	40.40	2.06×10^{-4}

* These values are exact (not rounded off).

** These data are taken from the following source: Shand, E. B., Glass Engineering Handbook, McGraw-Hill, 2nd Ed., 1958.

TABLE III

Comparison of Heat Flux Calculations with and without Corrections for Thermal Effects on Gage Properties -- Digital Data Reduction Program

Surface Temperature* History = $\gamma t^{1/2} + 70°F$

Time, t, sec.	Heat Flux, Btu/ft^{2}sec With Corrections			
	$\gamma = 3.062 \times 10^3$	$\gamma = 4.593 \times 10^3$	$\gamma = 6.124 \times 10^3$	$\gamma = 9.186 \times 10^3$
.001	210.77	322.80	439.52	687.86
.002	214.42	331.35	455.24	721.03
.003	217.30	338.18	467.67	743.14
.004	219.80	344.06	476.97	761.54
.005	222.07	349.28	484.57	777.81
.006	224.10	353.66	491.10	792.96
.007	226.01	357.32	497.06	807.28
.008	227.77	360.74	502.56	821.14
.009	229.48	363.78	507.83	834.54
.010	231.08	366.61	512.74	847.79
	Without Corrections			
	200.00	300.00	400.00	600.00

*The surface temperature history is taken to be that measured by the gage (T_m of Eq. 6).

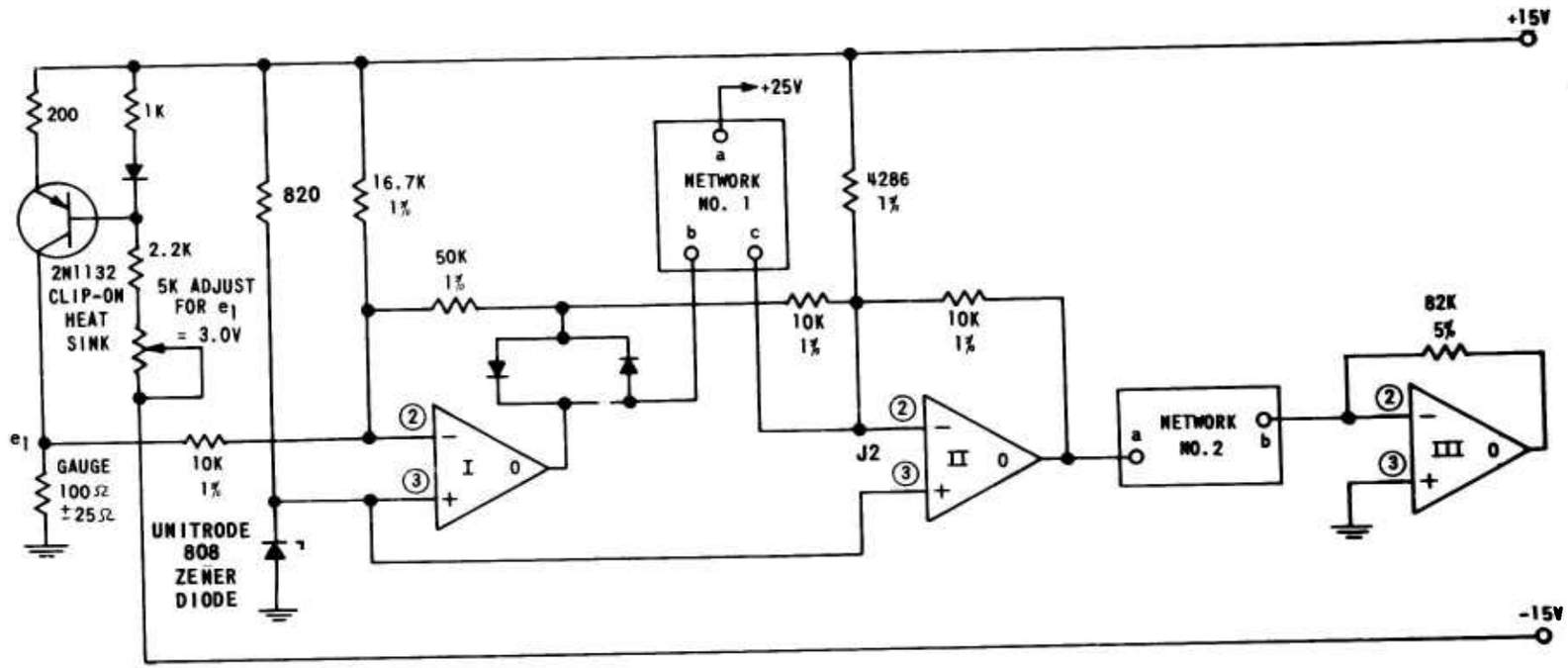

NOTE :
ALL AMPLIFIERS FAIRCHILD U5B770939X
ALL DIODES ARE TYPE IN914

Figure 1 SCHEMATIC DIAGRAM - COMPENSATED ANALOG CIRCUIT

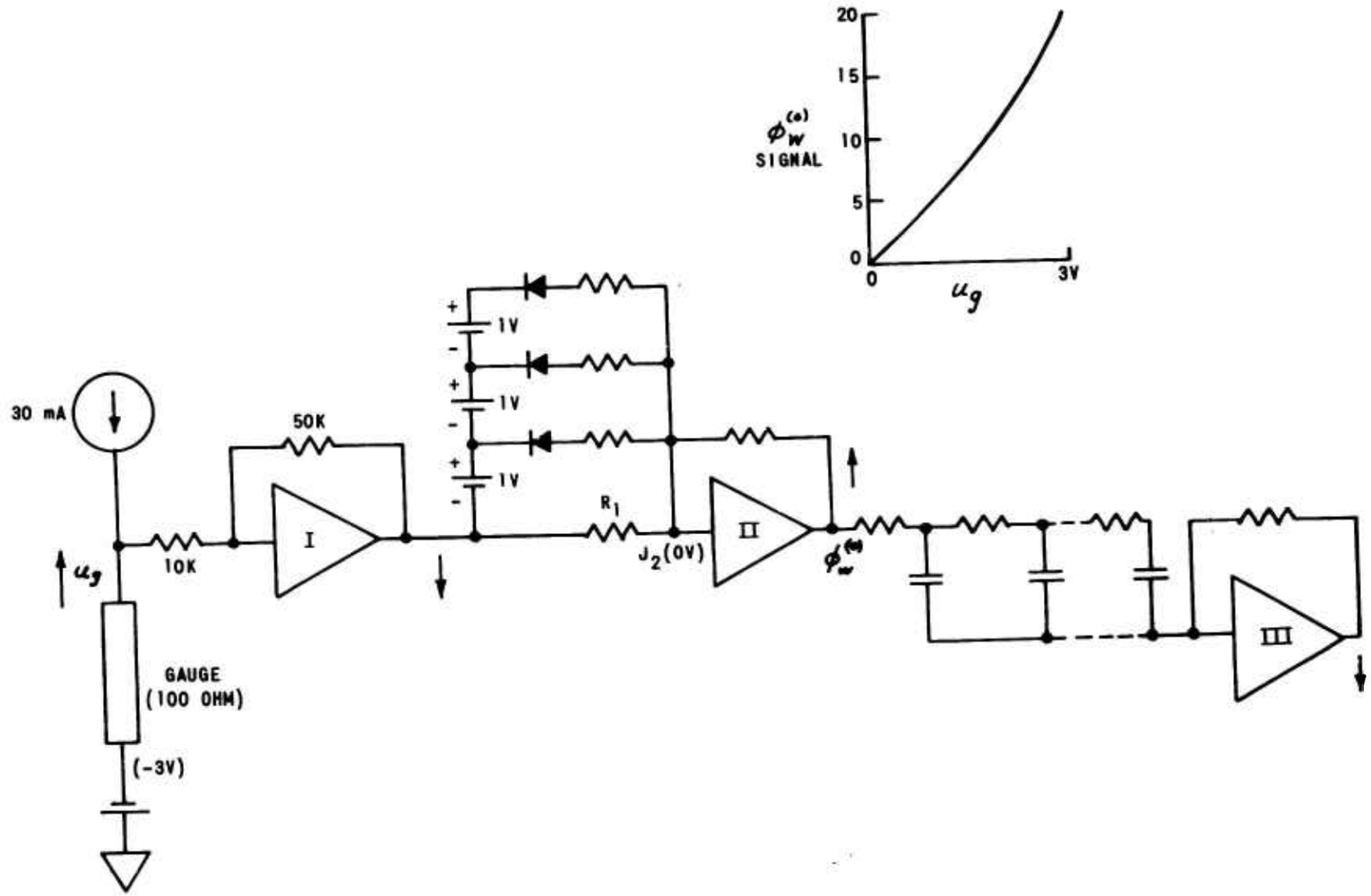

Figure 2 SIMPLIFIED SCHEMATIC-COMPENSATED ANALOG CIRCUIT

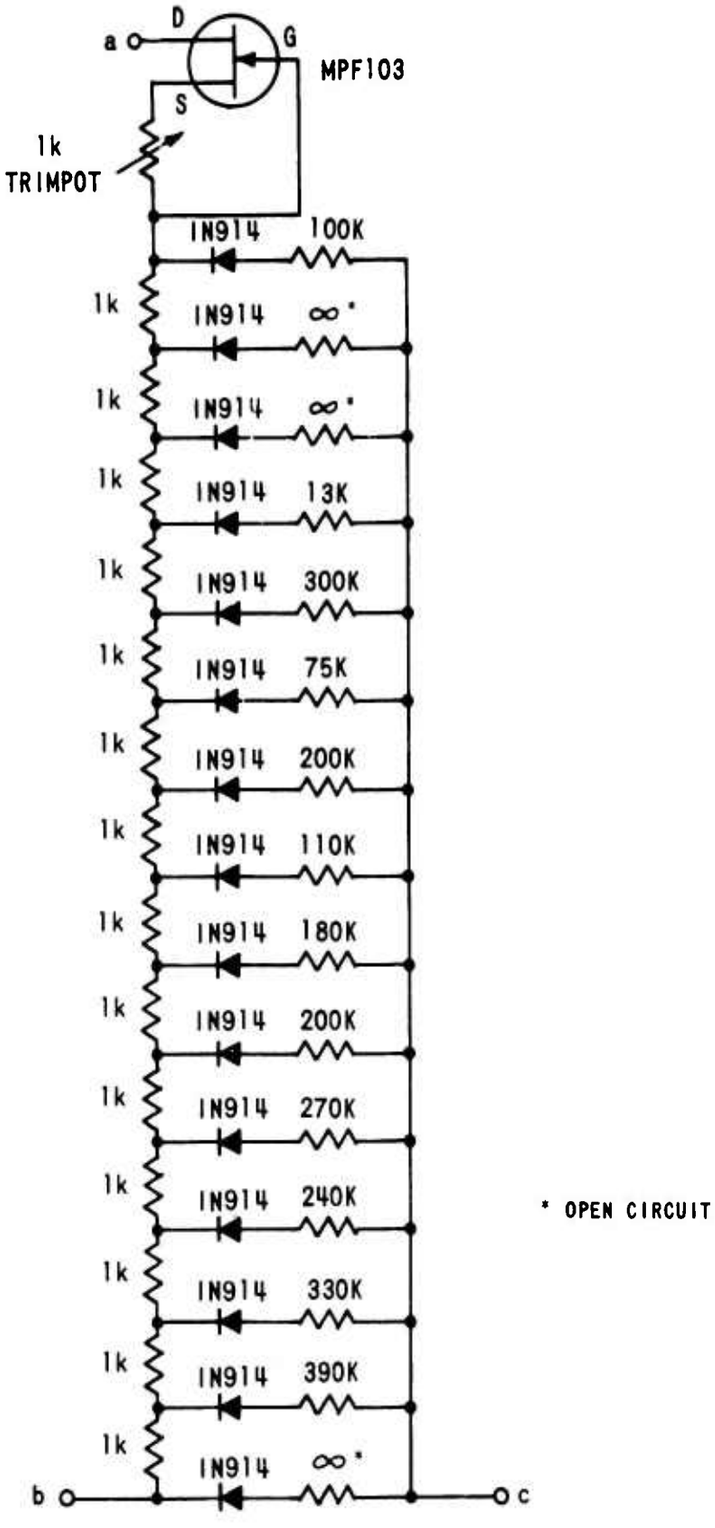

NETWORK NO. 1

Figure 3 FIFTEEN ELEMENT DIODE FUNCTION GENERATOR

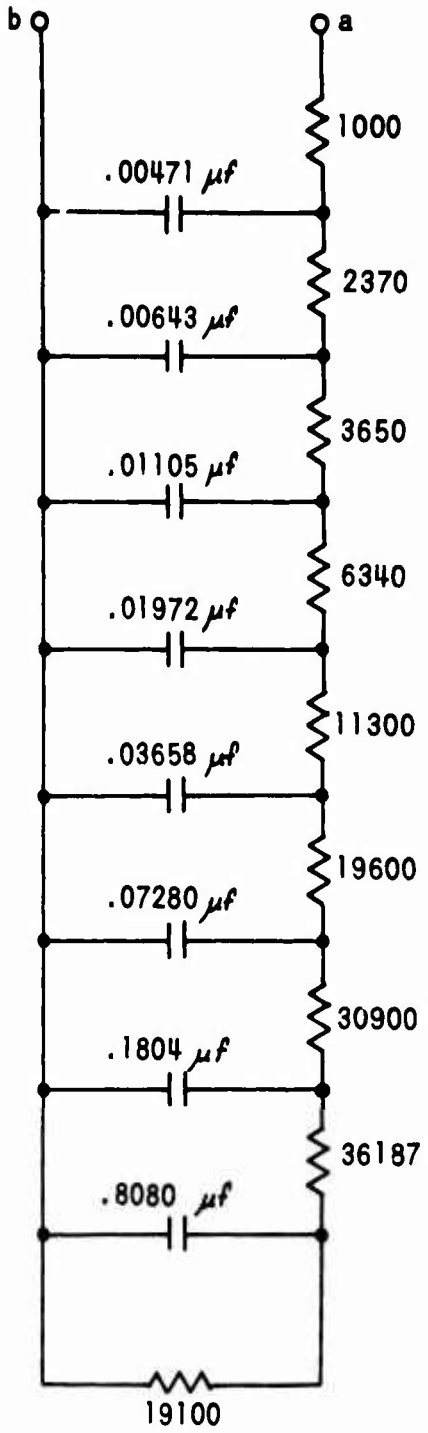

NETWORK NO. 2

NOTE:
ALL RESISTORS IN OHMS.

Figure 4 LINEAR EIGHT-SECTION ANALOG NETWORK

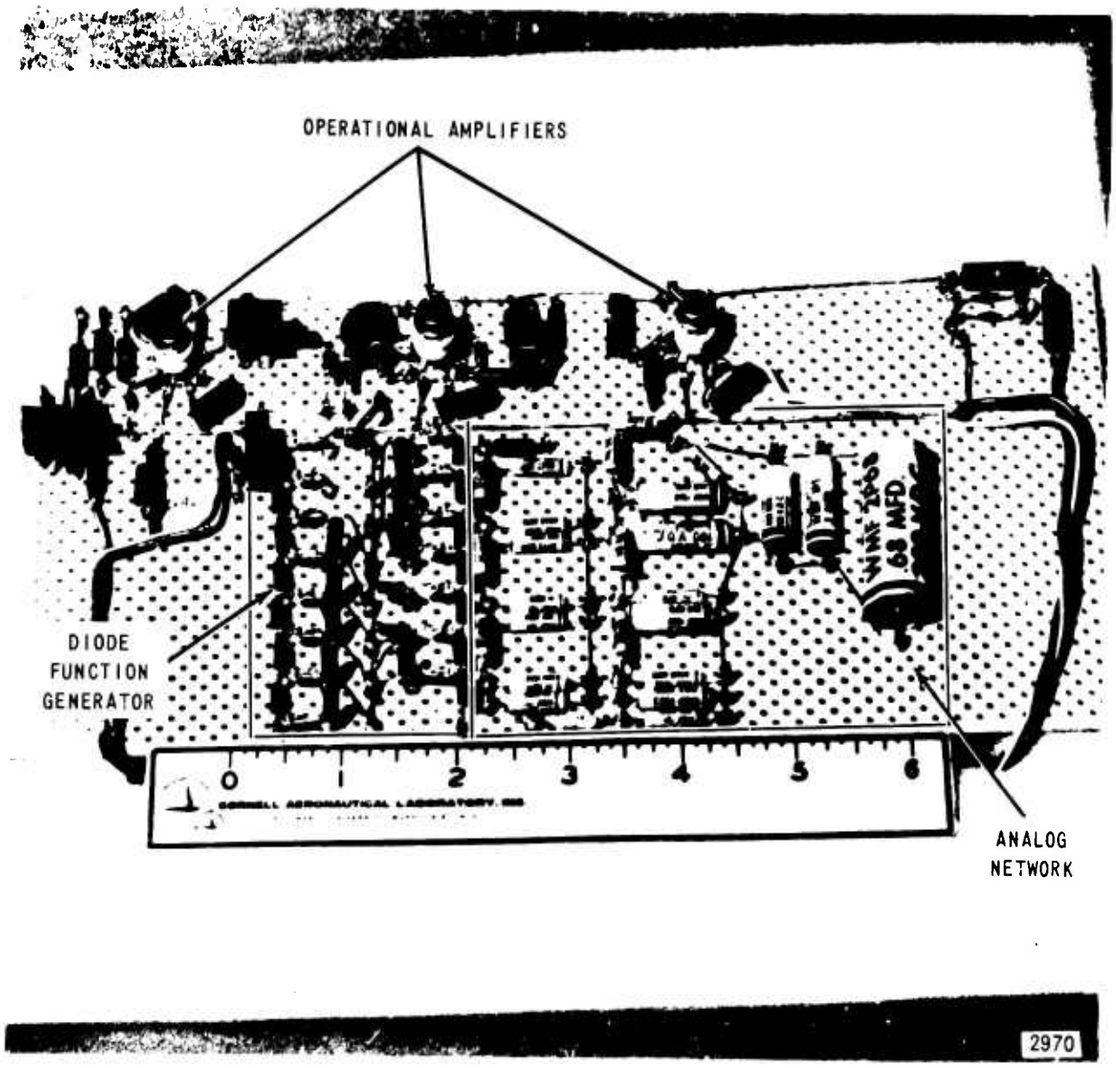

Figure 5 COMPENSATED ANALOG CIRCUIT BREADBOARD MODEL

APPENDIX A

1. INTRODUCTION

Solutions to the nonlinear heat diffusion equation were obtained in the COMCOR analog computer in terms of the incident heat transfer rates corresponding to specified substrate surface temperature histories. Basically, the primary input has been a parabolic function with lesser emphasis on ramp and step type inputs. Perturbations to these basic functions were added to simulate such factors as noise, gage abrasion, and tunnel starting phenomena.

Temperature excursions of the order of 1000°F were used to ascertain the full effects of variations in substrate properties on the computed heat flux. These effects are quantitatively illustrated by obtaining two separate solutions for the trial case, one with the substrate properties held constant and one with the properties permitted to vary with temperature. This procedure has been followed in all instances except for those unique situations where the principal objective was to demonstrate the relative changes in heat flux resulting from a modification in the input function. In these circumstances, it was felt that permitting the substrate properties to vary would only add unnecessary confusion.

Smoothing of the data by an electronic filter was provided as an option to demonstrate the efficiency of this technique when applied to various test situations.

Both the input temperature function and the resultant heat transfer rate were recorded by an x-y plotter on a single graph. Each record is annotated with a tabulation of the pertinent test variables. A total of 46 trial solutions were made. These are included in this appendix and identified as Run #1 through Run #46. The records are self-explanatory to a large degree, however, concise observations and comments of the various salient features of each record are given in the commentary that follows.

2. COMMENTS ON ANALOG COMPUTER RUNS*

Run #

1 Test conditions: parabolic temperature input with ΔT equal to 1000°F in 10 msec, initial temperature 70°F and substrate thermal properties assumed constant. Calculated heating rate, $\dot{q}$ is 652.2 BTU/ft^2 sec. Recorded trace shows slight "droop" in $\dot{q}$ level with time as a result of the finite number (and spacing) of substrate slabs used in programming the problem. Parabolic input is generated by a diode function generator and represents a composite of individual straight line segments. Scallop-effect on $\dot{q}$ signal arises from the segmented nature of the ΔT curve. Starting transient in $\dot{q}$ signal is solely attributable to the recording instrument dynamic characteristics.

* In all cases the temperatures used correspond to actual substrate values.

Run #

2 Test conditions: same as above with the exception that heat transfer gage substrate thermal properties are permitted to vary with temperature. Error in $\dot{q}$ resulting from assumption of constant substrate properties is seen to be negative and increases in amplitude with increasing temperature (at 10 msec $\dot{q}$ is approximately 87% of the proper value). Most rapid change in $\dot{q}$ (due to changes in substrate properties) occurs at the early portion of the record (for $\Delta T \propto t^{1/2}$) since the rate of change of temperature is greatest here.

3 Test conditions: same as #1 except that the temperature input signal has been processed through a quadratic filter* with a corner frequency of 5KHz and a damping factor of 0.7. Effect of the filter is relatively small and is evidenced by a rounding off of the scallop peaks in the $\dot{q}$ trace and a small time lag in both traces relative to both Run #1 and Run #2.

4 Test conditions: identical to above except that gage substrate properties are permitted to vary with temperature. Comments for Run #2 and Run #3 are appropriate.

5 Test conditions: same as #3 except for a change of filter corner frequency to 2.5 KHz. Filter effects are more pronounced: "scallop" amplitude well suppressed, $\dot{q}$ trace initial rise time still slower, time lags in temperature and $\dot{q}$ traces more obvious. Lag caused by filtering can be detected by noting temperature amplitude at some fixed time (see tabulation below):

time	temp., °F	filter
0.5 msec	297	out
0.5 msec	287	5 KHz, $\phi = 0.7$
0.5 msec	275	2.5 KHz, $\phi = 0.7$

A second $\dot{q}$ trace was recorded with the filter damping factor changed to 1.0 (critical damping). Whereas the rise time** has been considerably slowed, the time required to settle at the ultimate steady-state amplitude is the same but without the attendant overshoot. Consequently, for all succeeding cases employing filtering, $\phi = 1.0$.

---

* A quadratic filter is characterized by a transfer function of the following form:

$$e_o/e_1 = \frac{s^2}{s^2 + 2\phi\omega_o s + \omega_o^2}$$ where s is the complex frequency, $j\omega$, ω_o is the corner frequency, and ϕ is the damping factor.

** Rise time, in the sense used here, refers to the time required for the signal to first attain the amplitude of the final steady level.

Run #

6 Test conditions: same as above with substrate properties variable with temperature. Note increase in time lag in temperature trace (relative to Run #5) resulting from the change in the damping factor, ϕ, from 0.7 to 1.0 (at 0.5 msec temperature is now approximately 262°F). Except for the transient portions of the record and the presence of time lags, $\dot{q}$ amplitudes are not affected by the filtering employed.

7 Test conditions: same as Run #1 with the addition of random noise to the temperature signal. Despite the random nature of the noise, this particular 10 msec segment of noise could be faithfully reproduced (in both a time and amplitude relationship). This capability was necessitated since separate computer runs were required to acquire first the temperature trace and then the $\dot{q}$ trace on the x-y plotter. With the noise input reproducible, there is a direct correspondence of the noise components on the two traces. The high level of sensitivity of the $\dot{q}$ signal to fluctuations in temperature is dramatically illustrated.

8 Test condition: same as above with the temperature signal processed through a 2.5 KHz filter.

9 Test conditions: same as above with filter corner frequency changed to 5 KHz. The desirability of filtering the temperature signal is amply demonstrated by the results shown in this record and the preceding one.

10 Test conditions: temperature input a 50°F step of 1 msec duration intersecting a parabolic temperature trace having a vertex at 70°F. This input function is designed to simulate a possible type of tunnel starting phenomena. With a step temperature change, the corresponding $\dot{q}$ varies inversely with the square root of time as shown in the first msec of the record. The recovery of the $\dot{q}$ trace after 1 msec appears slow (despite the absence of filtering) because the parabola is intersected at a point ($\sim$ 120°F) where its time derivative is much smaller than it is at the vertex where it is infinite. Since $\dot{q}$ is approximately related to the temperature derivative, its rate of rise to the final level is less rapid than had the parabolic function been intersected at the vertex. The final value of $\dot{q}$ is not affected by the presence of the 1 msec duration step (compare with Run #1), however, the time to reach steady state is approximately 4 msec compared to a few tenths msec for the equivalent case of Run #1.

11 Test conditions: same as above with the substrate properties permitted to vary with temperature. Comments as above apply.

12 Test conditions: same as Run #10 with the temperature signal processed through a 5 KHz filter. The leading edge of the step input is now rounded and the initial peak value of $\dot{q}$ is greatly reduced. Time for $\dot{q}$ to attain steady state level is still approximately 4 msec and unaffected by filtering.

Run #

13 Test conditions: identical with above except filter corner frequency changed to 2.5 KHz.

14 Test conditions: identical with above with substrate properties permitted to vary with temperature.

15 Test conditions: temperature input comprises a 50°F step of unlimited duration with a parabolic temperature function superimposed at 1 msec (vertex of the parabola is at 120°F). This test is a variant of the simulated tunnel starting phenomenon explored in Run #10. The net $\dot{q}$ in this case is the sum of heat fluxes from a step temperature ($\dot{q} \propto t^{-1/2}$) and a parabolic temperature variation ($\dot{q}$ = a constant). Since the decay of $\dot{q}$ due to the step is very slow with time, the net $\dot{q}$ at 10 msec is still considerably in error* (672 Btu/ft^{2}sec compared with 652 Btu/ft^{2}sec without the step).

16 Test conditions: same as above with the temperature signal processed through a 2.5 KHz filter. Initial peak amplitudes of the transients are effectively reduced, however, the after portions of the traces remain unaffected ($\dot{q}$ @ 10 msec is still $\sim$ 672 Btu/ft^{2}sec).

17 Test conditions: identical with above except for addition of random noise.

18 Test conditions: basic parabolic temperature input as in first test (Run #1) except for the addition of sinusoidal noise (10 KHz).

19 Test conditions: as above with temperature input processed through a 2.5 KHz filter.

20 Test conditions: identical with Run #18 except that substrate properties are permitted to vary with temperature.

21 Test conditions: same as above with temperature input processed through a 2.5 KHz filter**.

22 Test conditions: temperature input consists of a 50°F temperature step of unlimited duration with a parabolic function superimposed at time zero (vertex of the parabola is at 120°F). This test is a variant of Run #15 and as in the previous case $\dot{q}$ is the sum of heat fluxes corresponding to the step and parabolic components of the input. Amplitude-time coordinates for Runs #15 and #22 are seen to be very similar except for the initial portions of the record ($t \leq 2$ msec).

---

* It is presumed that only the $\dot{q}$ associated with the parabolic component of the temperature function is sought.

** Starting with this run a new batch of coordinate paper was used on the x-y plotter and had somewhat different grid dimensions from the initial batch. Note that run duration now appears to be 9.9 msec rather than 10 msec.

Run #

23 Test conditions: identical with above with input temperature signal conditioned by 2.5 KHz filter. Except for initial transient amplitude and time lag, $\dot{q}$ signal is the same as for above test case.

24 Test conditions: identical with above with the exception that the amplitude of the step component of the input signal has been reduced by one half to 25°F. Comparison of $\dot{q}$ traces from Run 23 and Run 24 shows that the $\dot{q}$ component resulting from the step input has been reduced by one half.

25 Test conditions: same as above except for removal of 2.5 KHz filter. As demonstrated by many previous test cases, the filter is only effective in modifying the early portions of the test records and is completely ineffective at later test times (presuming transients occur only at times near zero).

26 Test conditions: parabolic temperature input(vertex at 70°F) with a 50°F step superimposed at 2 msec. This test simulates the result of a particle striking a heat transfer gage and causing a permanent change in gage resistance corresponding to a 50°F change in surface temperature. The slow characteristic decay in $\dot{q}$ with time (for step temperature input) produces a sizable error in $\dot{q}$ at 9-10 msec.

27 Test conditions: identical with above except that the input temperature signal is conditioned by a 2.5 KHz filter.

28 Test conditions: parabolic temperature input (vertex at 70°F) with 50°F steps superimposed at 2 msec and 5 msec. As in Run #26, this test simulates gage damage by particle impact. The heat flux components resulting from the steps are additive so that the absolute incremental error in $\dot{q}$ is about twice as large (at 10 msec) as for Run #26.

29 Test conditions: identical with above except that the temperature signal is conditioned by a 2.5 KHz filter.

30 Test conditions: identical with Run #28 except that the amplitude of the step temperature change is 25°F. Since $\dot{q}$ corresponding to a step temperature changes extremely slowly after the initial few milliseconds, for the particular temperature record used here the net $\dot{q}$ increment at 10 msec represents approximately equal increments from each step. Thus, the $\dot{q}$ error increment at 10 msec (Run #30) resulting from two 25°F steps is approximately equal to that caused by a single 50°F step (Run #26).

31 Test conditions: as above with the temperature input signal conditioned by a 2.5 KHz filter.

Run #

32 Test conditions: a 50°F step input (with origin at 70°F) conditioned by a 2.5 KHz filter. Addition of the filter was necessitated to prevent the analog computer from overload (saturation) as a result of the step input (note the change in ordinate scale for this run).

33 Test conditions: temperature input signal is a 50°F step (origin at 70°F) with a parabola (30°F rise in 10 msec*) superimposed starting at 1 msec. This test is a variation of Run #15 with the step as the dominant component rather than the parabolic temperature function. A condition is simulated wherein the starting phenomenon overshadows the convective heating due to the steady flow. Comparing Run #32 and Run #33 with the net $\dot{q}$ at 10 msec is about equally divided between the two components (step and parabola). The temperature input signal is conditioned by a 2.5 KHz filter.

34 Test conditions: identical with above except that the parabolic component of temperature has been changed to a rise of 60° in 10 msec.

35 Test conditions: parabolic temperature input function with a horizontal step of 0.5 msec duration superimposed at 2 msec. The characteristic variation of $\dot{q}$ with $t^{-1/2}$ for a constant temperature input is seen in the 2.0 to 2.5 msec interval. A rather slow recovery of the $\dot{q}$ trace follows. This slow recovery occurs for the same reason given in the comments for Run #10. The error component resulting from a horizontal step is seen to be negative and persists for the entire run although decreasing slowly with time. The horizontal step is sometimes observed in shock tunnel test records. Reasons for its occurrence are not known.

36 Test conditions: identical with above except that the temperature input is conditioned by a 2.5 KHz filter.

37 Test conditions: parabolic temperature input function with two horizontal steps of 0.5 msec duration superimposed; one at 2 msec and the other 5 msec. It is interesting to compare the $\dot{q}$ traces for Run #37 with Run #29. In the latter case, the perturbation in $\dot{q}$ corresponding to each of the two vertical steps in temperature is identical whereas in the former case the $\dot{q}$ disturbances corresponding to the two horizontal steps in the temperature function are of different magnitude (although of the same general shape). The reasons for this behavior are to be found in the comments for Run #10. As stated therein, to a crude approximation, the $\dot{q}$ signal is dependent on the slope (time derivative) of the temperature function. In a region of sudden temperature change (such as a vertical or horizontal step) the changes in the

*10 msec as measured from the origin of the parabola and not from t = 0 on the record.

Run #	
	$\dot{q}$ signal will be related to the relative changes in the slopes of the temperature signal. In the case of Run #10, the slope of the vertical step is infinite so that the $\dot{q}$ response is the same regardless of the slope of the parabola function at which the step is applied (that is, the $\dot{q}$ response is dominated by the step disturbance). In Run #37, the slope of the horizontal steps is zero, therefore, the slope of the parabolic function dominates the changes in the $\dot{q}$ signal. Since the slope of the parabola changes continuously with time, it follows the relative time position of the horizontal step will determine the corresponding $\dot{q}$ response. The relative effect of a horizontal step on the $\dot{q}$ signal decreases as the time at which the step is applied increases.
38	Test conditions: identical with above except that the temperature input function is conditioned by a 2.5 KHz filter.
39	Test conditions: parabolic temperature input function with a 0.25 msec horizontal step at 2 msec.
40	Test conditions: identical with above except that the temperature input function is conditioned by a 2.5 KHz filter.
41	Test conditions: a linearly increasing temperature input function with the origin at 70° and achieving an increase of 1000°F in 10 msec. For constant substrate properties, the $\dot{q}$ signal varies as $t^{1/2}$.
42	Test conditions: identical with above except substrate properties are permitted to vary with temperature. Because of the linear rate of increase of temperature, the $\dot{q}$ error (relative to the constant properties case above) increases continuously.
43	Test conditions: identical with Run #41 except that the temperature function is conditioned by a 2.5 KHz filter.
44	Test conditions: identical with above except that substrate properties are permitted to vary with temperature.
45	Test conditions: identical with Run #41 with random noise superimposed.
46	Test conditions: identical to above except that the temperature input signal is conditioned by a 2.5 KHz filter.

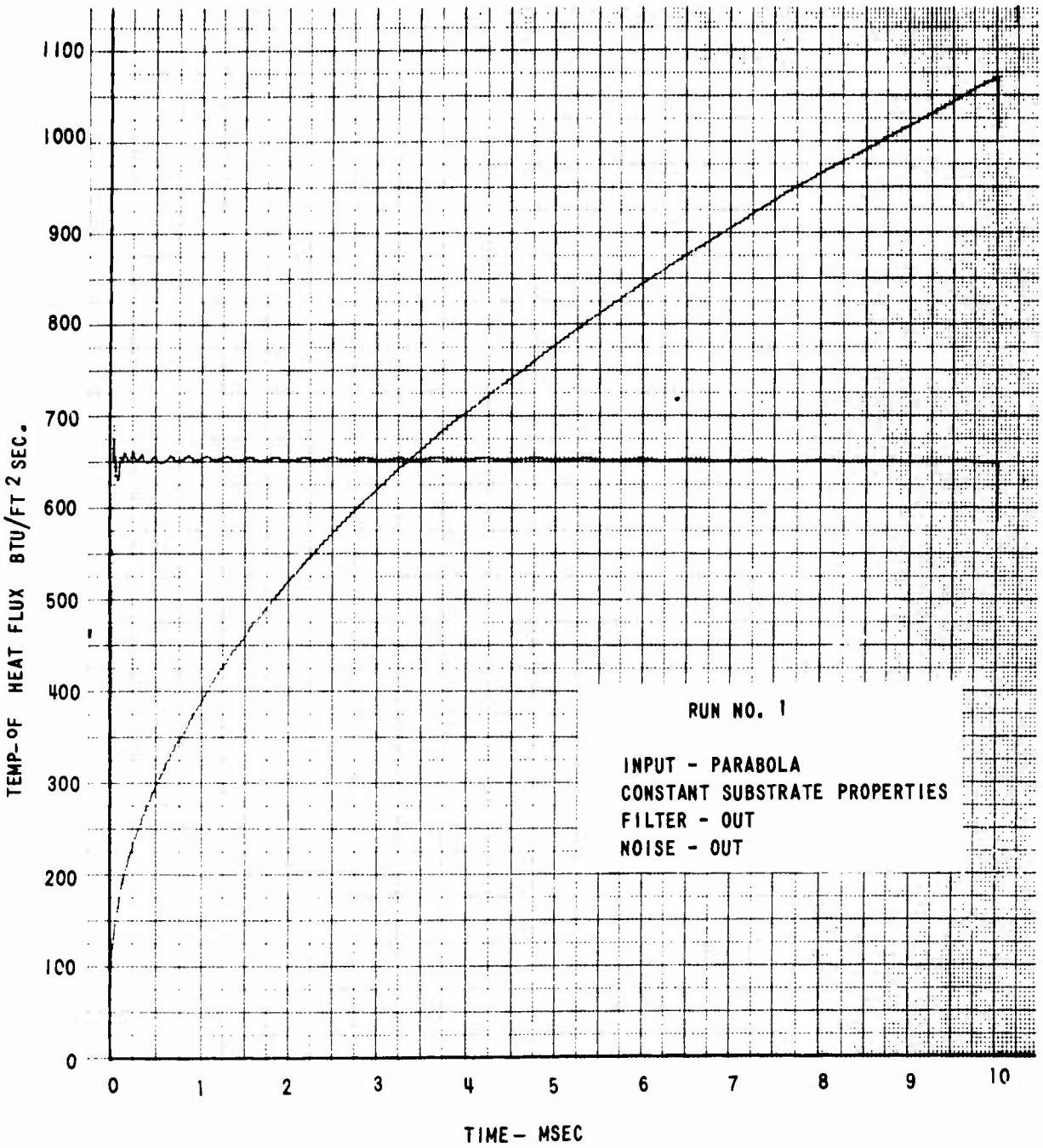
TEMP-OF HEAT FLUX BTU/FT 2 SEC.
1100
1000
900
800
700
600
500
400
300
200
100
0
0
1
2
3
4
5
6
7
8
9
10
TIME – MSEC
RUN NO. 1
INPUT - PARABOLA
CONSTANT SUBSTRATE PROPERTIES
FILTER - OUT
NOISE - OUT

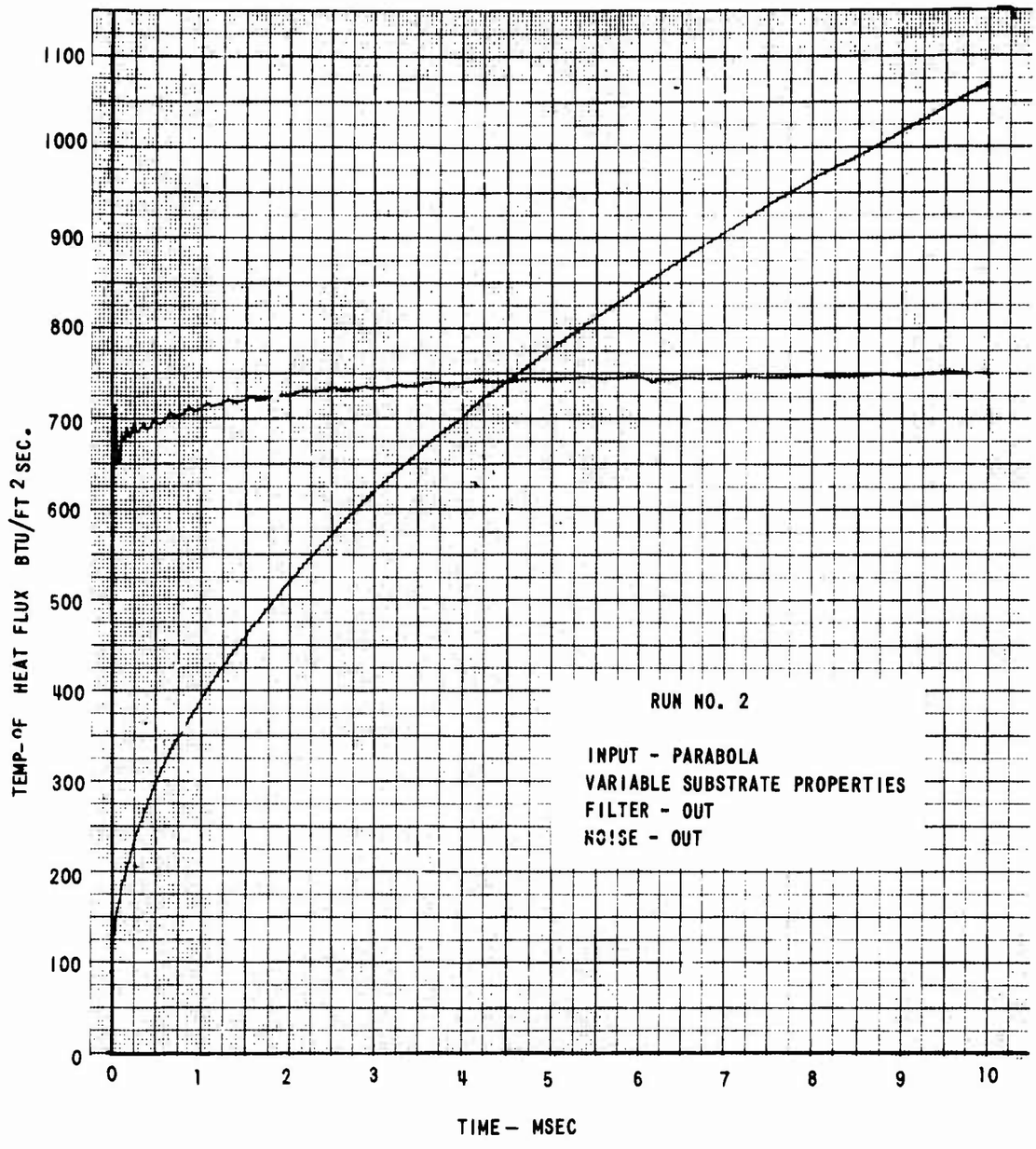
1100
1000
900
800
700
600
500
400
300
200
100
0
TEMP-°F HEAT FLUX BTU/FT 2 SEC.
0
1
2
3
4
5
6
7
8
9
10
TIME— MSEC
RUN NO. 2
INPUT - PARABOLA
VARIABLE SUBSTRATE PROPERTIES
FILTER - OUT
NOISE - OUT

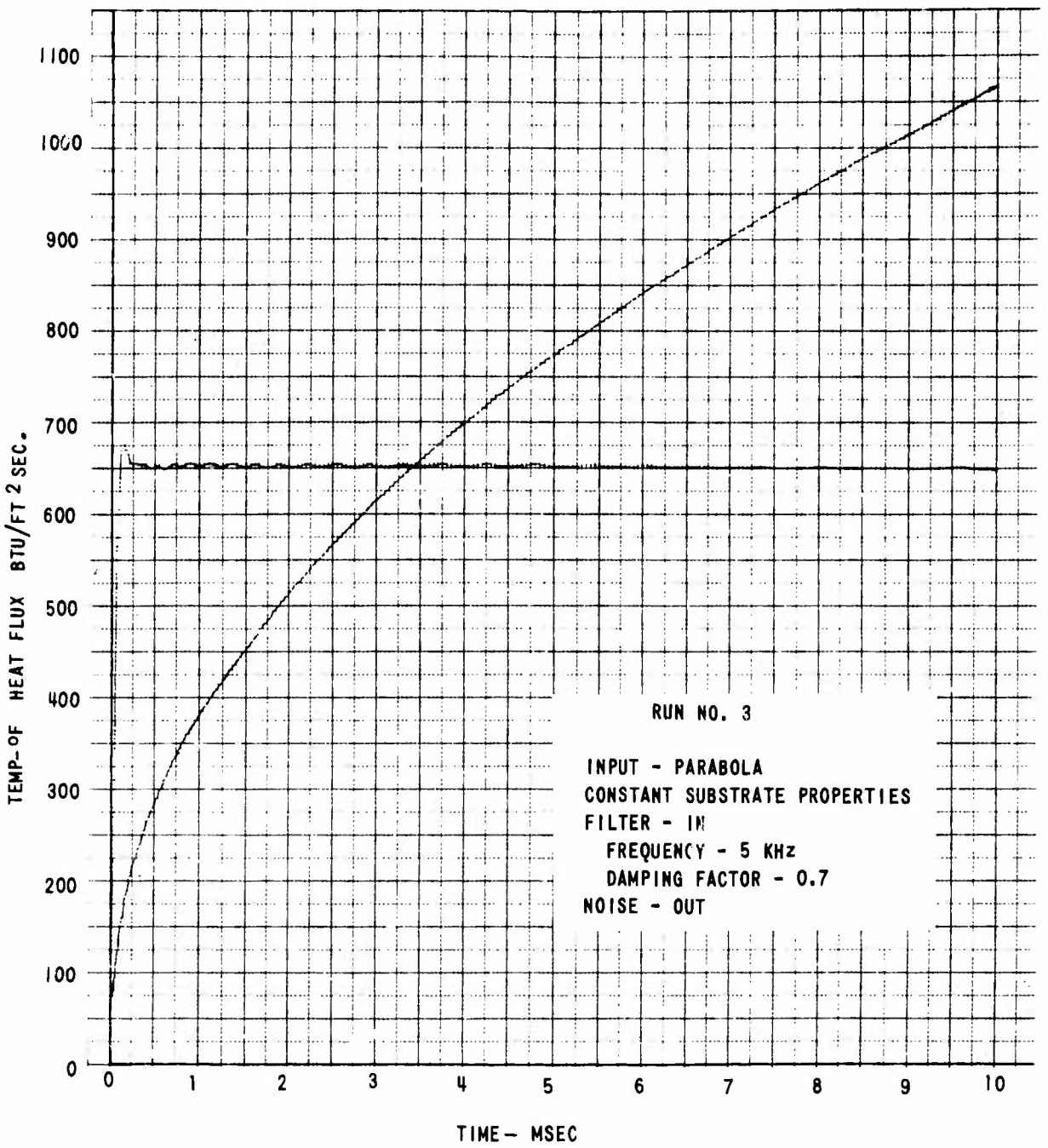
TEMP-OF HEAT FLUX BTU/FT 2 SEC.
1100
1000
900
800
700
600
500
400
300
200
100
0
0
1
2
3
4
5
6
7
8
9
10
TIME— MSEC
RUN NO. 3
INPUT - PARABOLA
CONSTANT SUBSTRATE PROPERTIES
FILTER - IN
FREQUENCY - 5 KHz
DAMPING FACTOR - 0.7
NOISE - OUT

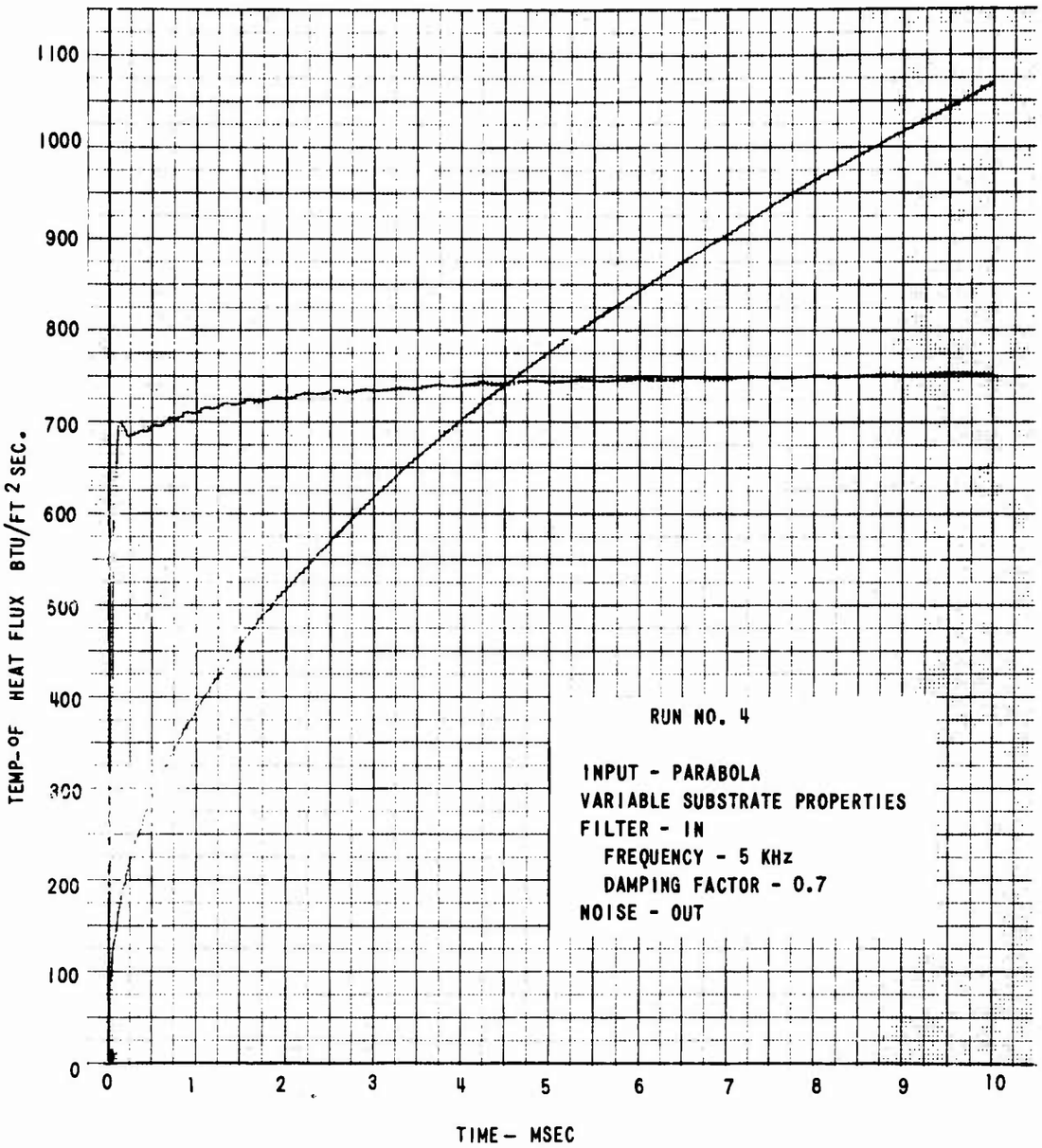
TEMP-°F HEAT FLUX BTU/FT 2 SEC.
1100
1000
900
800
700
600
500
400
300
200
100
0
0
1
2
3
4
5
6
7
8
9
10
TIME – MSEC
RUN NO. 4
INPUT - PARABOLA
VARIABLE SUBSTRATE PROPERTIES
FILTER - IN
FREQUENCY - 5 KHz
DAMPING FACTOR - 0.7
NOISE - OUT

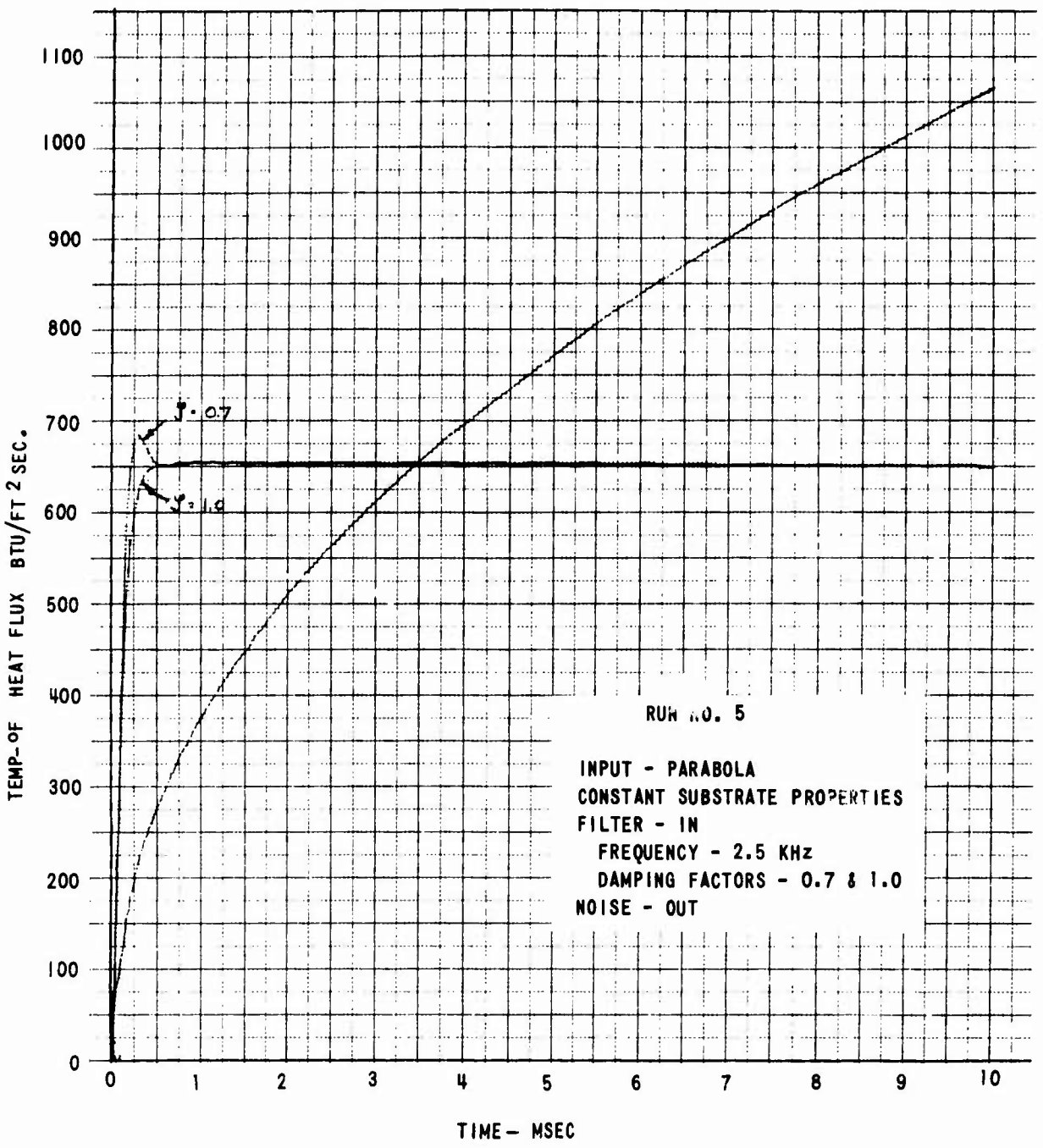
TEMP-OF HEAT FLUX BTU/FT 2 SEC.
1100
1000
900
800
700
600
500
400
300
200
100
0
0
1
2
3
4
5
6
7
8
9
10
TIME- MSEC
ζ = 0.7
ζ = 1.0
RUN NO. 5
INPUT - PARABOLA
CONSTANT SUBSTRATE PROPERTIES
FILTER - IN
FREQUENCY - 2.5 KHz
DAMPING FACTORS - 0.7 & 1.0
NOISE - OUT

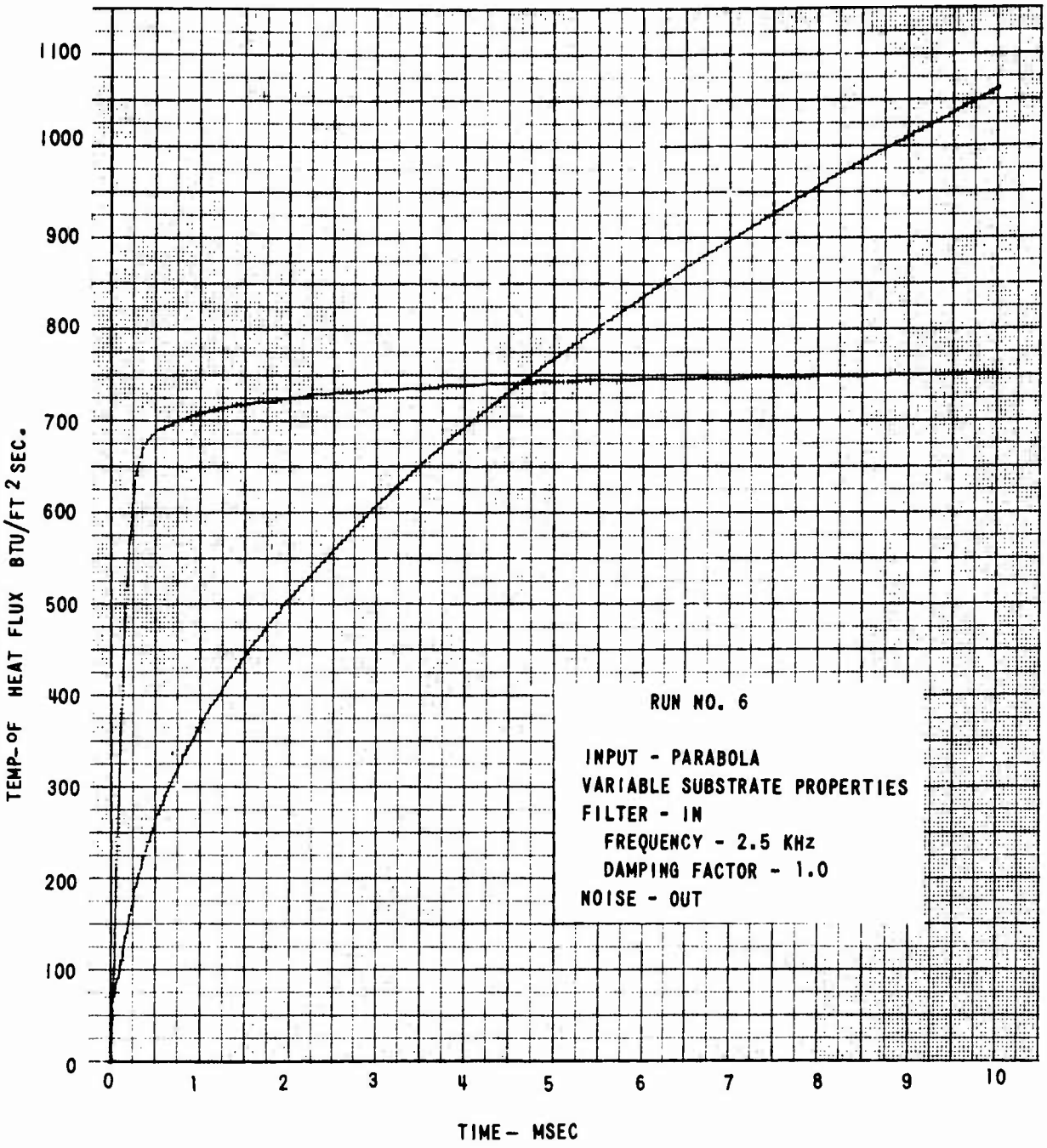
TEMP-°F HEAT FLUX BTU/FT 2 SEC.
1100
1000
900
800
700
600
500
400
300
200
100
0
0
1
2
3
4
5
6
7
8
9
10
TIME- MSEC
RUN NO. 6
INPUT - PARABOLA
VARIABLE SUBSTRATE PROPERTIES
FILTER - IN
FREQUENCY - 2.5 KHz
DAMPING FACTOR - 1.0
NOISE - OUT

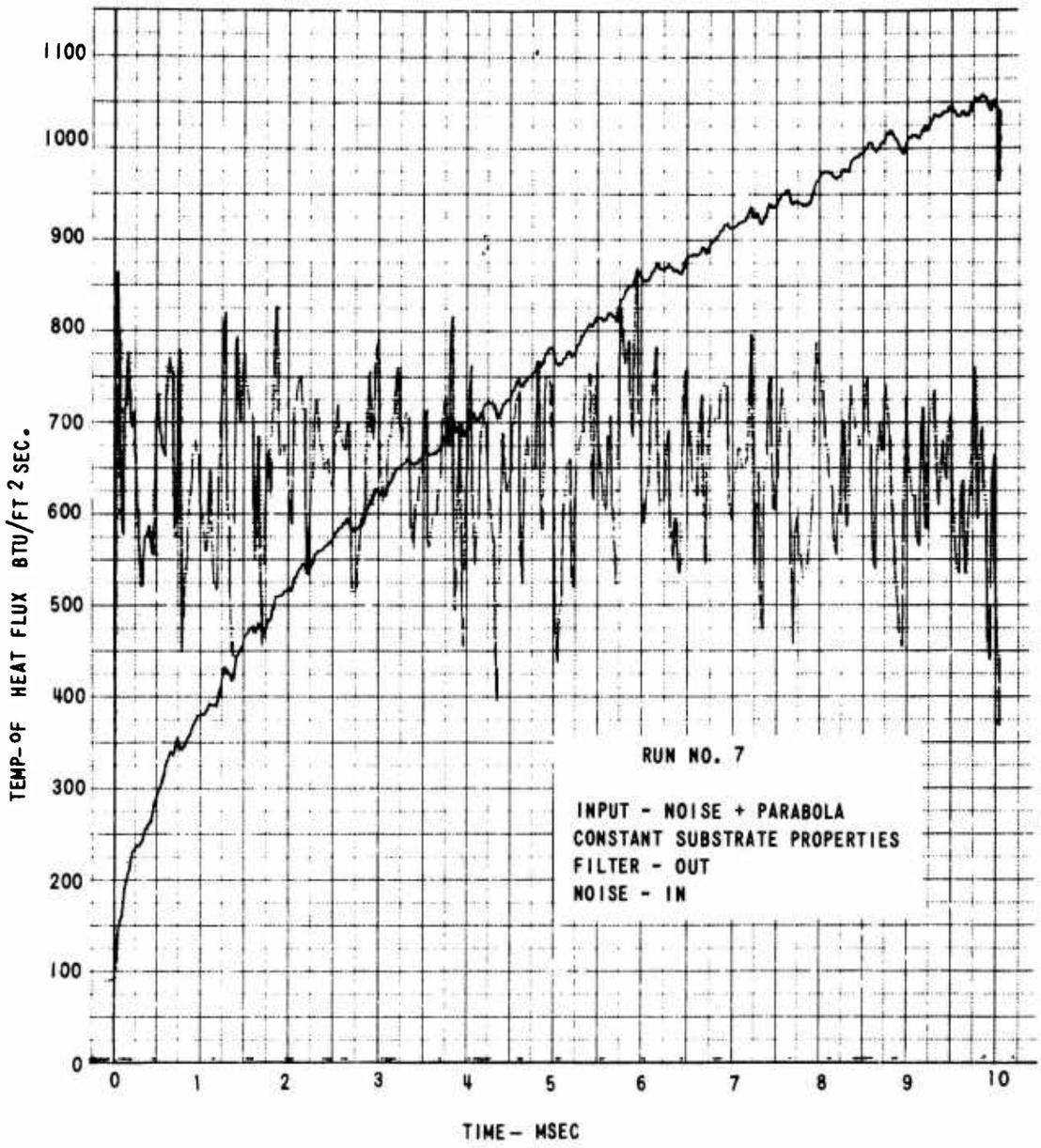
TEMP-OF HEAT FLUX BTU/FT 2 SEC.
1100
1000
900
800
700
600
500
400
300
200
100
0
0
1
2
3
4
5
6
7
8
9
10
TIME- MSEC
RUN NO. 7
INPUT - NOISE + PARABOLA
CONSTANT SUBSTRATE PROPERTIES
FILTER - OUT
NOISE - IN

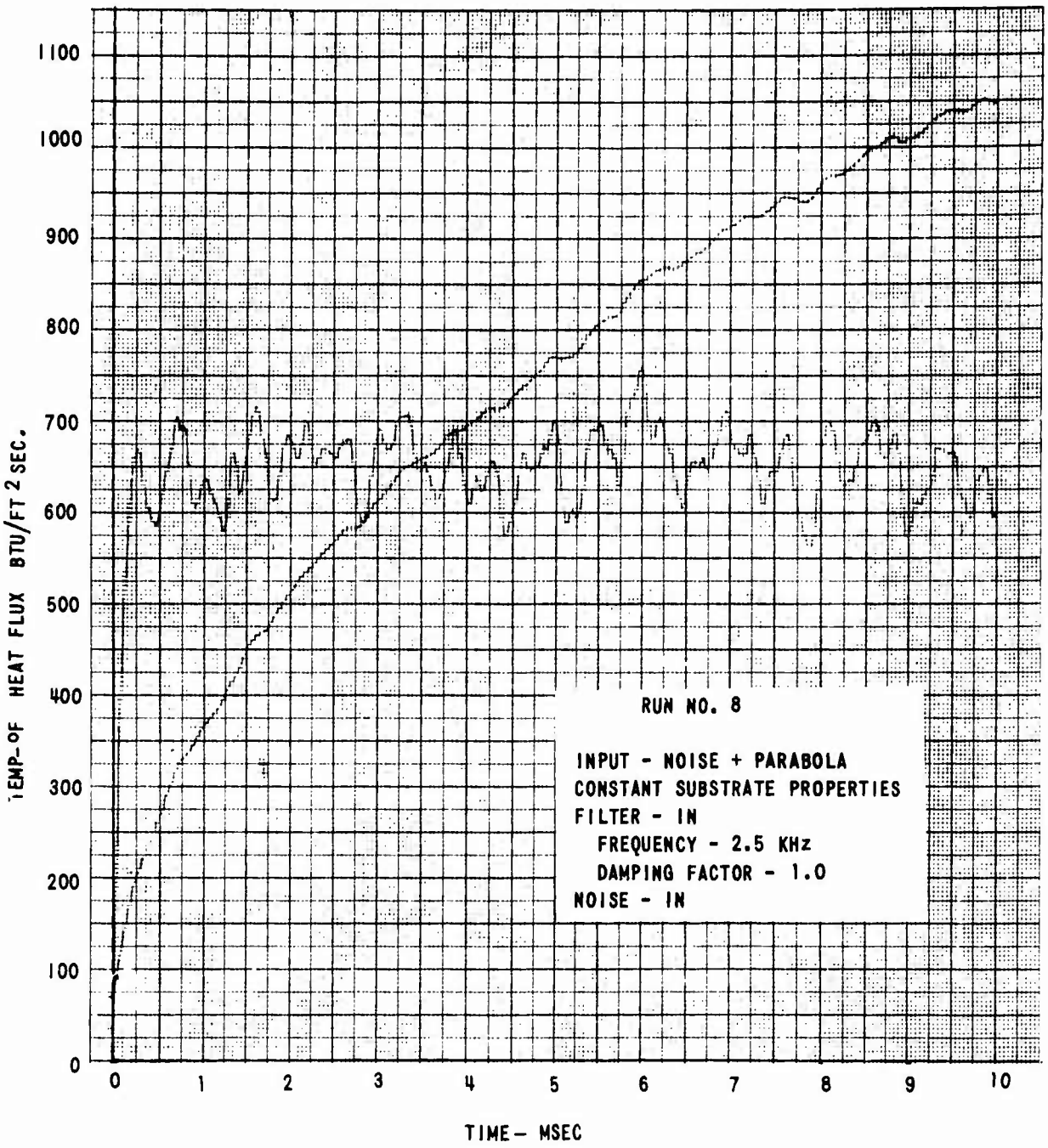
1100
1000
900
800
700
600
500
400
300
200
100
0
TEMP-OF HEAT FLUX BTU/FT 2 SEC.
0
1
2
3
4
5
6
7
8
9
10
TIME- MSEC
RUN NO. 8
INPUT - NOISE + PARABOLA
CONSTANT SUBSTRATE PROPERTIES
FILTER - IN
FREQUENCY - 2.5 KHz
DAMPING FACTOR - 1.0
NOISE - IN

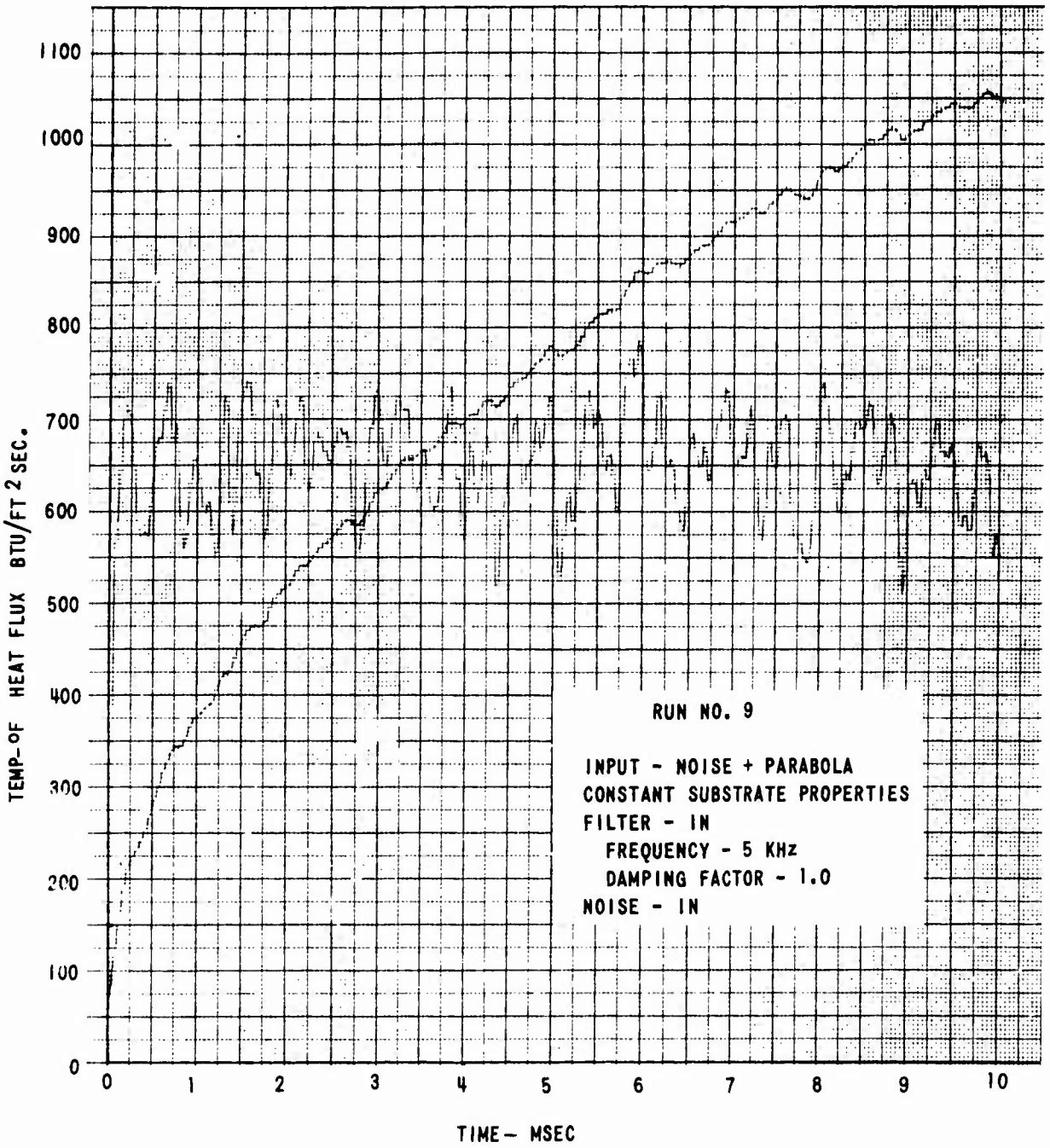
TEMP-OF HEAT FLUX BTU/FT 2 SEC.
1100
1000
900
800
700
600
500
400
300
200
100
0
0
1
2
3
4
5
6
7
8
9
10
TIME- MSEC
RUN NO. 9
INPUT - NOISE + PARABOLA
CONSTANT SUBSTRATE PROPERTIES
FILTER - IN
FREQUENCY - 5 KHz
DAMPING FACTOR - 1.0
NOISE - IN

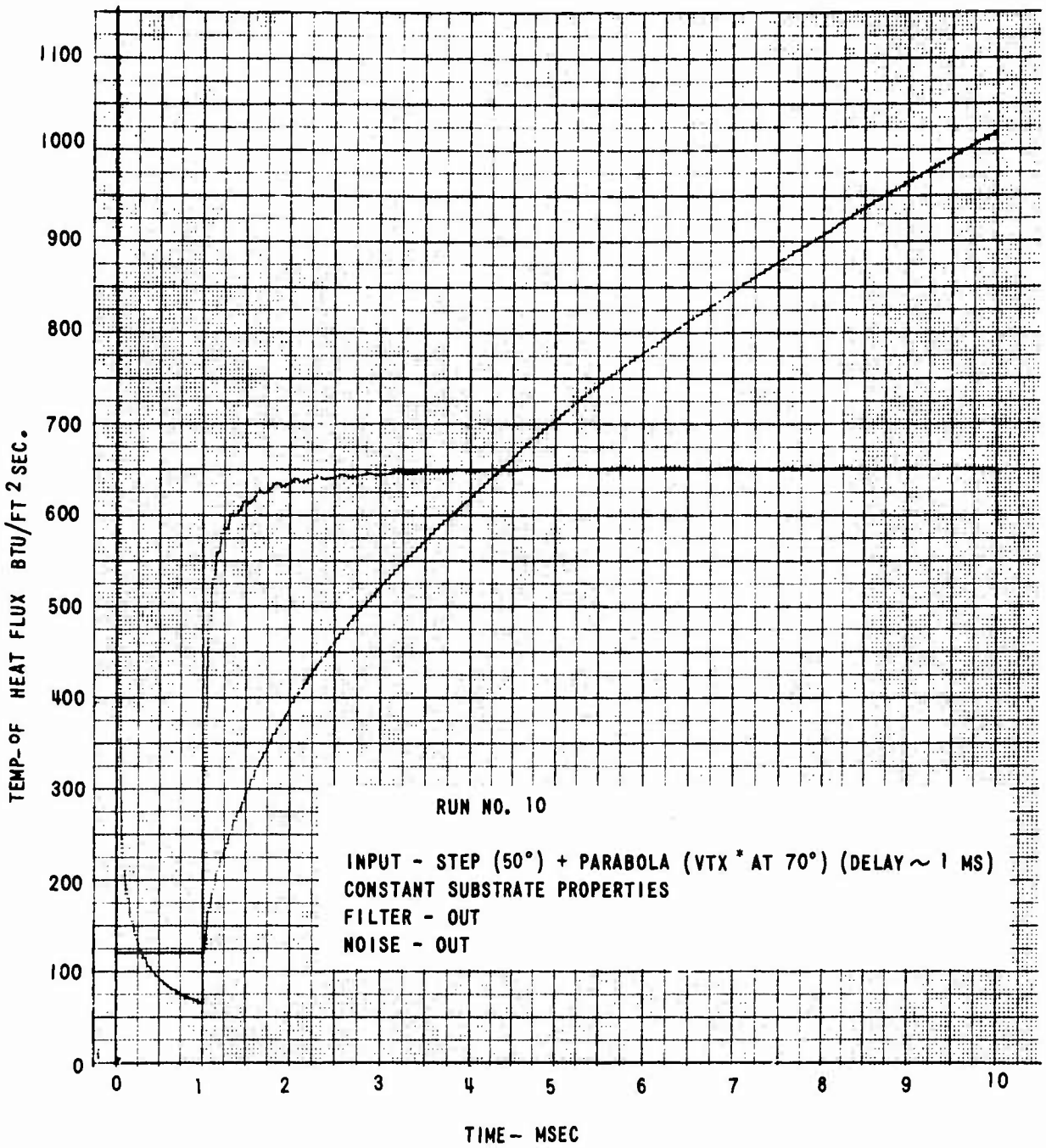
TEMP-°F HEAT FLUX BTU/FT 2 SEC.
1100
1000
900
800
700
600
500
400
300
200
100
0
0
1
2
3
4
5
6
7
8
9
10
TIME- MSEC
RUN NO. 10
INPUT - STEP (50°) + PARABOLA (VTX * AT 70°) (DELAY ~ 1 MS)
CONSTANT SUBSTRATE PROPERTIES
FILTER - OUT
NOISE - OUT

* VTX = VERTEX

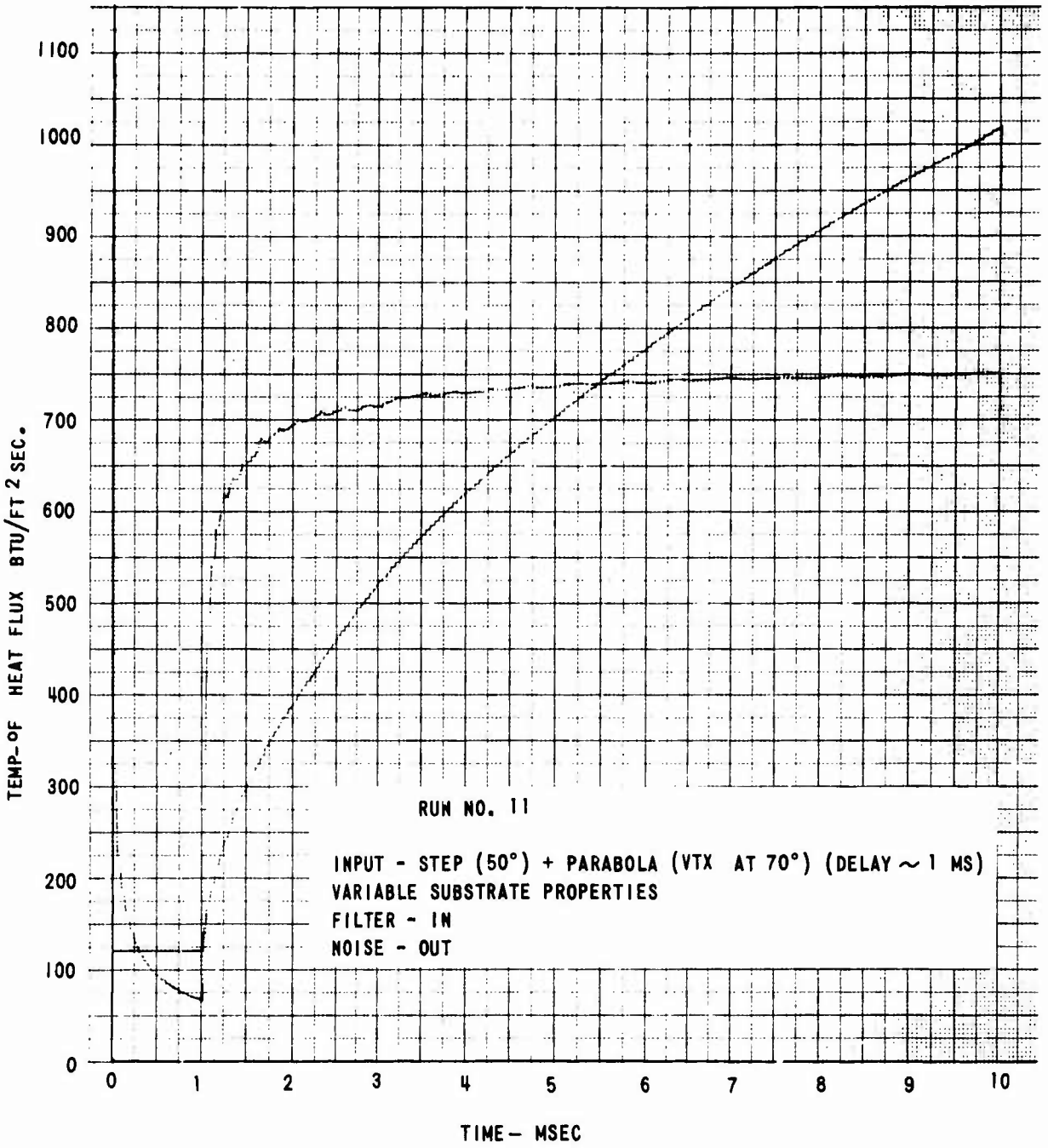
TEMP-OF HEAT FLUX BTU/FT 2 SEC.
1100
1000
900
800
700
600
500
400
300
200
100
0
0
1
2
3
4
5
6
7
8
9
10
TIME- MSEC
RUN NO. 11
INPUT - STEP (50°) + PARABOLA (VTX AT 70°) (DELAY ~ 1 MS)
VARIABLE SUBSTRATE PROPERTIES
FILTER - IN
NOISE - OUT

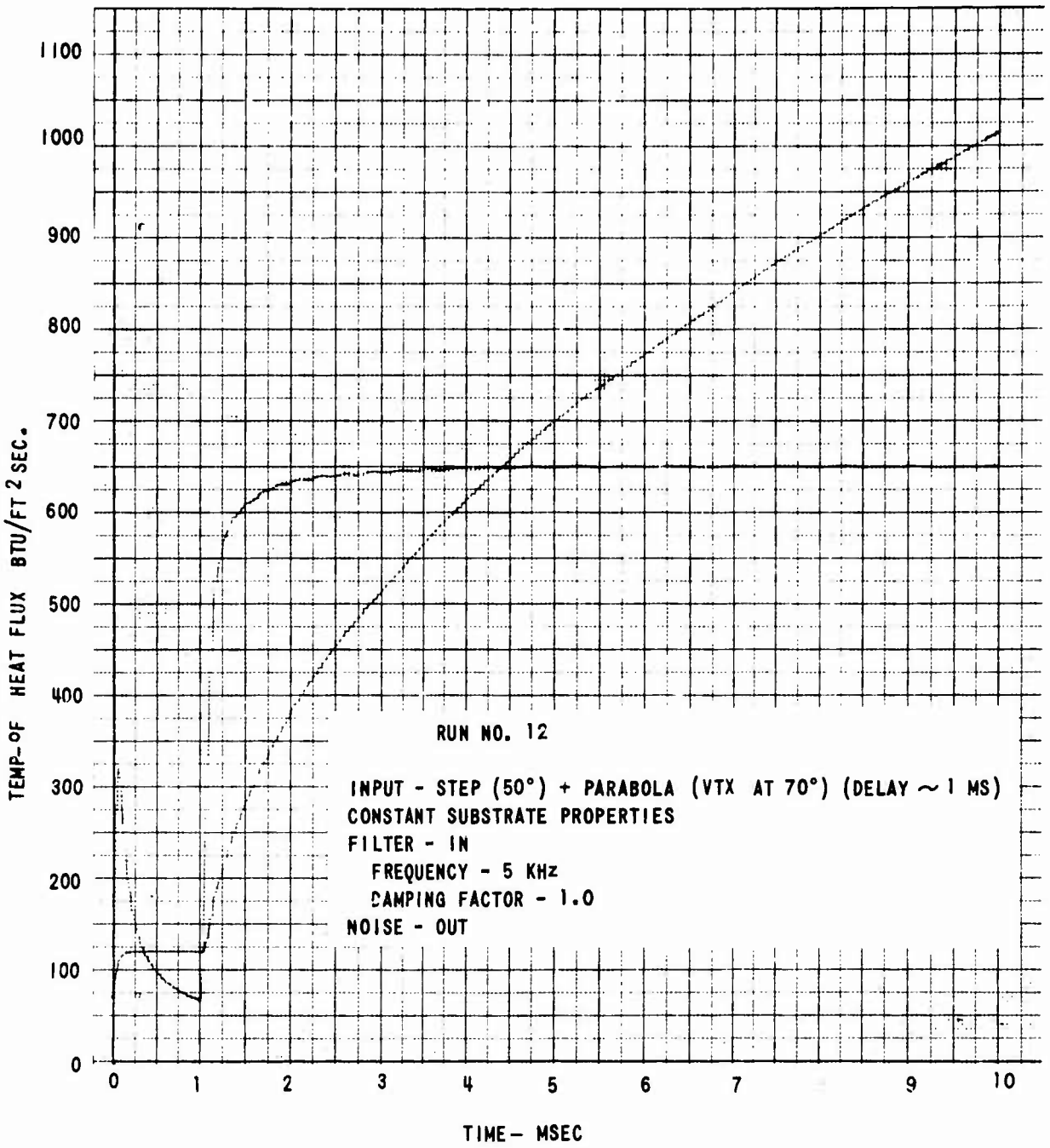
TEMP-OF HEAT FLUX BTU/FT 2 SEC.
1100
1000
900
800
700
600
500
400
300
200
100
0
0
1
2
3
4
5
6
7
9
10
TIME- MSEC
RUN NO. 12
INPUT - STEP (50°) + PARABOLA (VTX AT 70°) (DELAY ~ 1 MS)
CONSTANT SUBSTRATE PROPERTIES
FILTER - IN
FREQUENCY - 5 KHz
DAMPING FACTOR - 1.0
NOISE - OUT

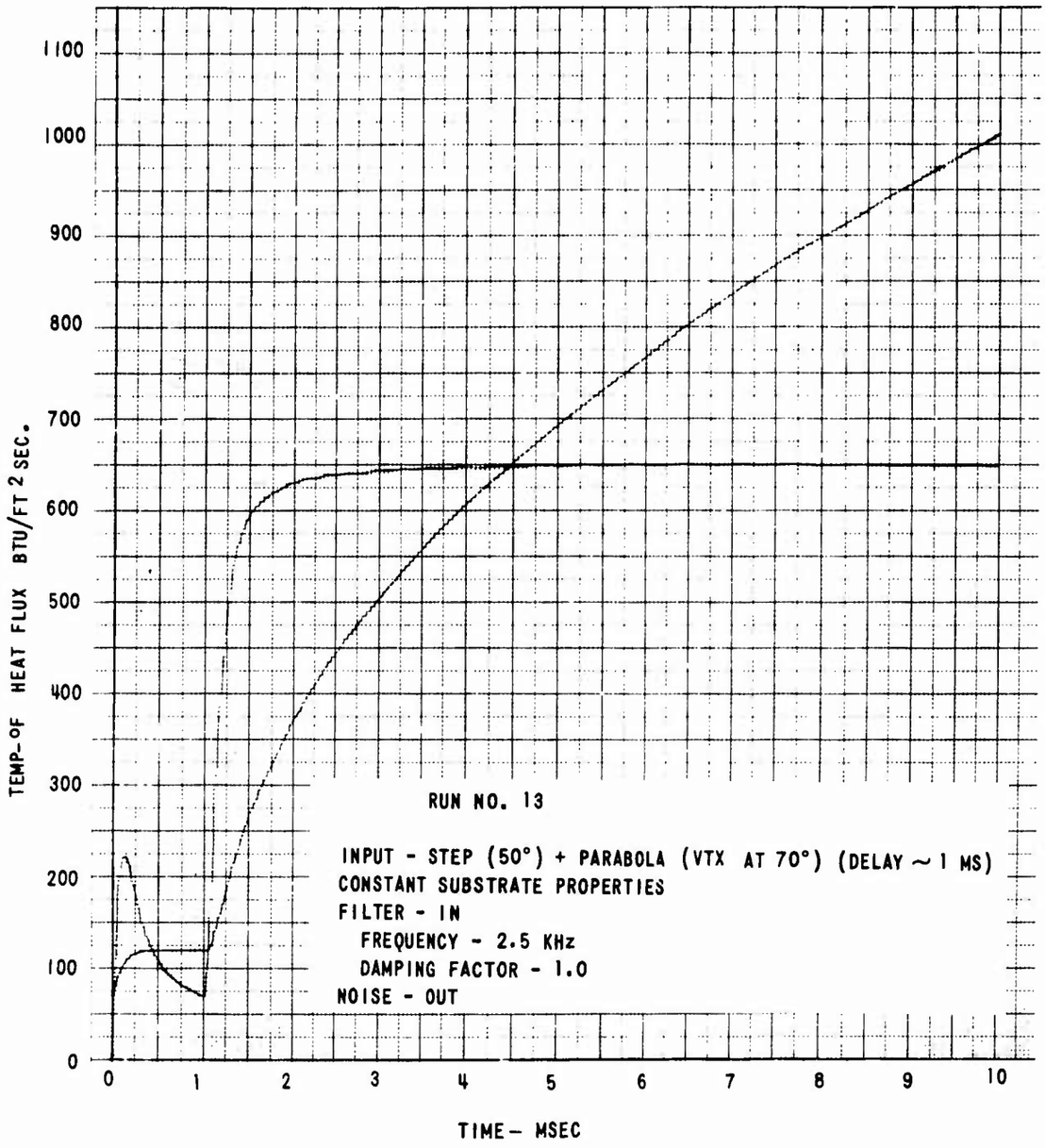
TEMP-OF HEAT FLUX BTU/FT 2 SEC.
1100
1000
900
800
700
600
500
400
300
200
100
0
0
1
2
3
4
5
6
7
8
9
10
TIME- MSEC
RUN NO. 13
INPUT - STEP (50°) + PARABOLA (VTX AT 70°) (DELAY ~ 1 MS)
CONSTANT SUBSTRATE PROPERTIES
FILTER - IN
FREQUENCY - 2.5 KHz
DAMPING FACTOR - 1.0
NOISE - OUT

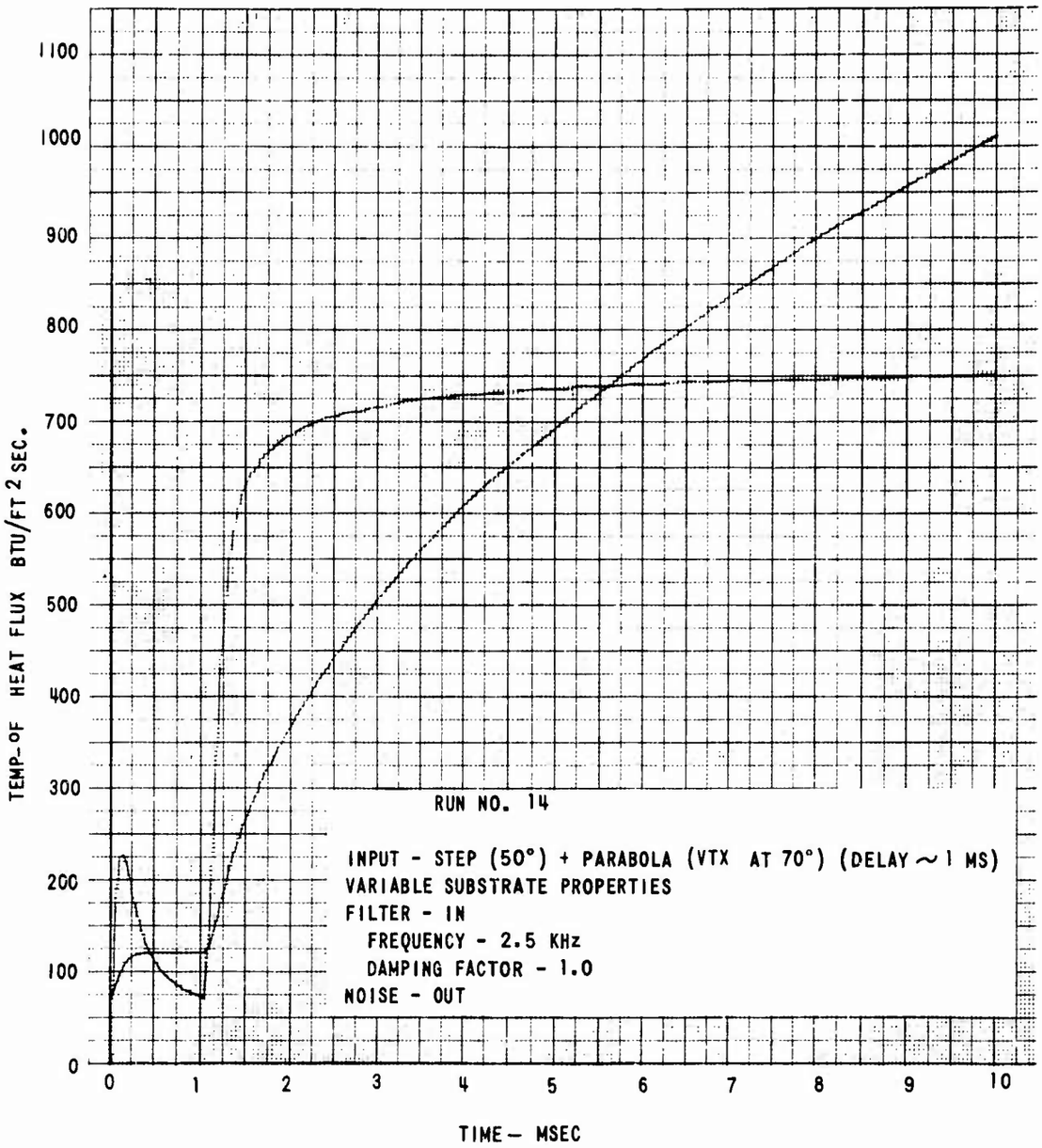
1100
1000
900
800
700
600
500
400
300
200
100
0
TEMP-OF HEAT FLUX BTU/FT 2 SEC.
0
1
2
3
4
5
6
7
8
9
10
TIME— MSEC
RUN NO. 14
INPUT - STEP (50°) + PARABOLA (VTX AT 70°) (DELAY ~ 1 MS)
VARIABLE SUBSTRATE PROPERTIES
FILTER - IN
FREQUENCY - 2.5 KHz
DAMPING FACTOR - 1.0
NOISE - OUT

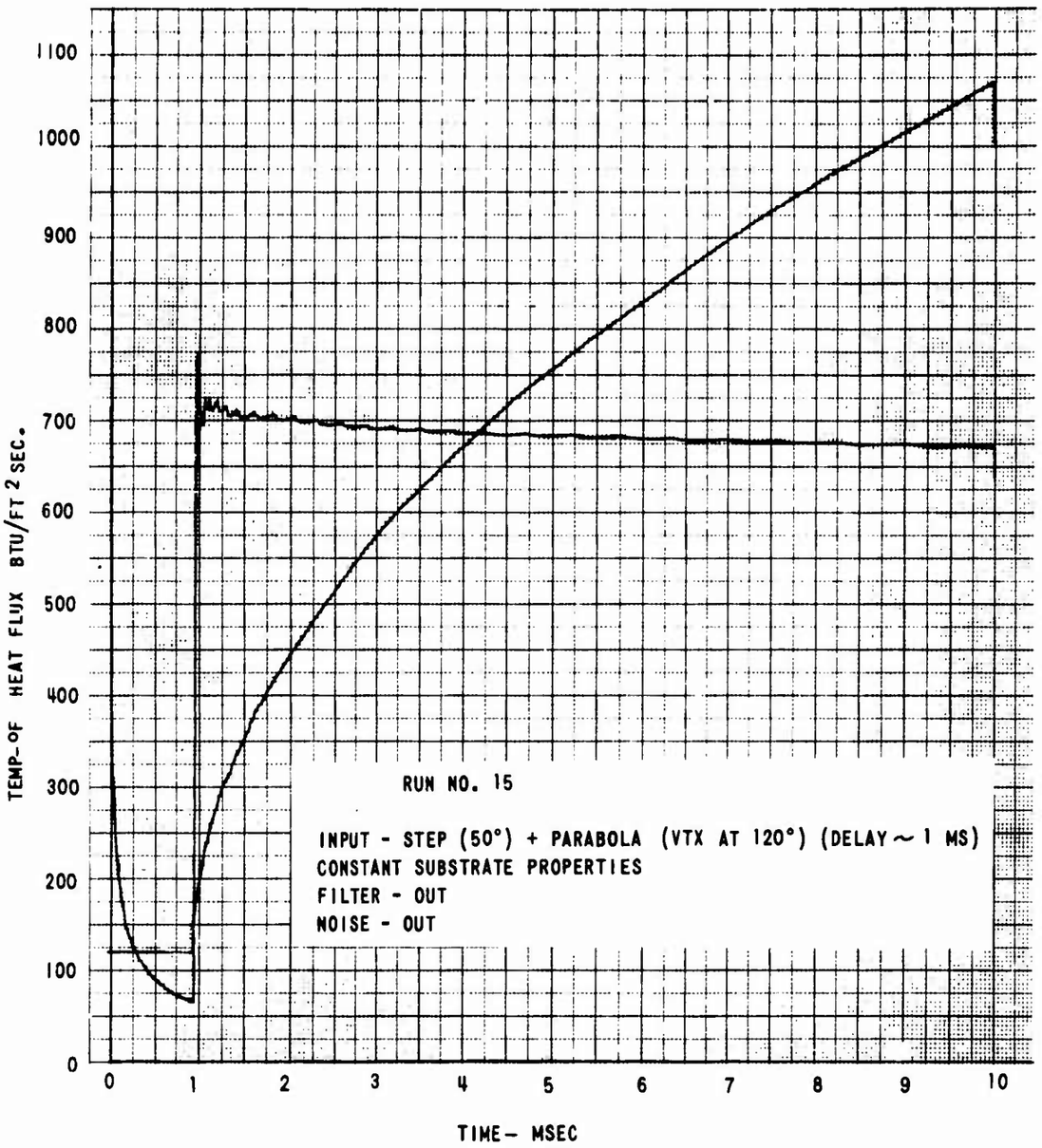
TEMP-OF HEAT FLUX BTU/FT 2 SEC.
1100
1000
900
800
700
600
500
400
300
200
100
0
0
1
2
3
4
5
6
7
8
9
10
TIME- MSEC
RUN NO. 15
INPUT - STEP (50°) + PARABOLA (VTX AT 120°) (DELAY ~ 1 MS)
CONSTANT SUBSTRATE PROPERTIES
FILTER - OUT
NOISE - OUT

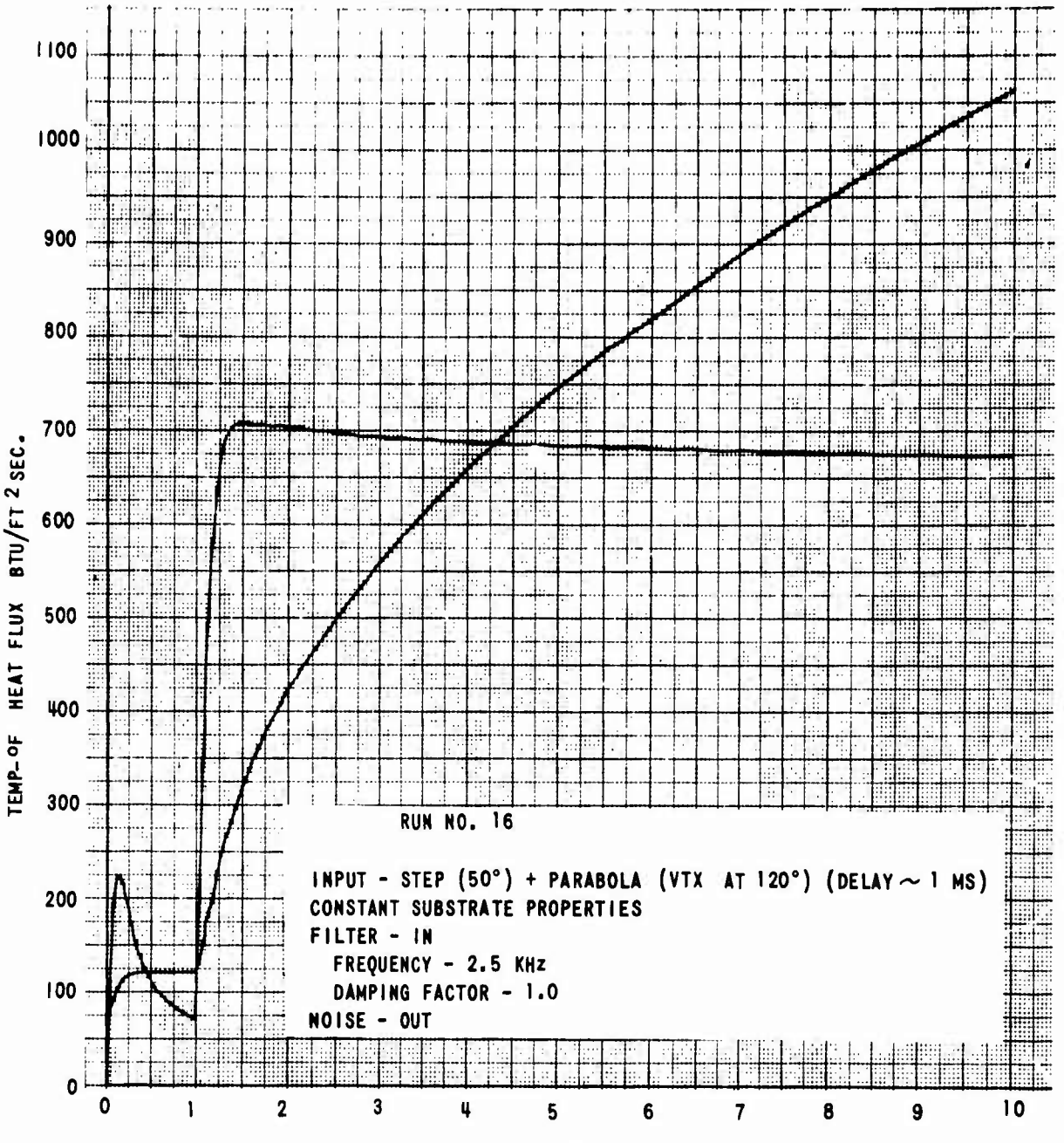
TEMP-OF HEAT FLUX BTU/FT 2 SEC.
1100
1000
900
800
700
600
500
400
300
200
100
0
0
1
2
3
4
5
6
7
8
9
10
TIME- MSEC
RUN NO. 16
INPUT - STEP (50°) + PARABOLA (VTX AT 120°) (DELAY ~ 1 MS)
CONSTANT SUBSTRATE PROPERTIES
FILTER - IN
FREQUENCY - 2.5 KHz
DAMPING FACTOR - 1.0
NOISE - OUT

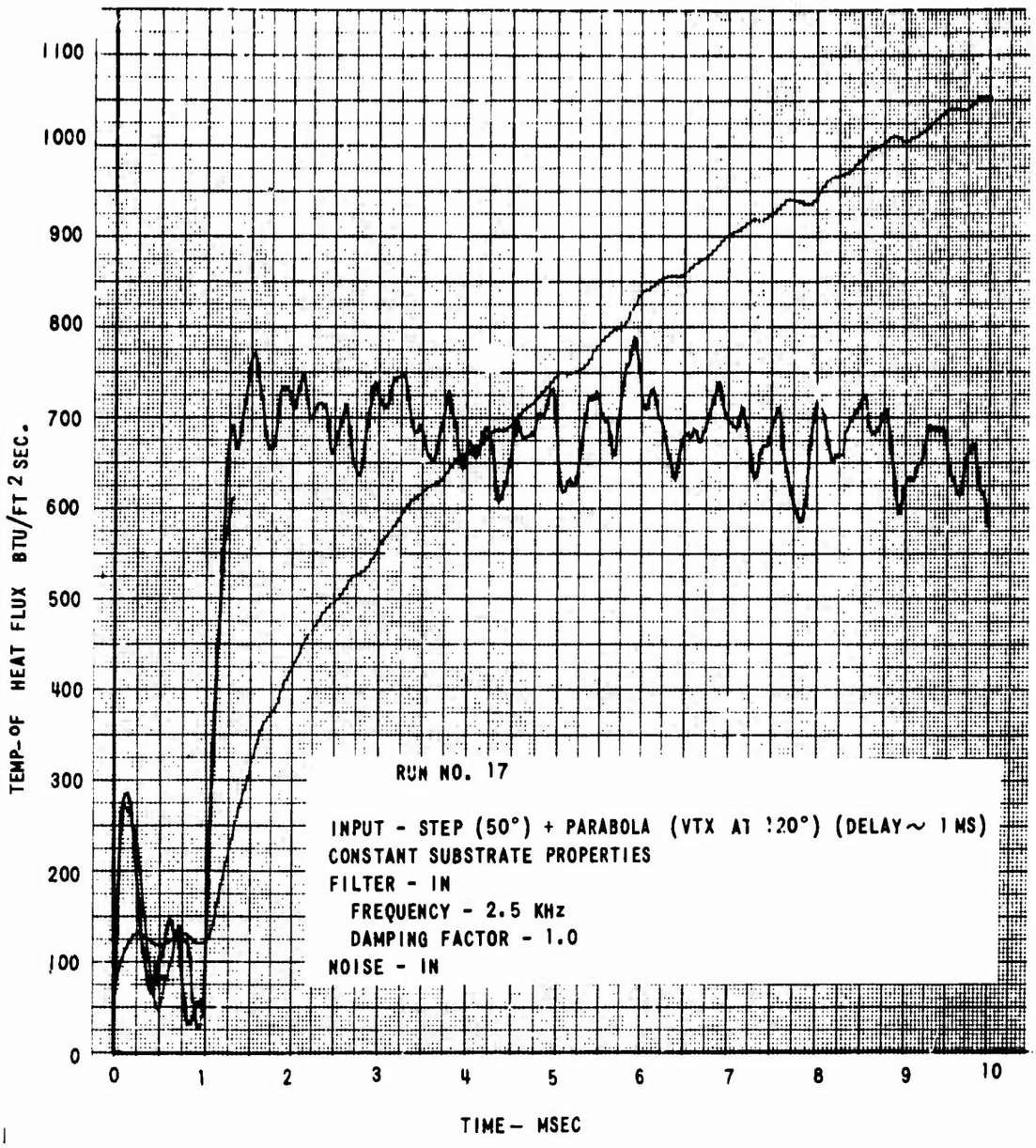
TEMP-OF HEAT FLUX BTU/FT 2 SEC.
1100
1000
900
800
700
600
500
400
300
200
100
0
0
1
2
3
4
5
6
7
8
9
10
TIME – MSEC
RUN NO. 17
INPUT - STEP (50°) + PARABOLA (VTX AT 120°) (DELAY ~ 1 MS)
CONSTANT SUBSTRATE PROPERTIES
FILTER - IN
FREQUENCY - 2.5 KHz
DAMPING FACTOR - 1.0
NOISE - IN

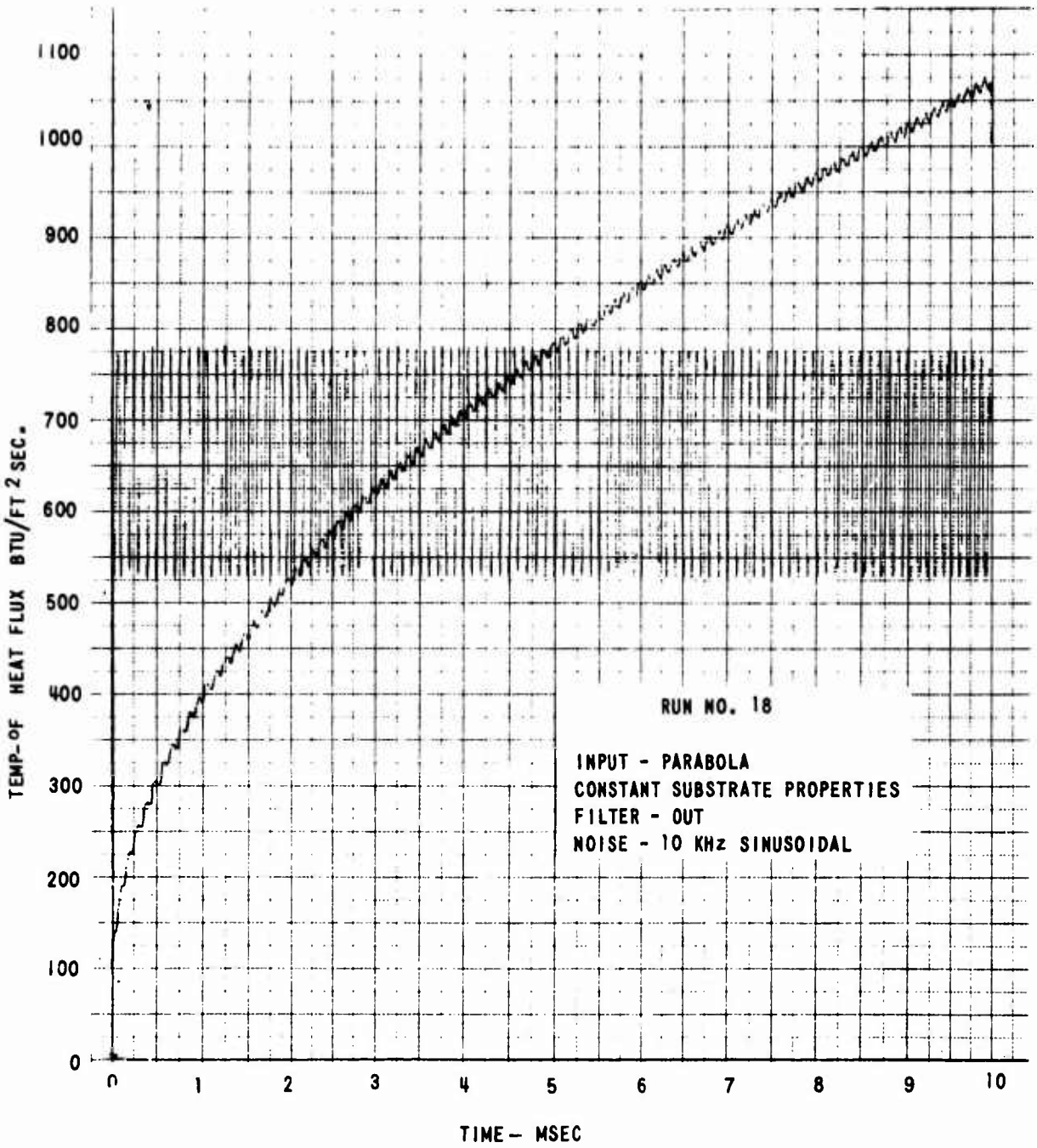
TEMP-OF HEAT FLUX BTU/FT 2 SEC.
1100
1000
900
800
700
600
500
400
300
200
100
0
0
1
2
3
4
5
6
7
8
9
10
TIME – MSEC
RUN NO. 18
INPUT - PARABOLA
CONSTANT SUBSTRATE PROPERTIES
FILTER - OUT
NOISE - 10 KHz SINUSOIDAL

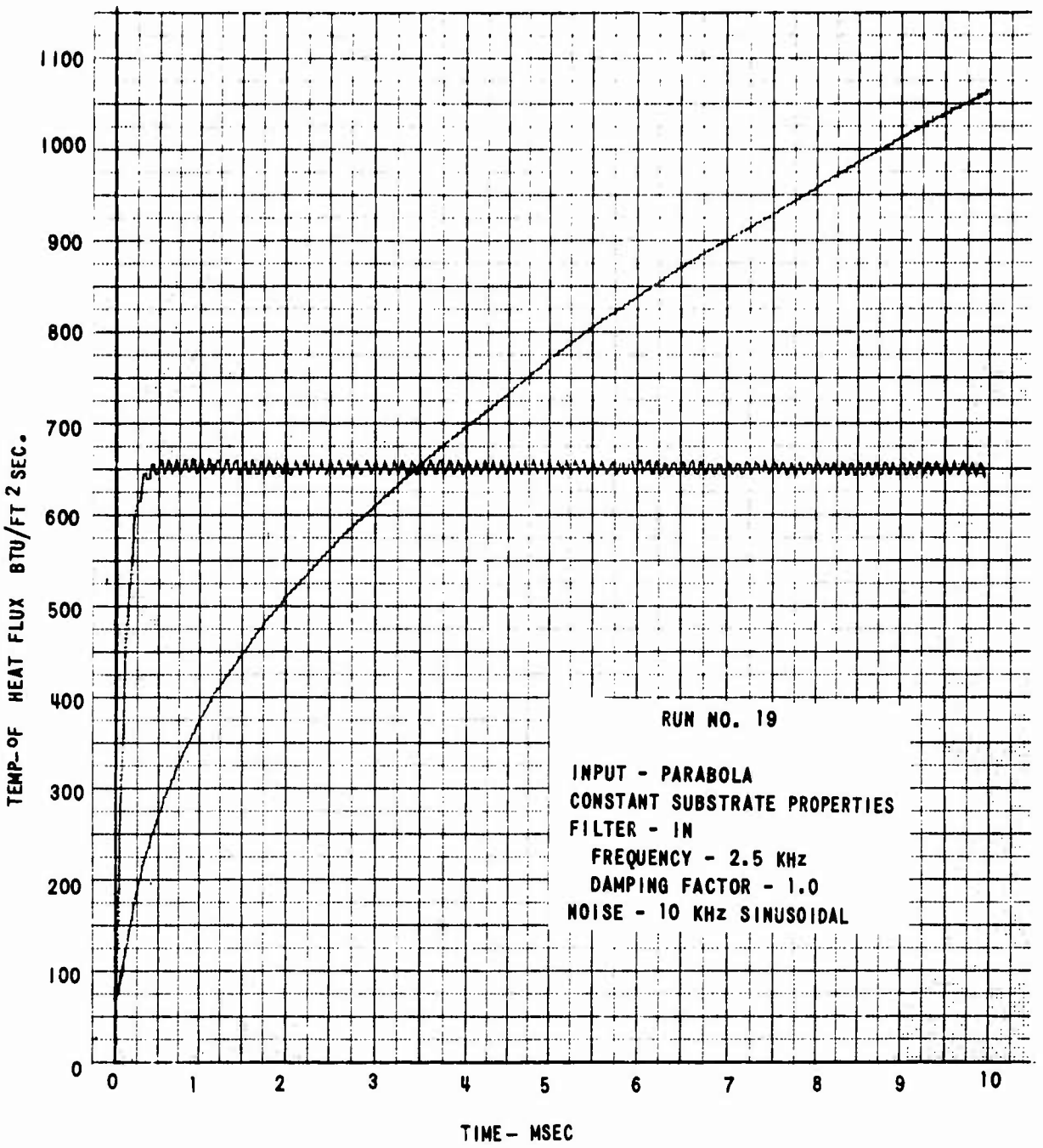
TEMP-OF
1100
1000
900
800
700
600
500
400
300
200
100
0
0
1
2
3
4
5
6
7
8
9
10
TIME- MSEC
OF HEAT FLUX BTU/FT 2 SEC.
RUN NO. 19
INPUT - PARABOLA
CONSTANT SUBSTRATE PROPERTIES
FILTER - IN
FREQUENCY - 2.5 KHz
DAMPING FACTOR - 1.0
NOISE - 10 KHz SINUSOIDAL

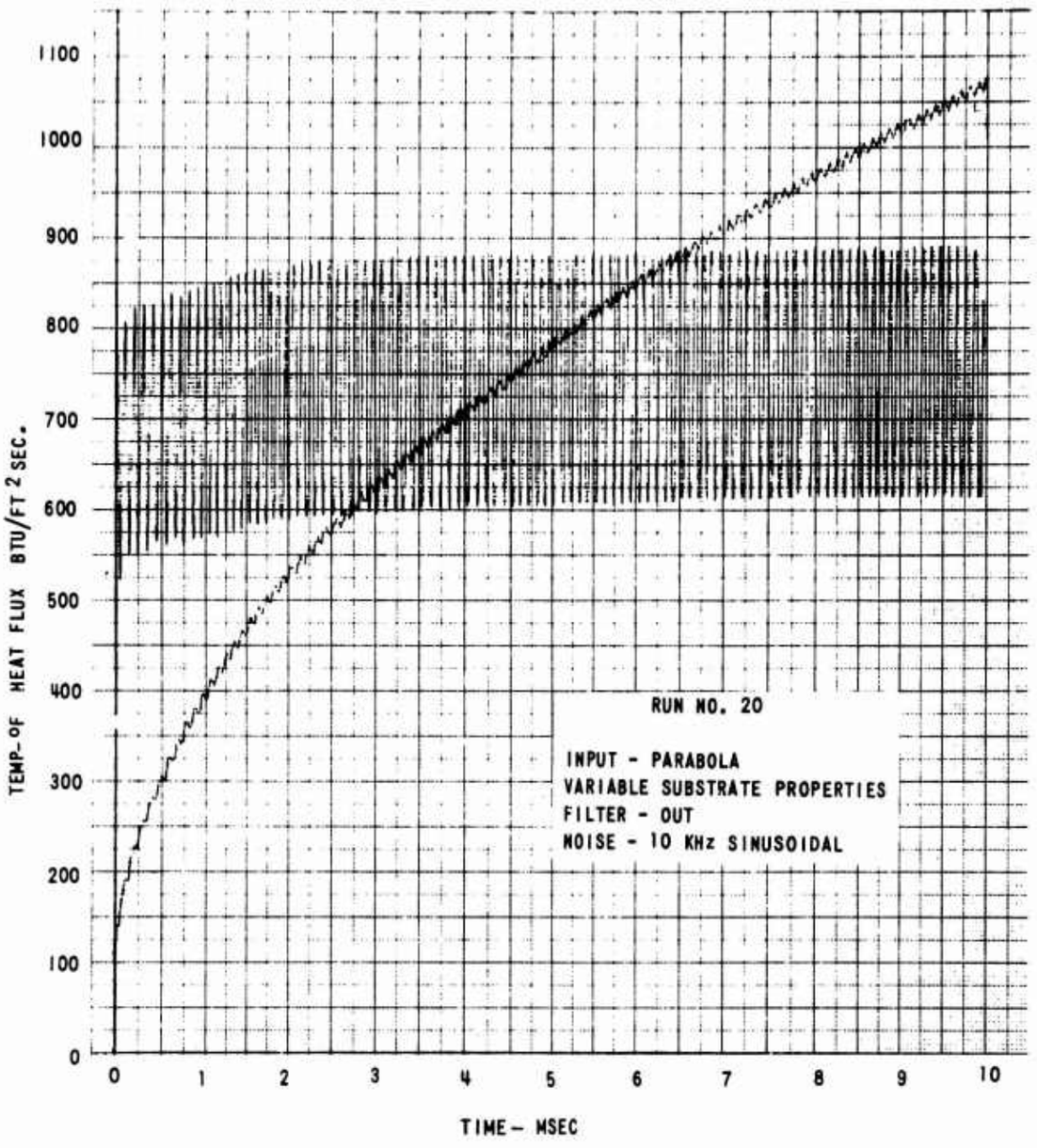
TEMP-OF HEAT FLUX BTU/FT 2 SEC.
1100
1000
900
800
700
600
500
400
300
200
100
0
0
1
2
3
4
5
6
7
8
9
10
TIME– MSEC
RUN NO. 20
INPUT - PARABOLA
VARIABLE SUBSTRATE PROPERTIES
FILTER - OUT
NOISE - 10 KHz SINUSOIDAL

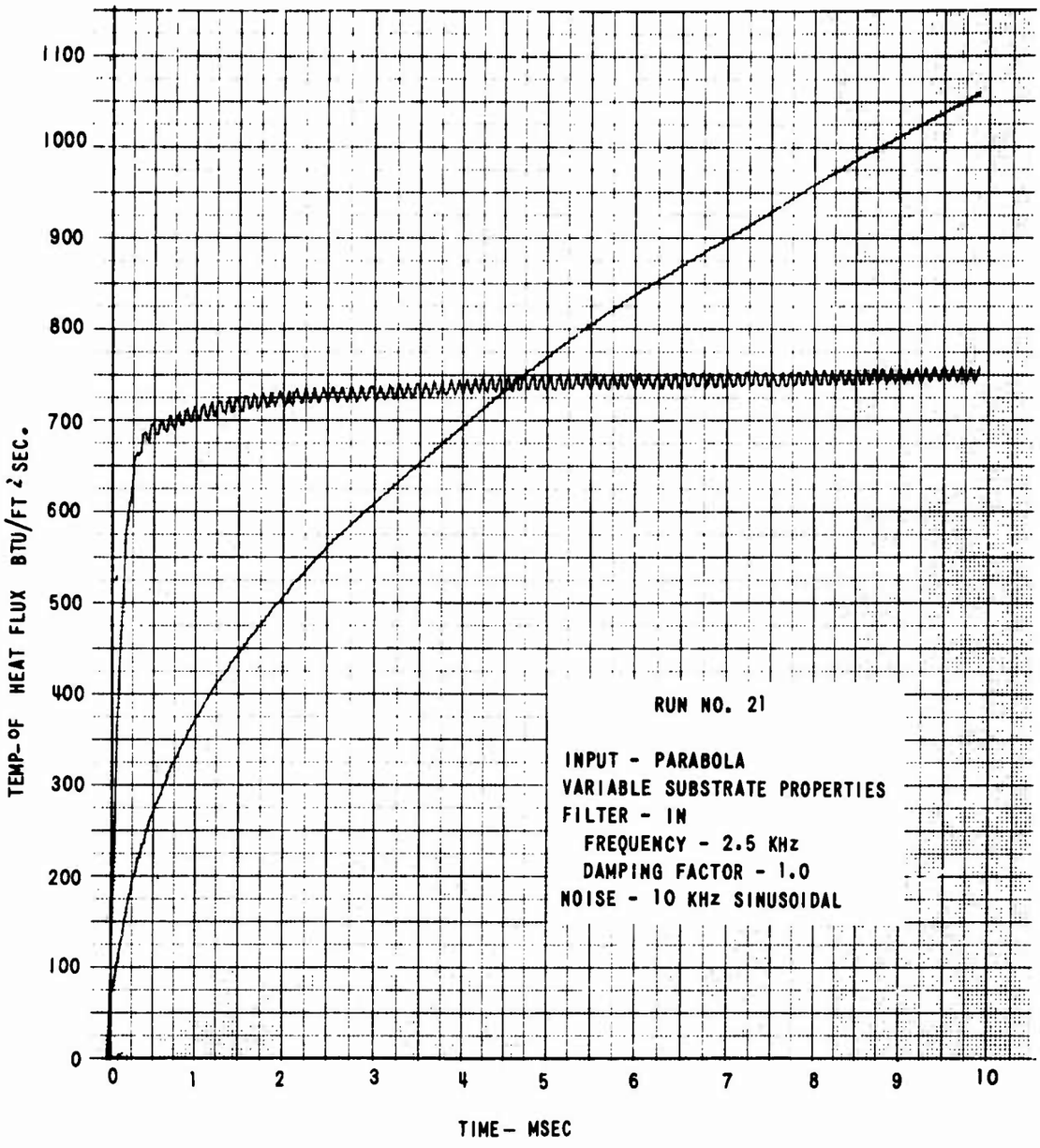
TEMP-OF HEAT FLUX BTU/FT²SEC.
1100
1000
900
800
700
600
500
400
300
200
100
0
0
1
2
3
4
5
6
7
8
9
10
TIME- MSEC
RUN NO. 21
INPUT - PARABOLA
VARIABLE SUBSTRATE PROPERTIES
FILTER - IN
FREQUENCY - 2.5 KHz
DAMPING FACTOR - 1.0
NOISE - 10 KHz SINUSOIDAL

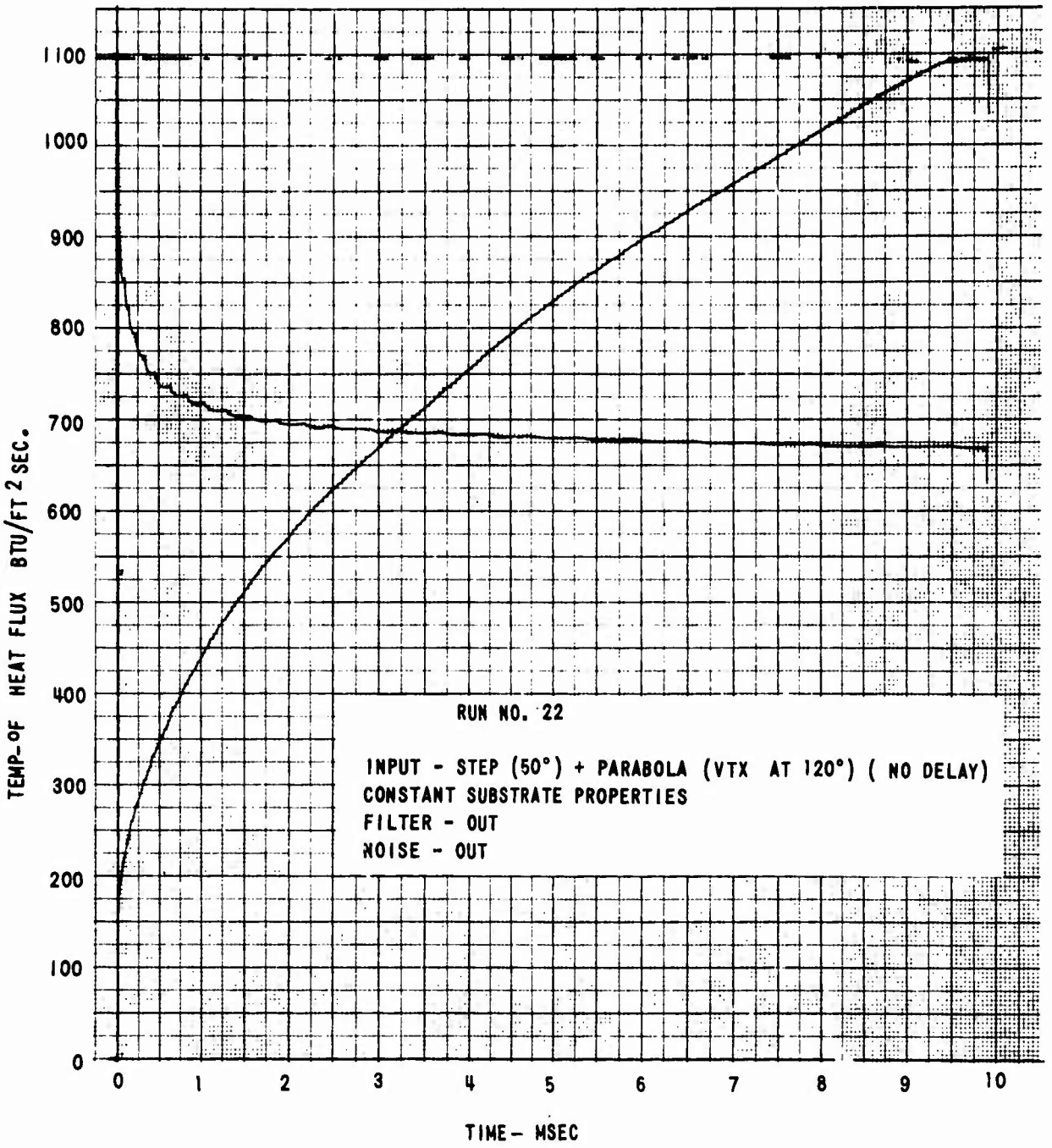
TEMP-OF HEAT FLUX BTU/FT 2 SEC.
1100
1000
900
800
700
600
500
400
300
200
100
0
0
1
2
3
4
5
6
7
8
9
10
TIME- MSEC
RUN NO. 22
INPUT - STEP (50°) + PARABOLA (VTX AT 120°) (NO DELAY)
CONSTANT SUBSTRATE PROPERTIES
FILTER - OUT
NOISE - OUT

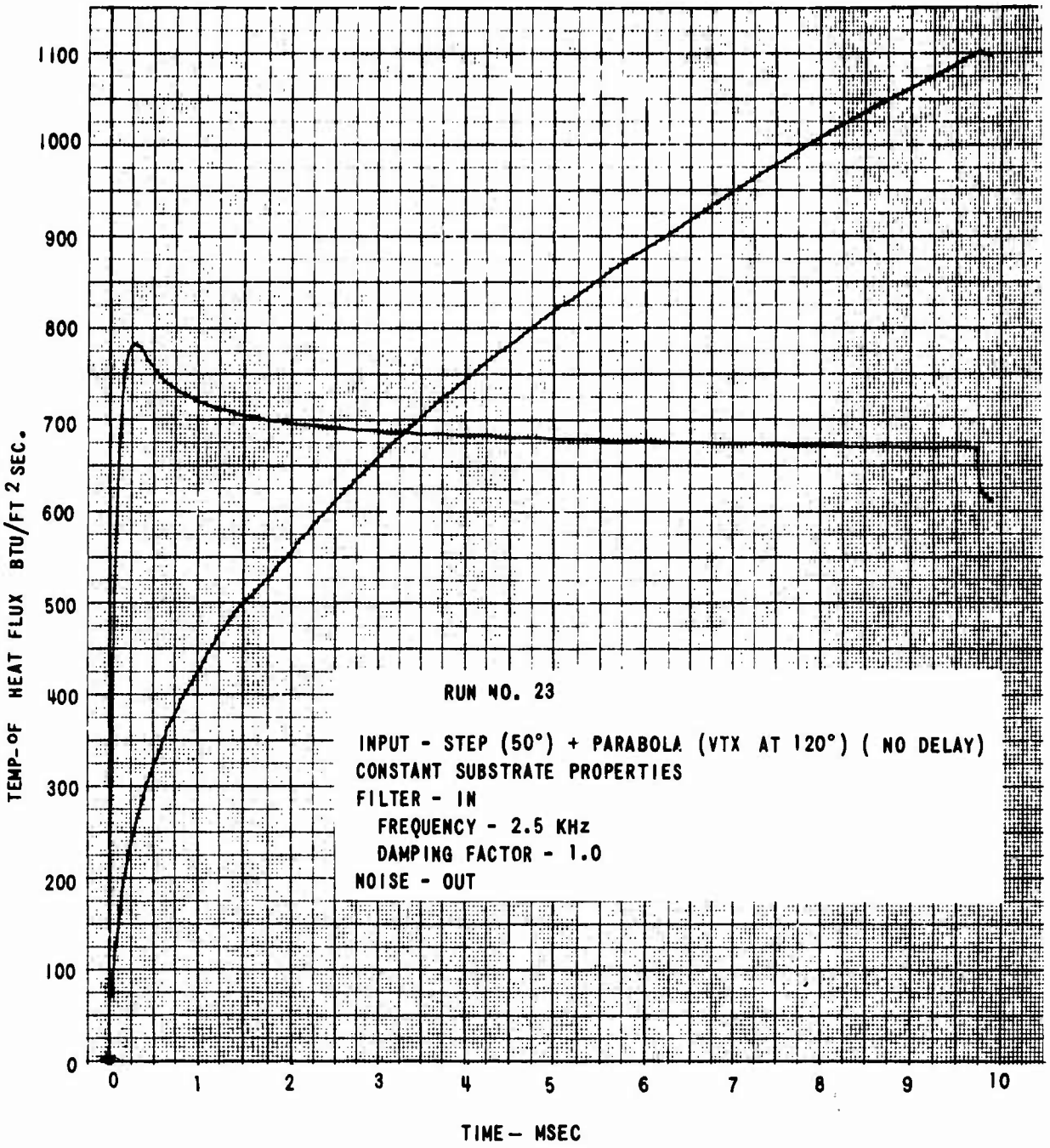
TEMP-OF HEAT FLUX BTU/FT 2 SEC.
1100
1000
900
800
700
600
500
400
300
200
100
0
0
1
2
3
4
5
6
7
8
9
10
TIME— MSEC
RUN NO. 23
INPUT - STEP (50°) + PARABOLA (VTX AT 120°) (NO DELAY)
CONSTANT SUBSTRATE PROPERTIES
FILTER - IN
FREQUENCY - 2.5 KHz
DAMPING FACTOR - 1.0
NOISE - OUT

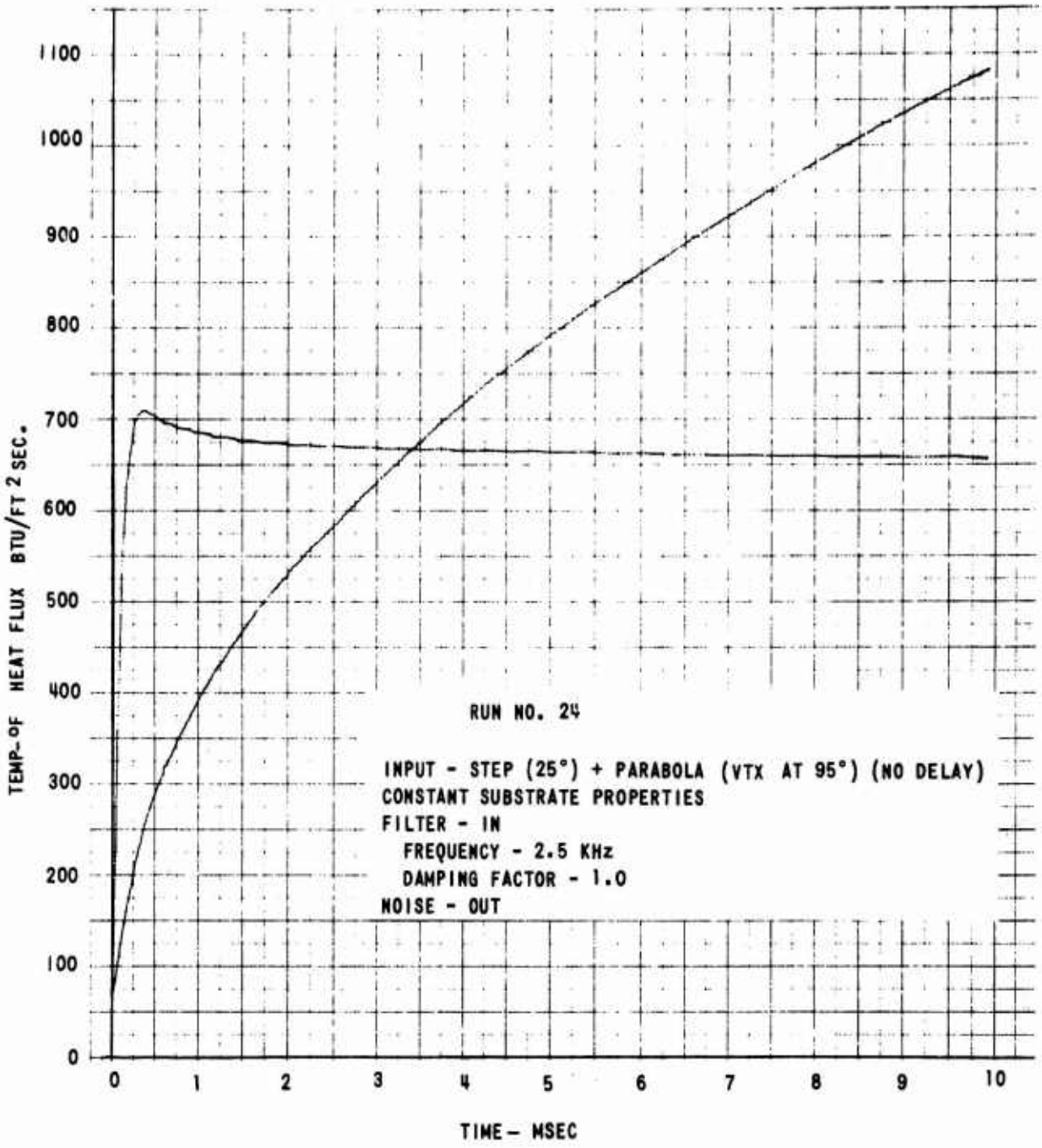
RUN NO. 24
INPUT - STEP (25°) + PARABOLA (VTX AT 95°) (NO DELAY)
CONSTANT SUBSTRATE PROPERTIES
FILTER - IN
FREQUENCY - 2.5 KHz
DAMPING FACTOR - 1.0
NOISE - OUT
TEMP-°F HEAT FLUX BTU/FT² SEC.
1100
1000
900
800
700
600
500
400
300
200
100
0
0
1
2
3
4
5
6
7
8
9
10
TIME - MSEC

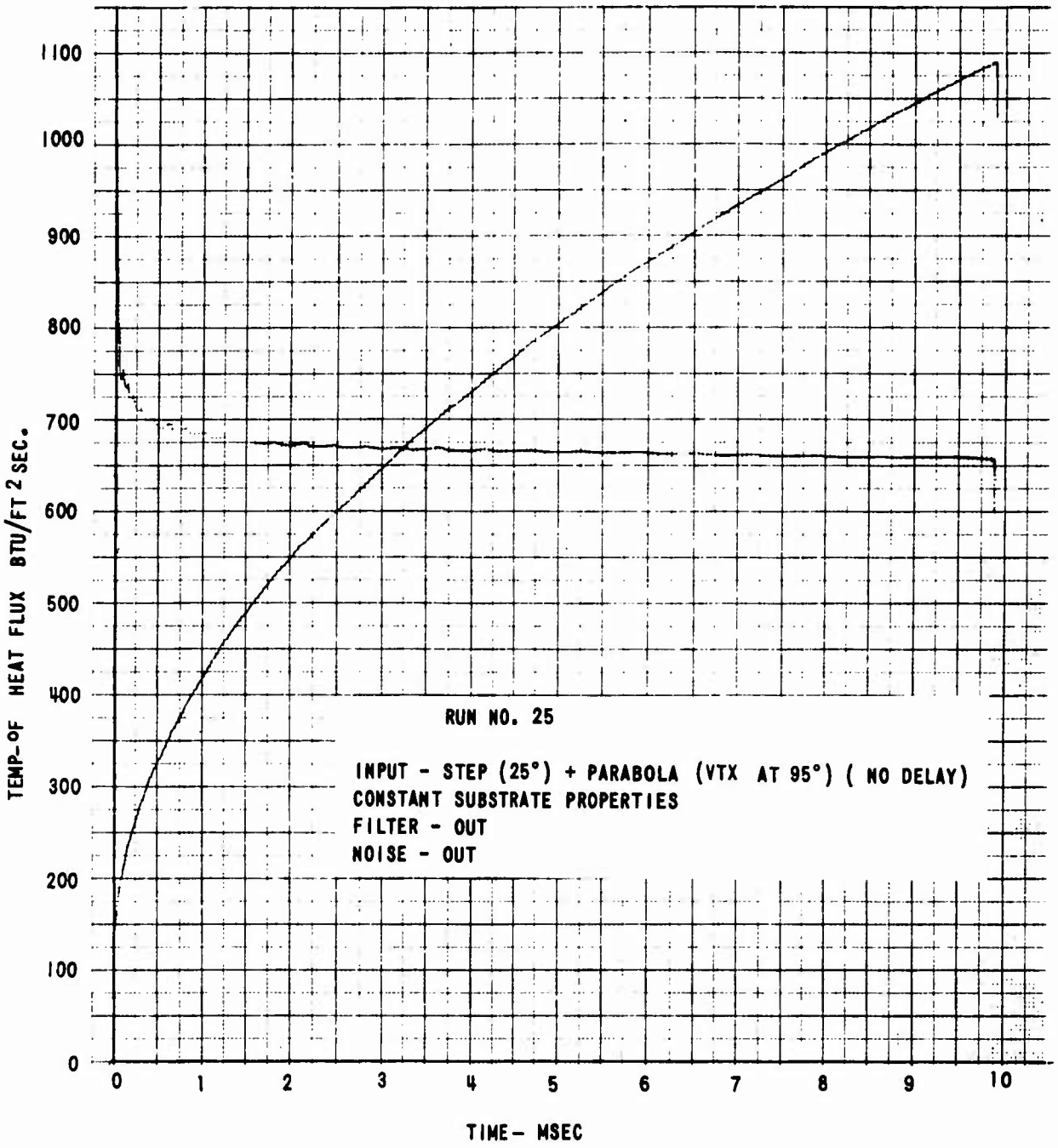
RUN NO. 25
INPUT - STEP (25°) + PARABOLA (VTX AT 95°) (NO DELAY)
CONSTANT SUBSTRATE PROPERTIES
FILTER - OUT
NOISE - OUT
TEMP-oF HEAT FLUX BTU/FT 2 SEC.
TIME- MSEC
0
100
200
300
400
500
600
700
800
900
1000
1100
0
1
2
3
4
5
6
7
8
9
10

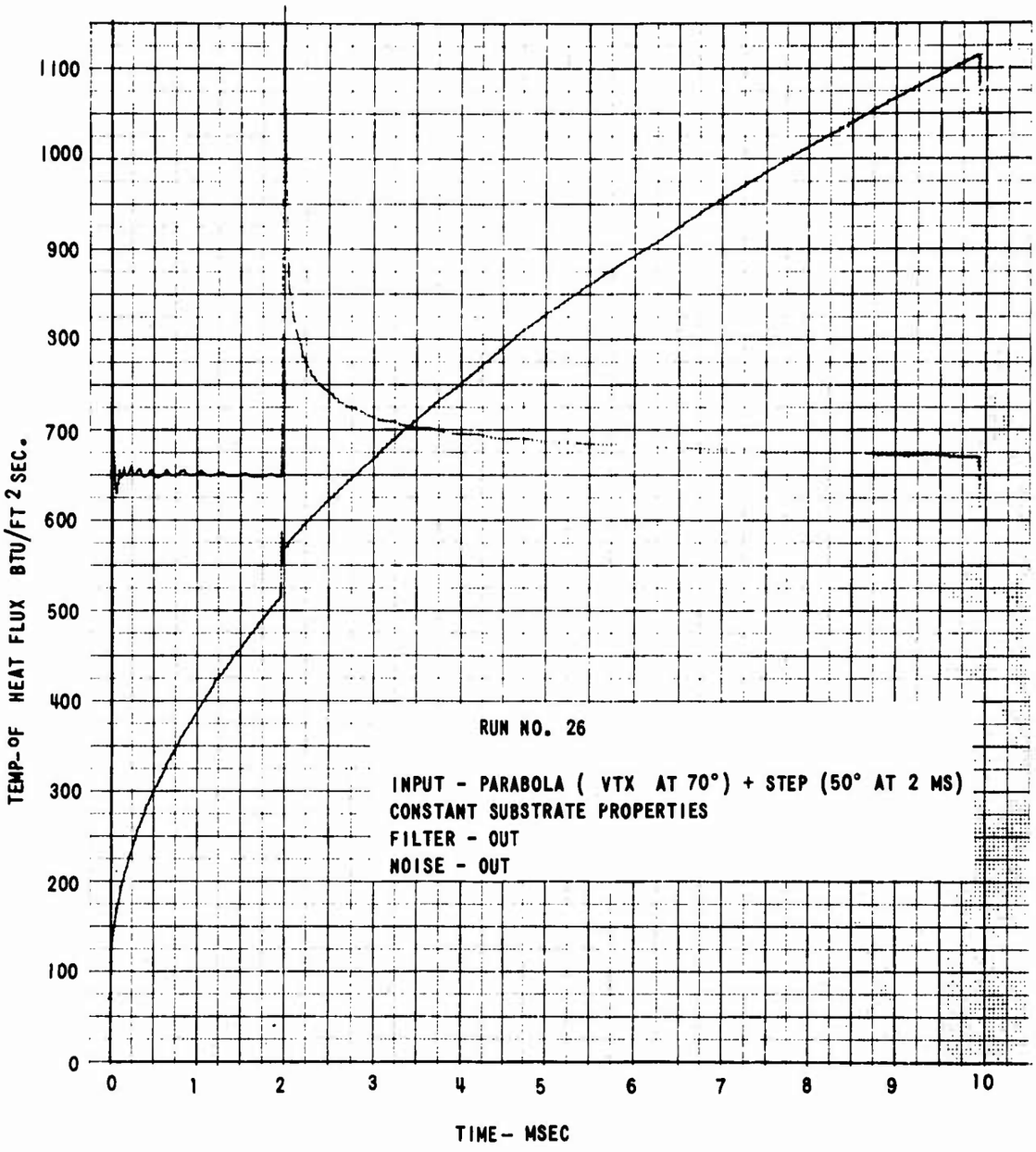
TEMP-OF HEAT FLUX BTU/FT 2 SEC.
1100
1000
900
300
700
600
500
400
300
200
100
0
0
1
2
3
4
5
6
7
8
9
10
TIME- MSEC
RUN NO. 26
INPUT - PARABOLA (VTX AT 70°) + STEP (50° AT 2 MS)
CONSTANT SUBSTRATE PROPERTIES
FILTER - OUT
NOISE - OUT

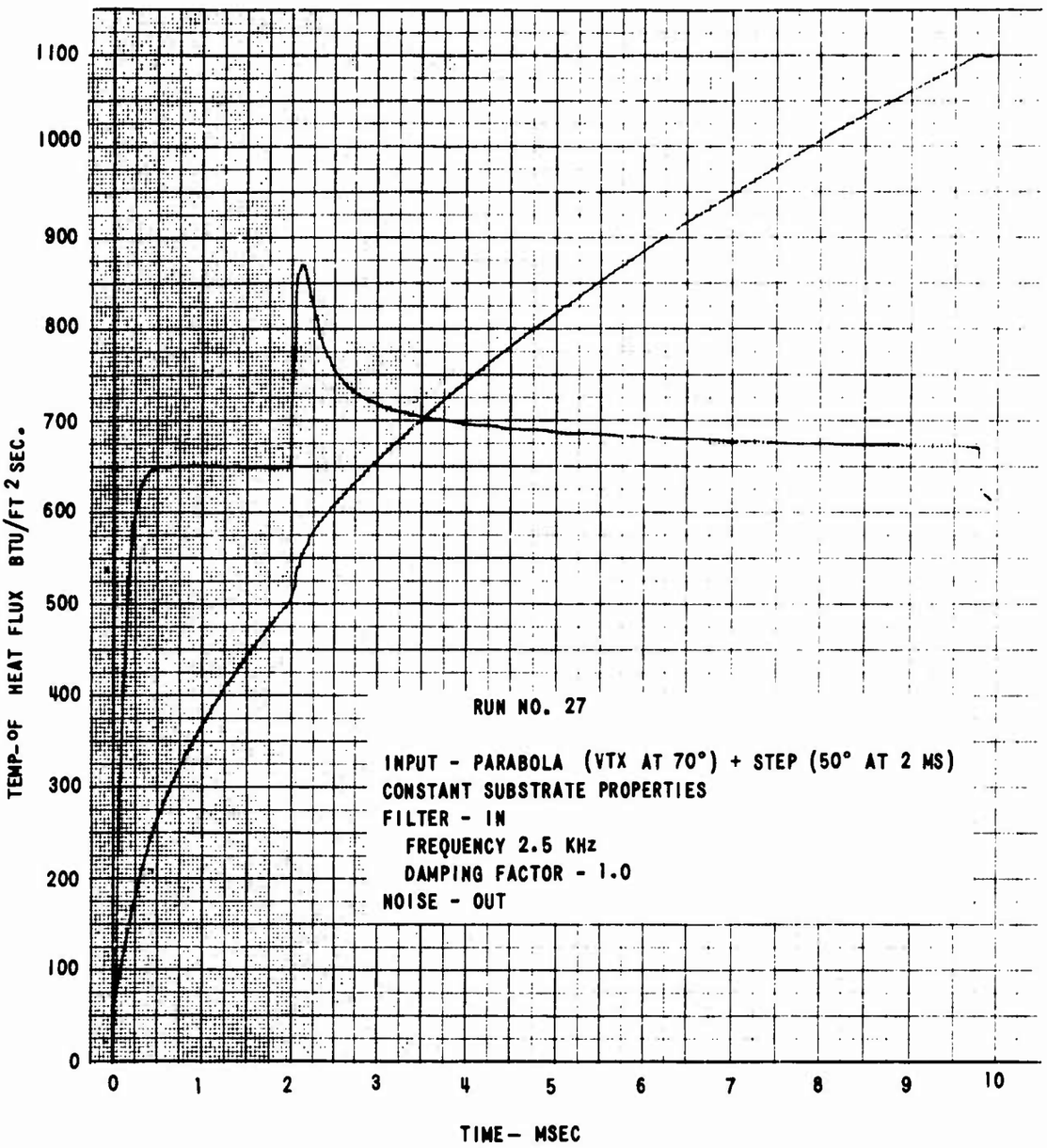
TEMP-°F HEAT FLUX BTU/FT² SEC.
1100
1000
900
800
700
600
500
400
300
200
100
0
0
1
2
3
4
5
6
7
8
9
10
TIME- MSEC
RUN NO. 27
INPUT - PARABOLA (VTX AT 70°) + STEP (50° AT 2 MS)
CONSTANT SUBSTRATE PROPERTIES
FILTER - IN
FREQUENCY 2.5 KHz
DAMPING FACTOR - 1.0
NOISE - OUT

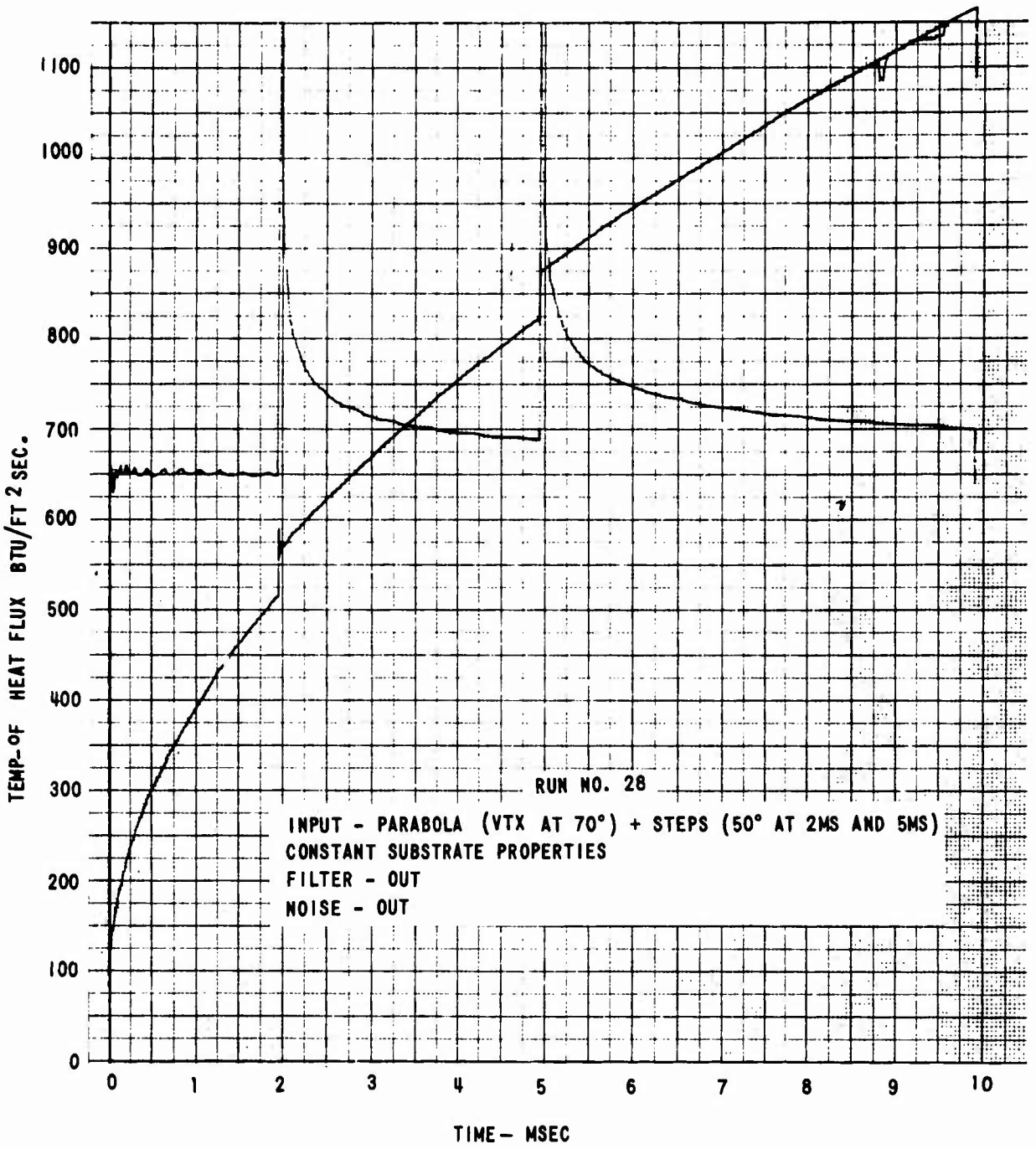
TEMP-OF HEAT FLUX BTU/FT 2 SEC.
1100
1000
900
800
700
600
500
400
300
200
100
0
0
1
2
3
4
5
6
7
8
9
10
TIME— MSEC
RUN NO. 28
INPUT - PARABOLA (VTX AT 70°) + STEPS (50° AT 2MS AND 5MS)
CONSTANT SUBSTRATE PROPERTIES
FILTER - OUT
NOISE - OUT

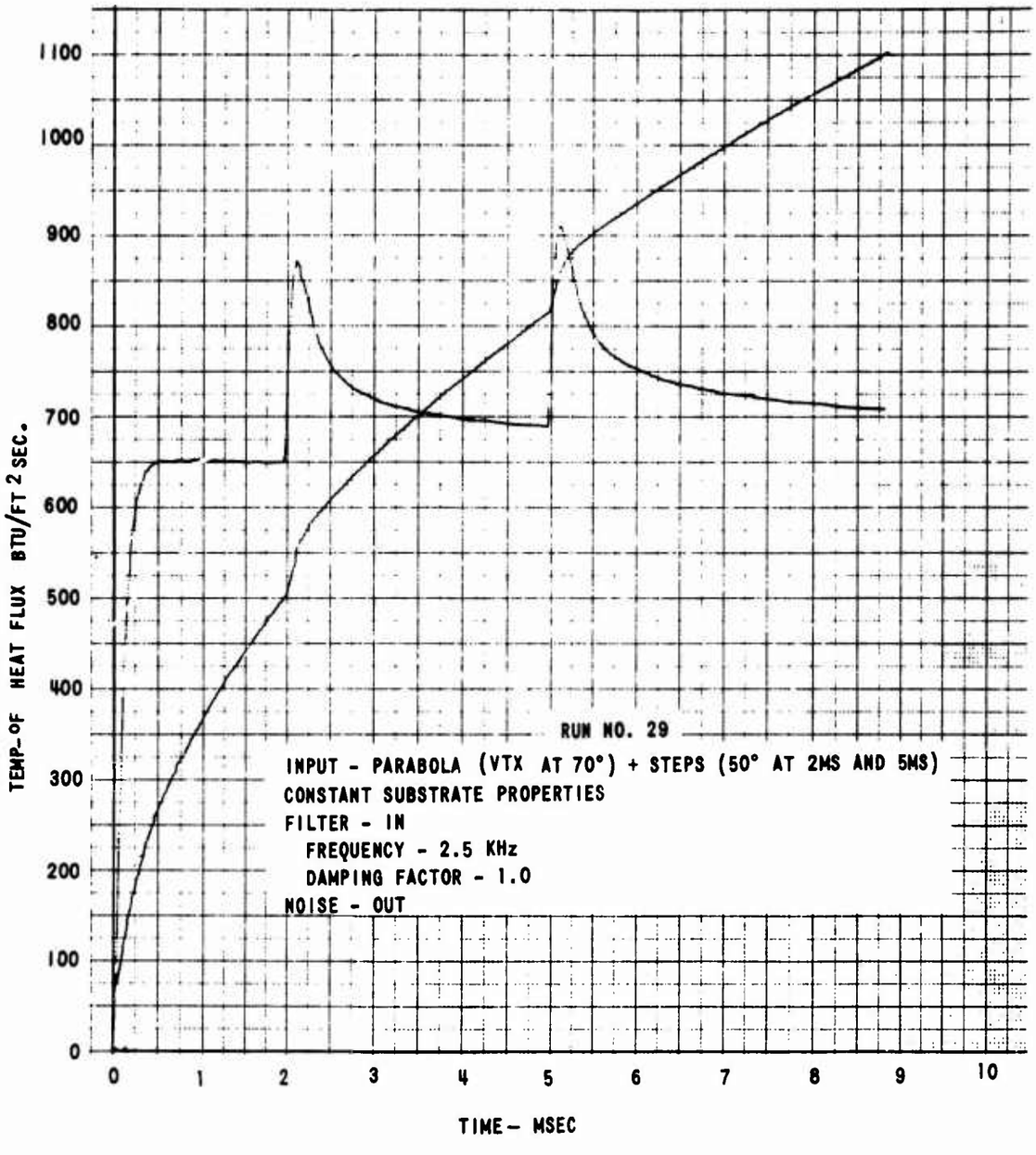
TEMP-°F HEAT FLUX BTU/FT 2 SEC.
1100
1000
900
800
700
600
500
400
300
200
100
0
0
1
2
3
4
5
6
7
8
9
10
TIME- MSEC
RUN NO. 29
INPUT - PARABOLA (VTX AT 70°) + STEPS (50° AT 2MS AND 5MS)
CONSTANT SUBSTRATE PROPERTIES
FILTER - IN
FREQUENCY - 2.5 KHz
DAMPING FACTOR - 1.0
NOISE - OUT

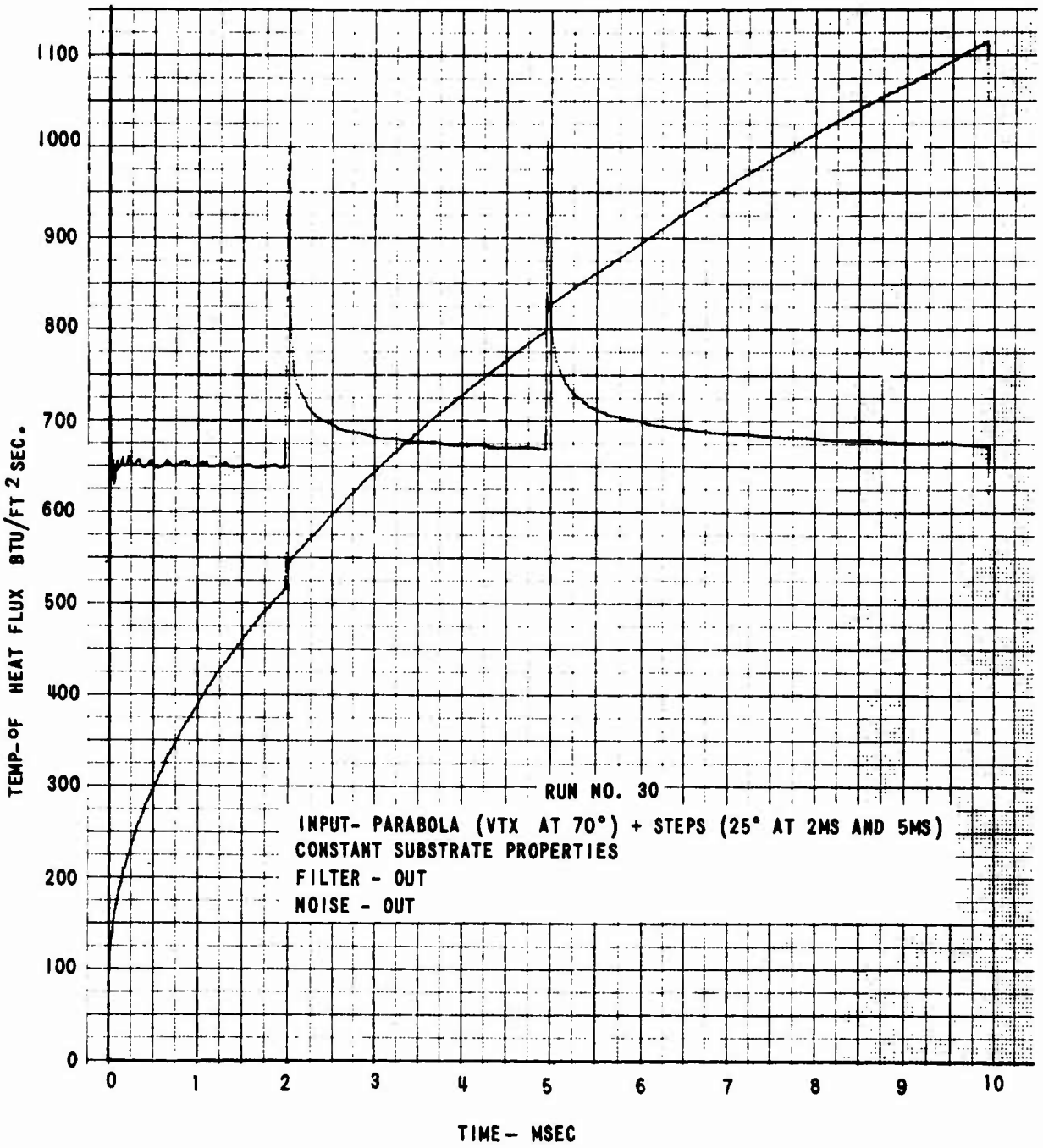
TEMP-°F HEAT FLUX BTU/FT 2 SEC.
1100
1000
900
800
700
600
500
400
300
200
100
0
0
1
2
3
4
5
6
7
8
9
10
TIME- MSEC
RUN NO. 30
INPUT- PARABOLA (VTX AT 70°) + STEPS (25° AT 2MS AND 5MS)
CONSTANT SUBSTRATE PROPERTIES
FILTER - OUT
NOISE - OUT

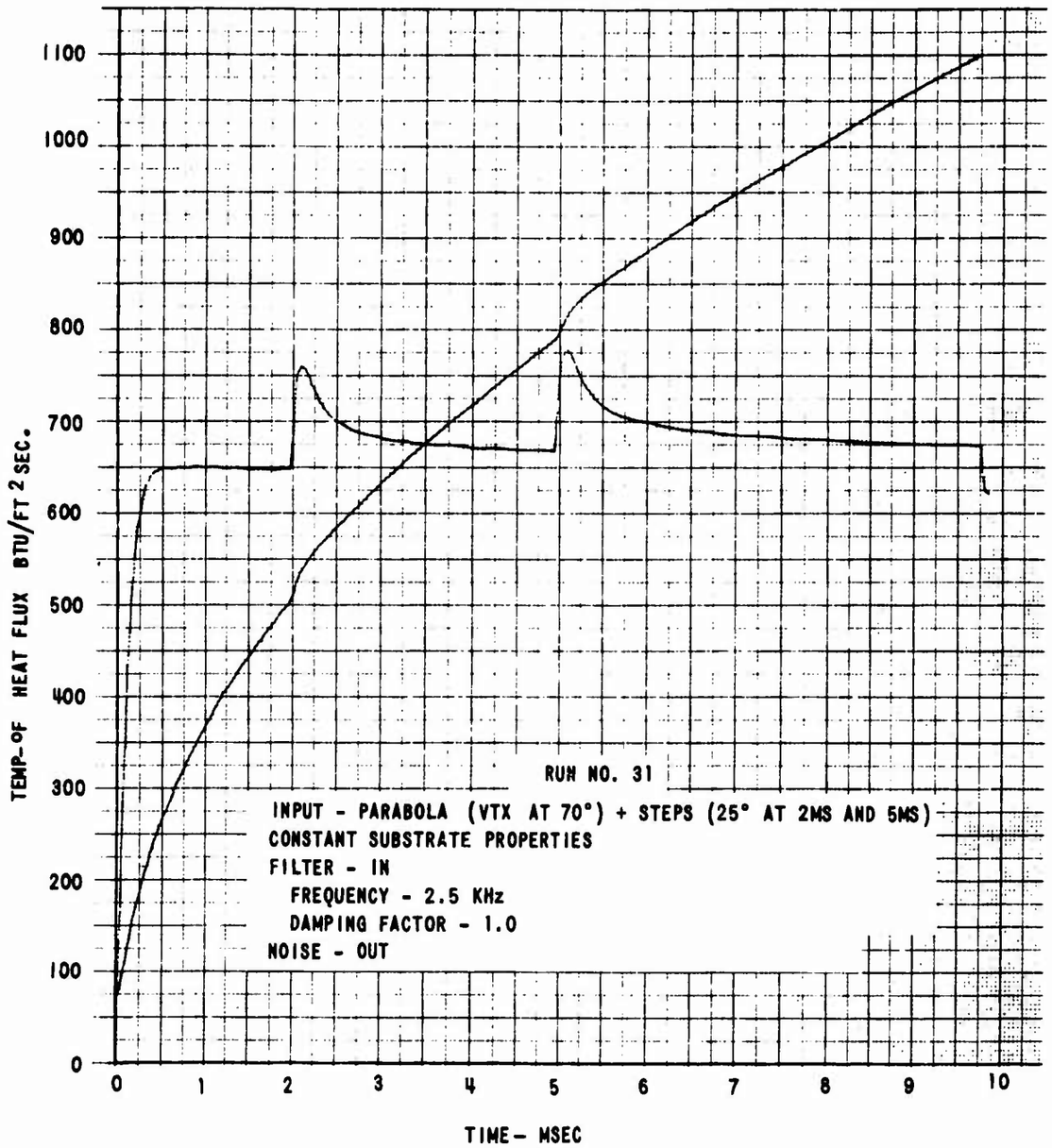
TEMP-°F HEAT FLUX BTU/FT 2 SEC.
1100
1000
900
800
700
600
500
400
300
200
100
0
0
1
2
3
4
5
6
7
8
9
10
TIME- MSEC
RUN NO. 31
INPUT - PARABOLA (VTX AT 70°) + STEPS (25° AT 2MS AND 5MS)
CONSTANT SUBSTRATE PROPERTIES
FILTER - IN
FREQUENCY - 2.5 KHz
DAMPING FACTOR - 1.0
NOISE - OUT

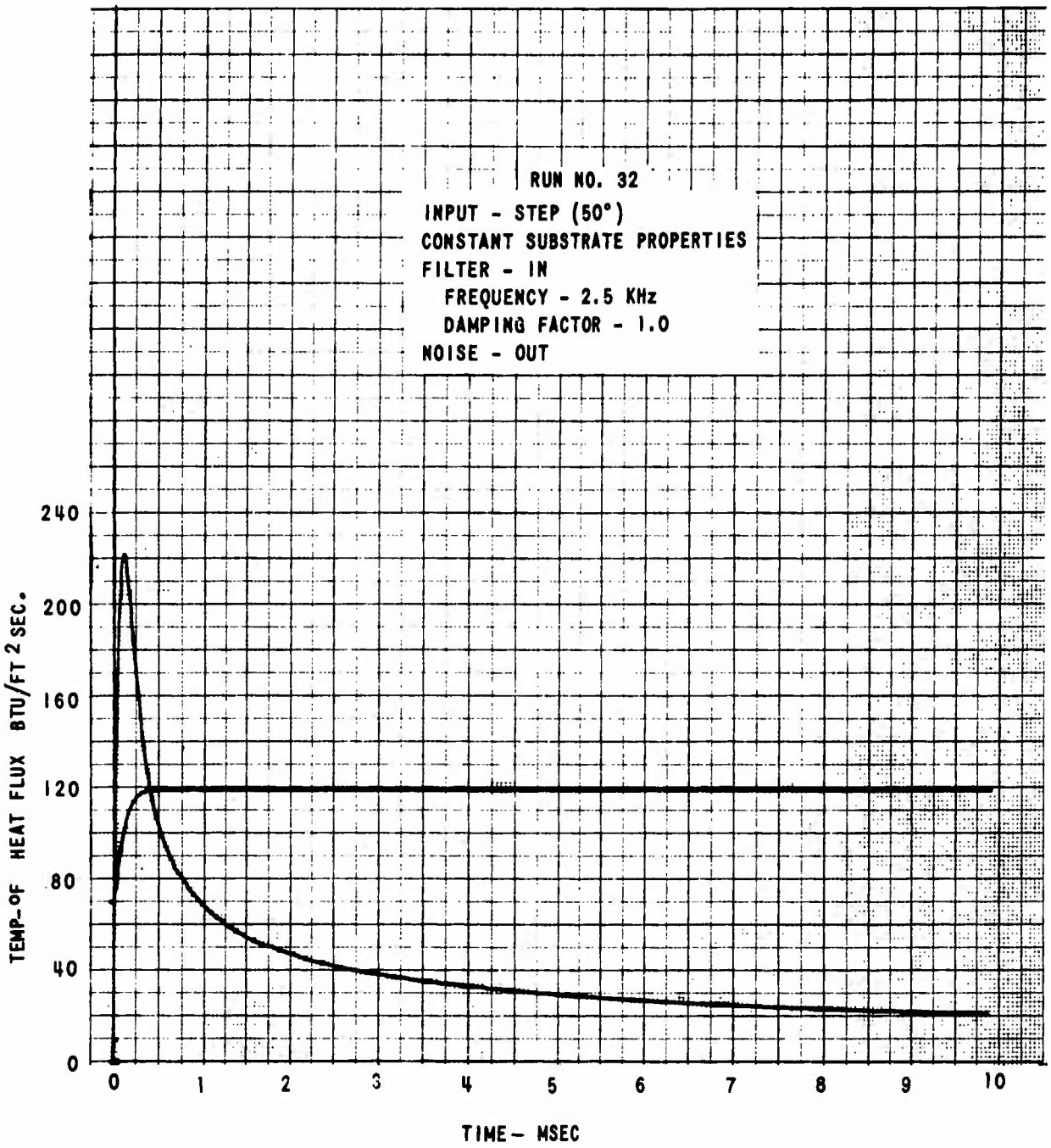
RUN NO. 32
INPUT - STEP (50°)
CONSTANT SUBSTRATE PROPERTIES
FILTER - IN
FREQUENCY - 2.5 KHz
DAMPING FACTOR - 1.0
NOISE - OUT
TEMP-°F HEAT FLUX BTU/FT 2 SEC.
240
200
160
120
80
40
0
0
1
2
3
4
5
6
7
8
9
10
TIME - MSEC

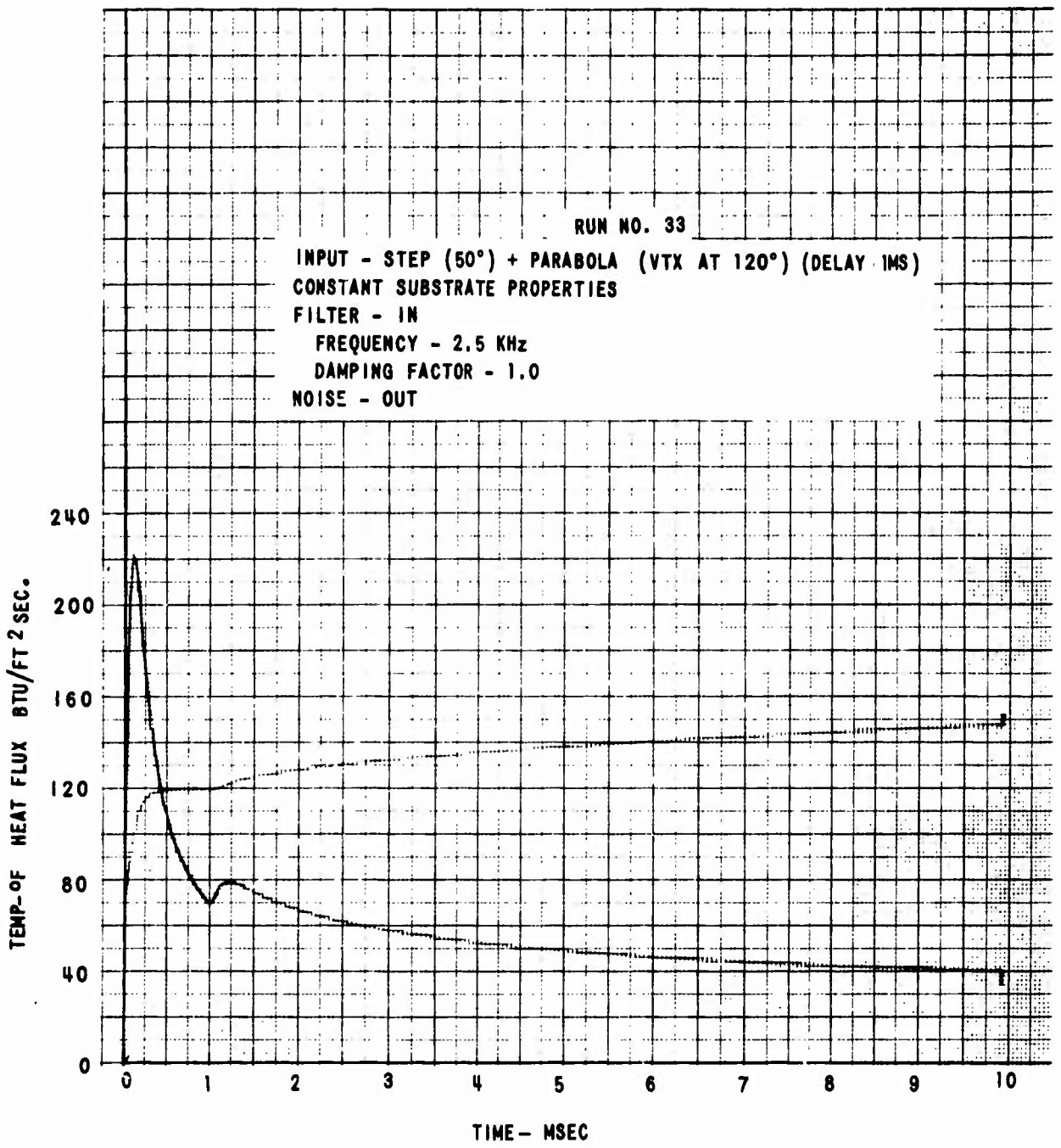
RUN NO. 33
INPUT - STEP (50°) + PARABOLA (VTX AT 120°) (DELAY 1MS)
CONSTANT SUBSTRATE PROPERTIES
FILTER - IN
FREQUENCY - 2.5 KHz
DAMPING FACTOR - 1.0
NOISE - OUT
TEMP-°F HEAT FLUX BTU/FT 2 SEC.
240
200
160
120
80
40
0
0
1
2
3
4
5
6
7
8
9
10
TIME - MSEC

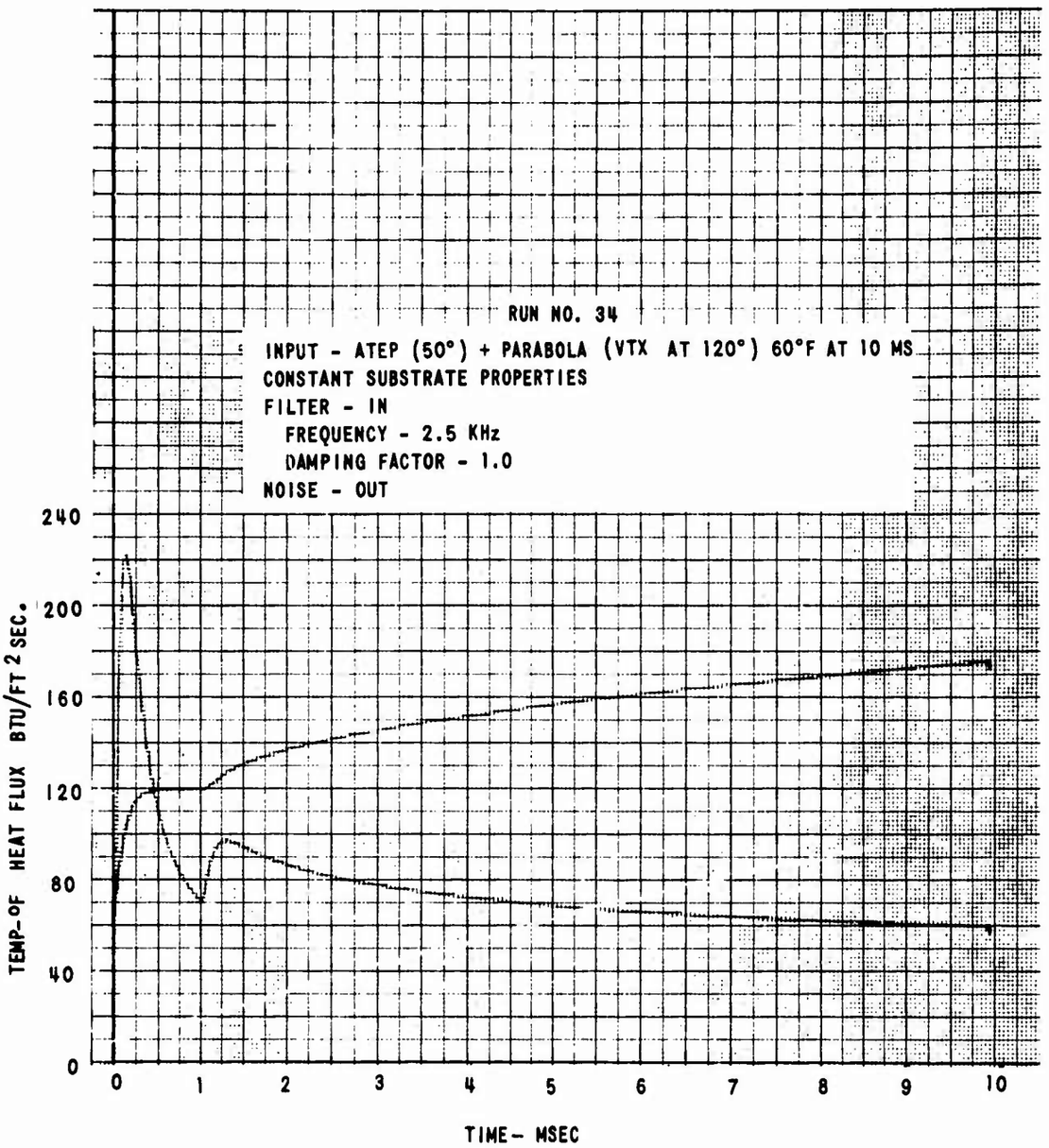
RUN NO. 34
INPUT - ATEP (50°) + PARABOLA (VTX AT 120°) 60°F AT 10 MS
CONSTANT SUBSTRATE PROPERTIES
FILTER - IN
FREQUENCY - 2.5 KHz
DAMPING FACTOR - 1.0
NOISE - OUT
TEMP-OF HEAT FLUX BTU/FT 2 SEC.
240
200
160
120
80
40
0
0
1
2
3
4
5
6
7
8
9
10
TIME- MSEC

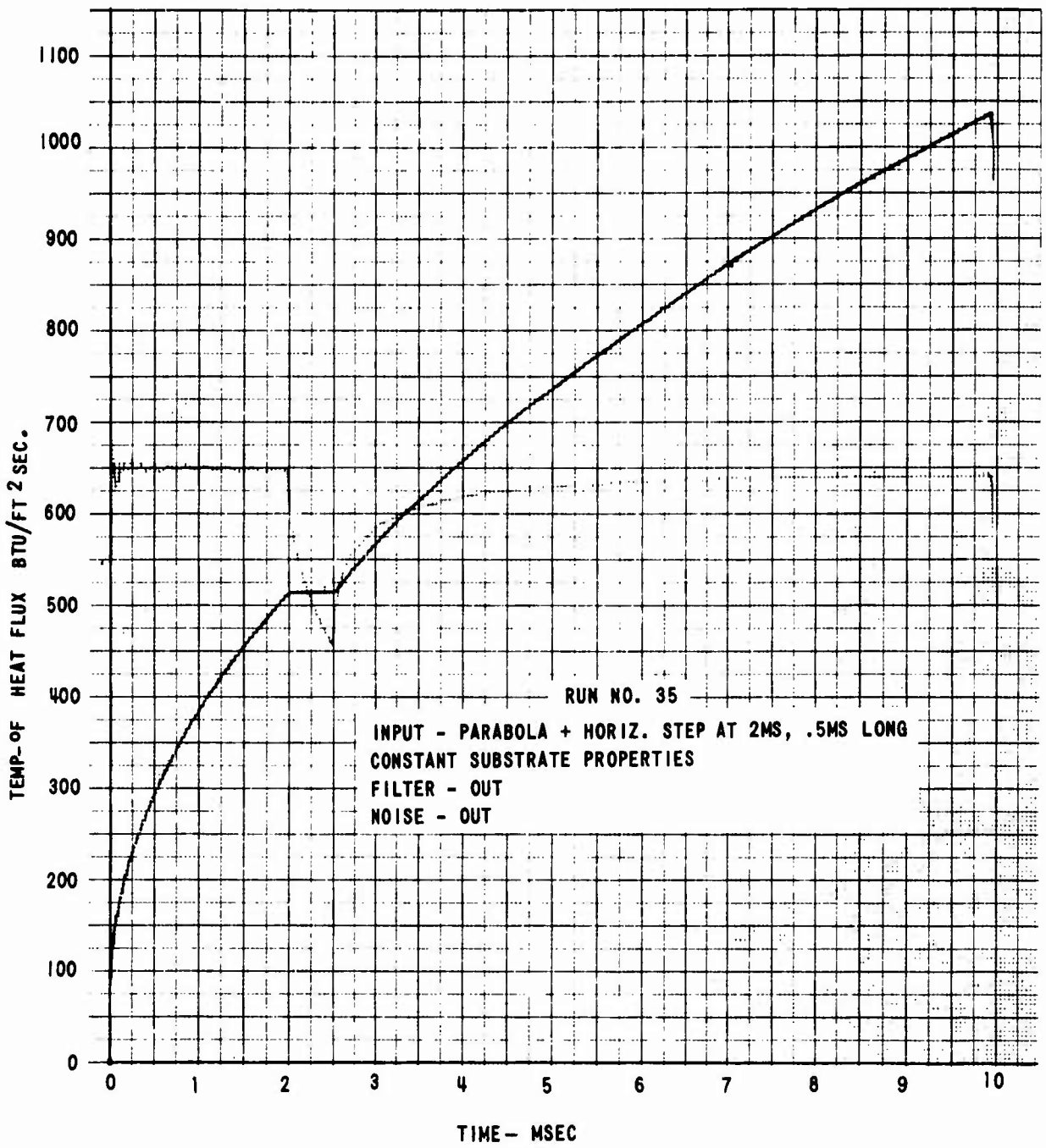
RUN NO. 35
INPUT - PARABOLA + HORIZ. STEP AT 2MS, .5MS LONG
CONSTANT SUBSTRATE PROPERTIES
FILTER - OUT
NOISE - OUT
TEMP-OF HEAT FLUX BTU/FT 2 SEC.
1100
1000
900
800
700
600
500
400
300
200
100
0
0
1
2
3
4
5
6
7
8
9
10
TIME- MSEC

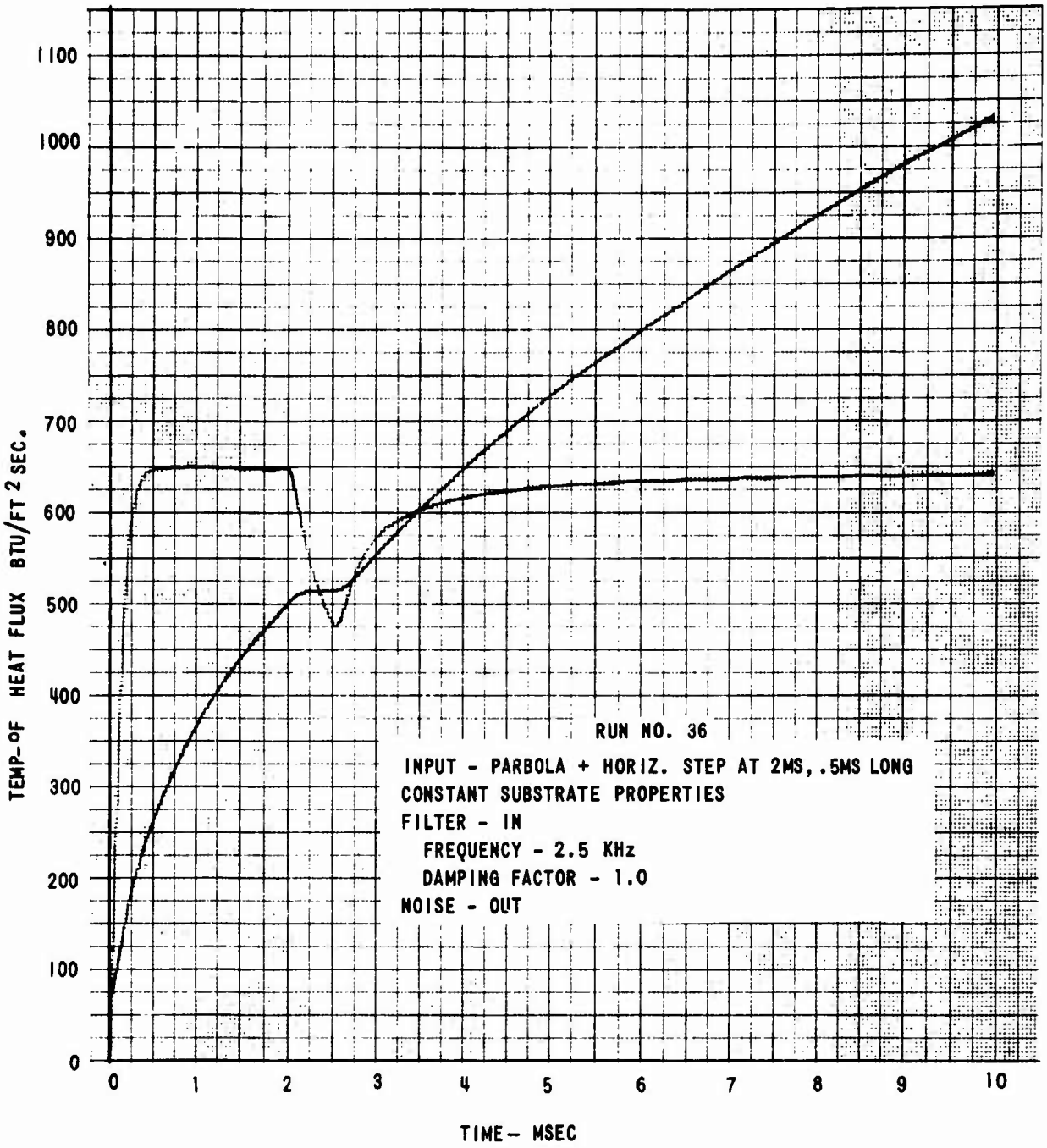
TEMP-OF HEAT FLUX BTU/FT 2 SEC.
1100
1000
900
800
700
600
500
400
300
200
100
0
0
1
2
3
4
5
6
7
8
9
10
TIME- MSEC
RUN NO. 36
INPUT - PARBOLA + HORIZ. STEP AT 2MS, .5MS LONG
CONSTANT SUBSTRATE PROPERTIES
FILTER - IN
FREQUENCY - 2.5 KHz
DAMPING FACTOR - 1.0
NOISE - OUT

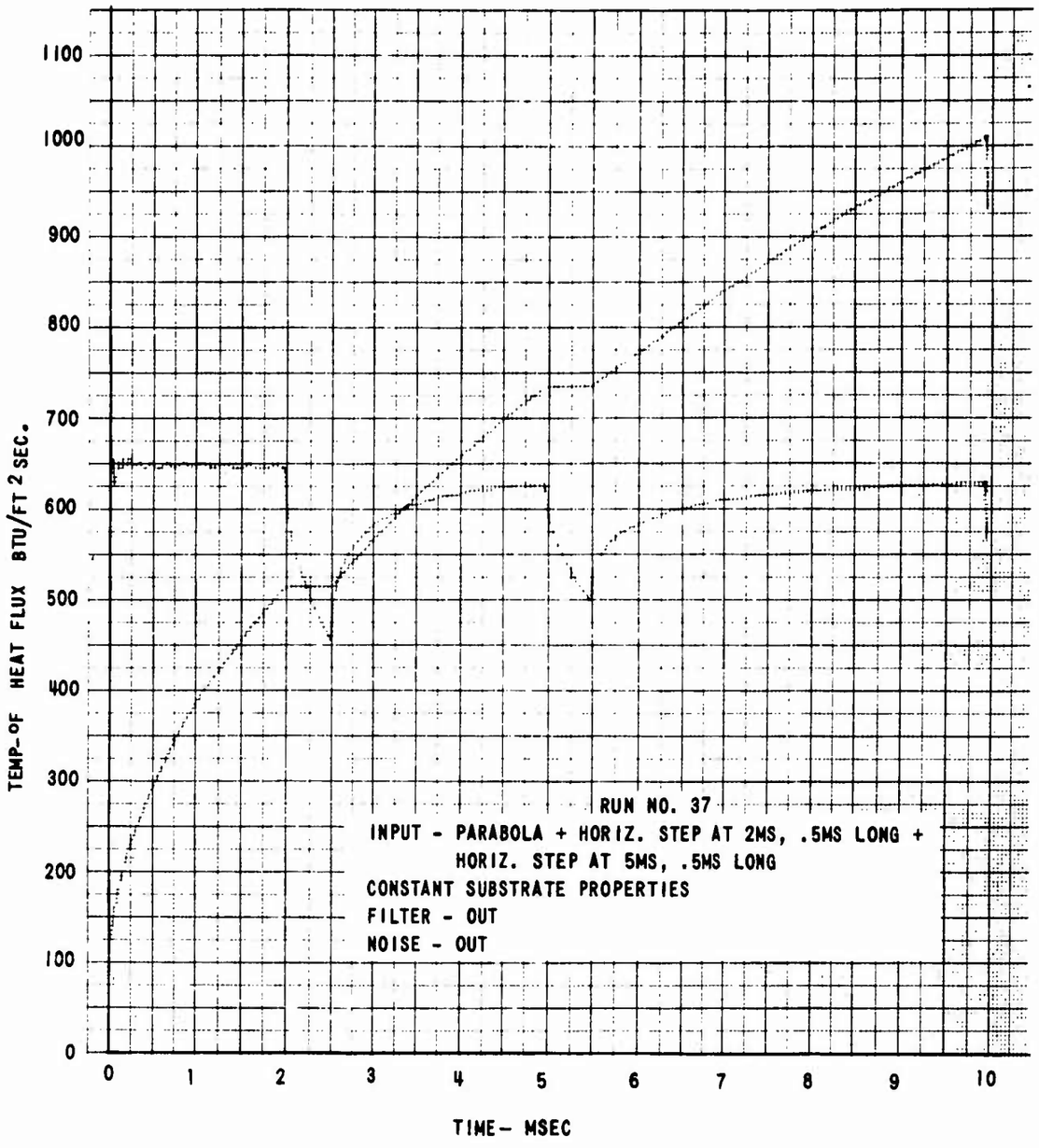
TEMP-OF HEAT FLUX BTU/FT 2 SEC.
1100
1000
900
800
700
600
500
400
300
200
100
0
0
1
2
3
4
5
6
7
8
9
10
TIME- MSEC
RUN NO. 37
INPUT - PARABOLA + HORIZ. STEP AT 2MS, .5MS LONG +
HORIZ. STEP AT 5MS, .5MS LONG
CONSTANT SUBSTRATE PROPERTIES
FILTER - OUT
NOISE - OUT

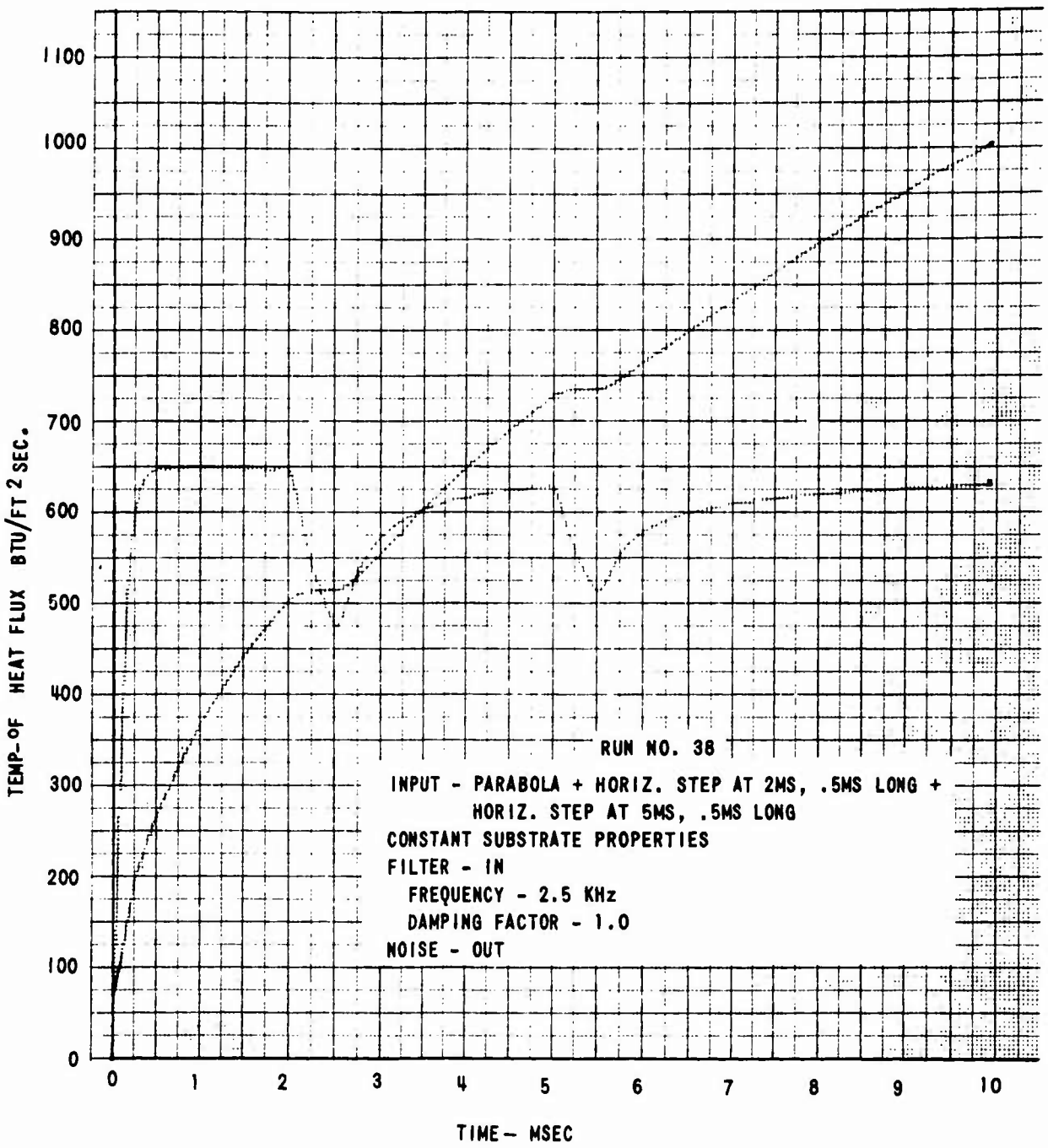
TEMP-OF HEAT FLUX BTU/FT 2 SEC.
1100
1000
900
800
700
600
500
400
300
200
100
0
0
1
2
3
4
5
6
7
8
9
10
TIME— MSEC
RUN NO. 38
INPUT - PARABOLA + HORIZ. STEP AT 2MS, .5MS LONG +
HORIZ. STEP AT 5MS, .5MS LONG
CONSTANT SUBSTRATE PROPERTIES
FILTER - IN
FREQUENCY - 2.5 KHz
DAMPING FACTOR - 1.0
NOISE - OUT

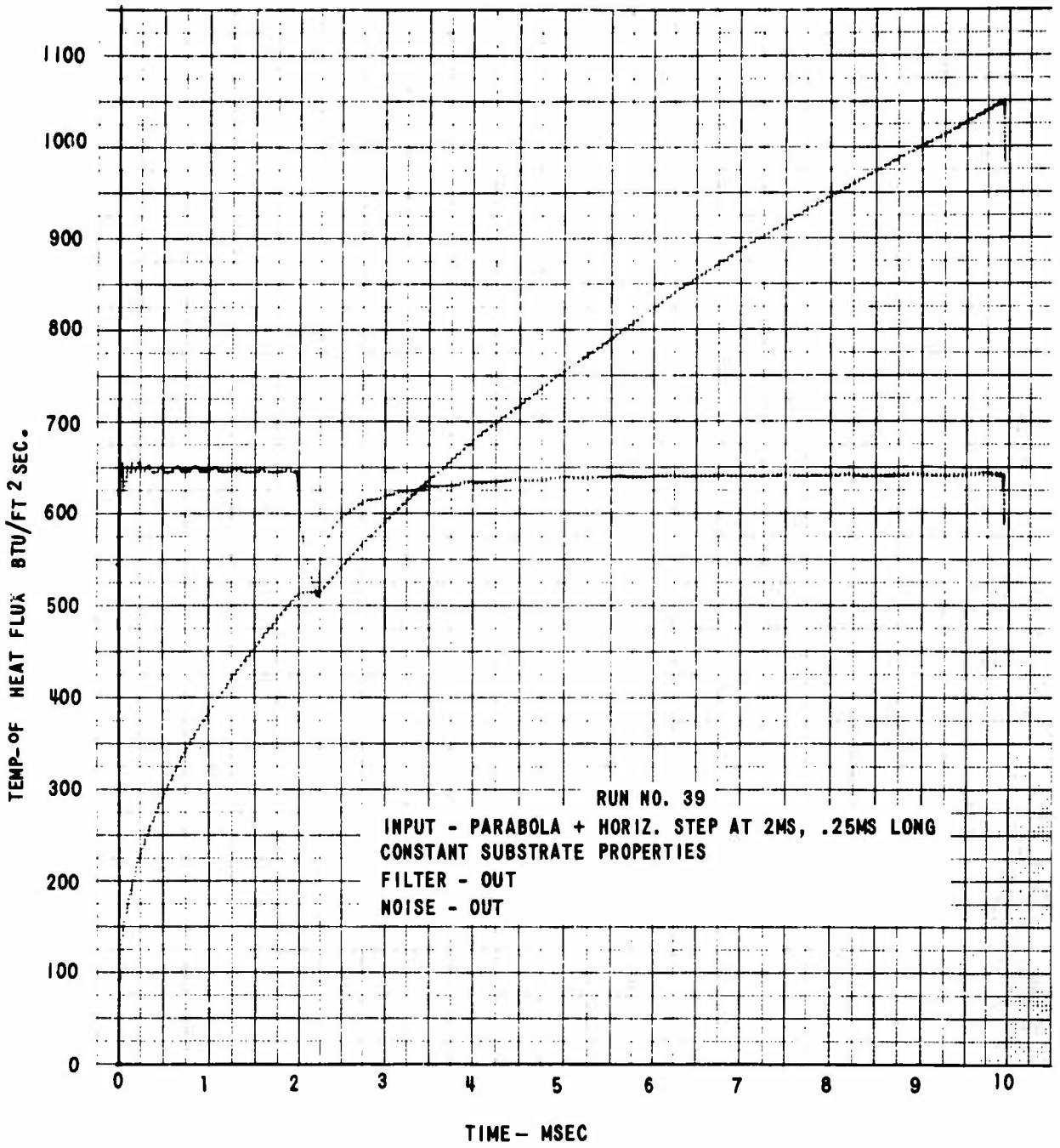
TEMP-OF HEAT FLUX BTU/FT 2 SEC.
1100
1000
900
800
700
600
500
400
300
200
100
0
0
1
2
3
4
5
6
7
8
9
10
TIME – MSEC
RUN NO. 39
INPUT - PARABOLA + HORIZ. STEP AT 2MS, .25MS LONG
CONSTANT SUBSTRATE PROPERTIES
FILTER - OUT
NOISE - OUT

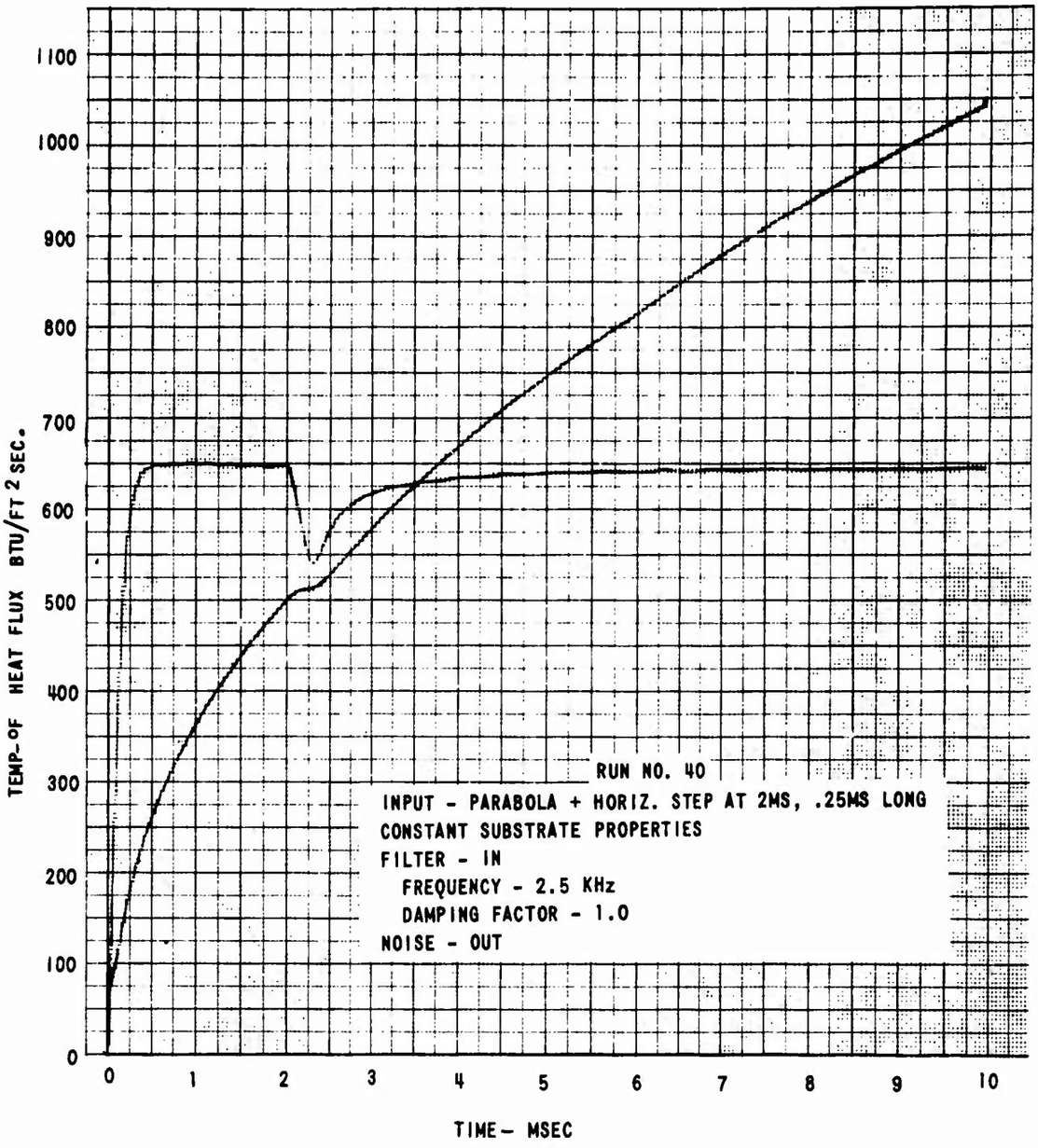
TEMP-OF HEAT FLUX BTU/FT 2 SEC.
1100
1000
900
800
700
600
500
400
300
200
100
0
0
1
2
3
4
5
6
7
8
9
10
TIME- MSEC
RUN NO. 40
INPUT - PARABOLA + HORIZ. STEP AT 2MS, .25MS LONG
CONSTANT SUBSTRATE PROPERTIES
FILTER - IN
FREQUENCY - 2.5 KHz
DAMPING FACTOR - 1.0
NOISE - OUT

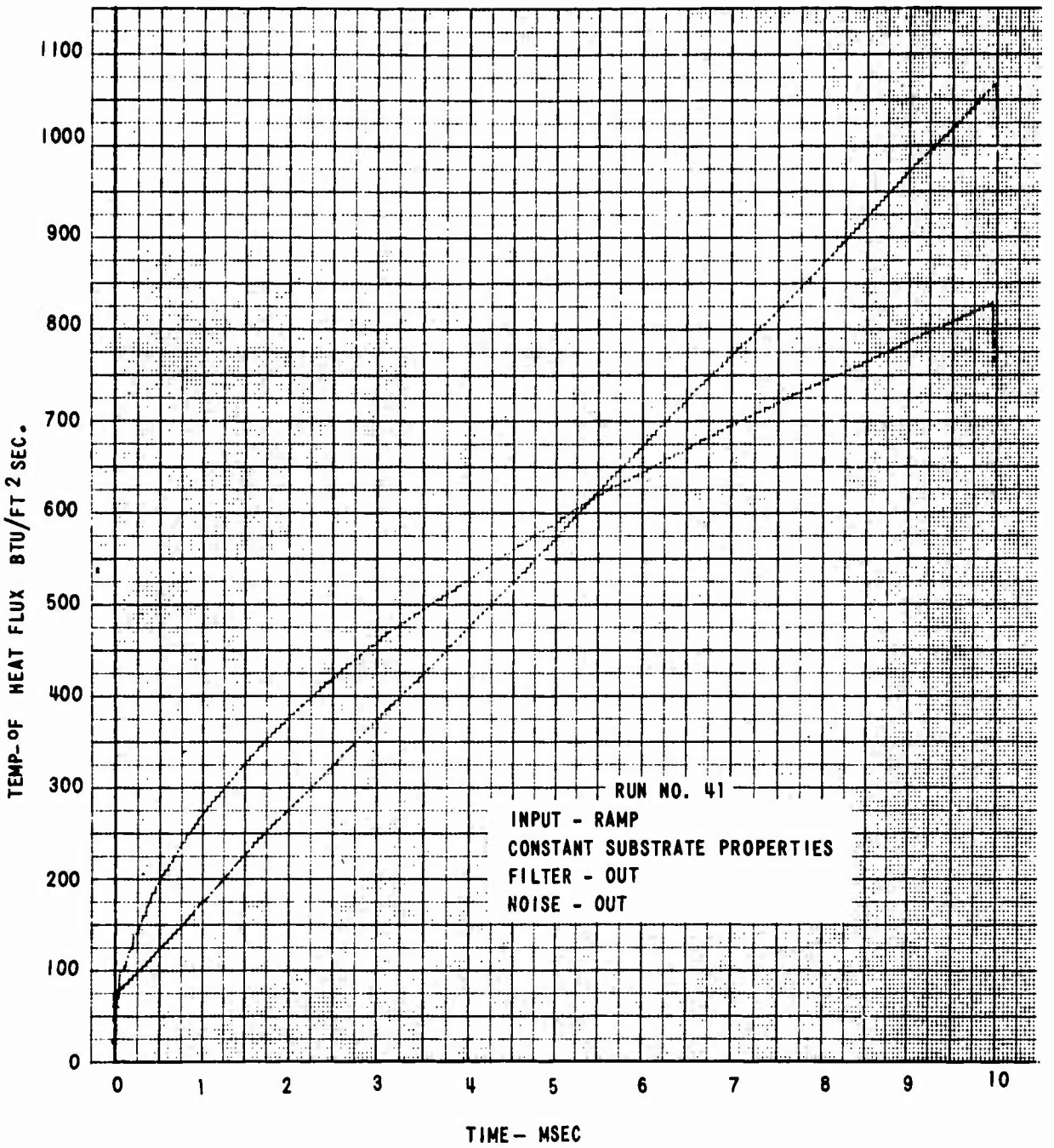
TEMP-OF HEAT FLUX BTU/FT 2 SEC.
1100
1000
900
800
700
600
500
400
300
200
100
0
0
1
2
3
4
5
6
7
8
9
10
TIME- MSEC
RUN NO. 41
INPUT - RAMP
CONSTANT SUBSTRATE PROPERTIES
FILTER - OUT
NOISE - OUT

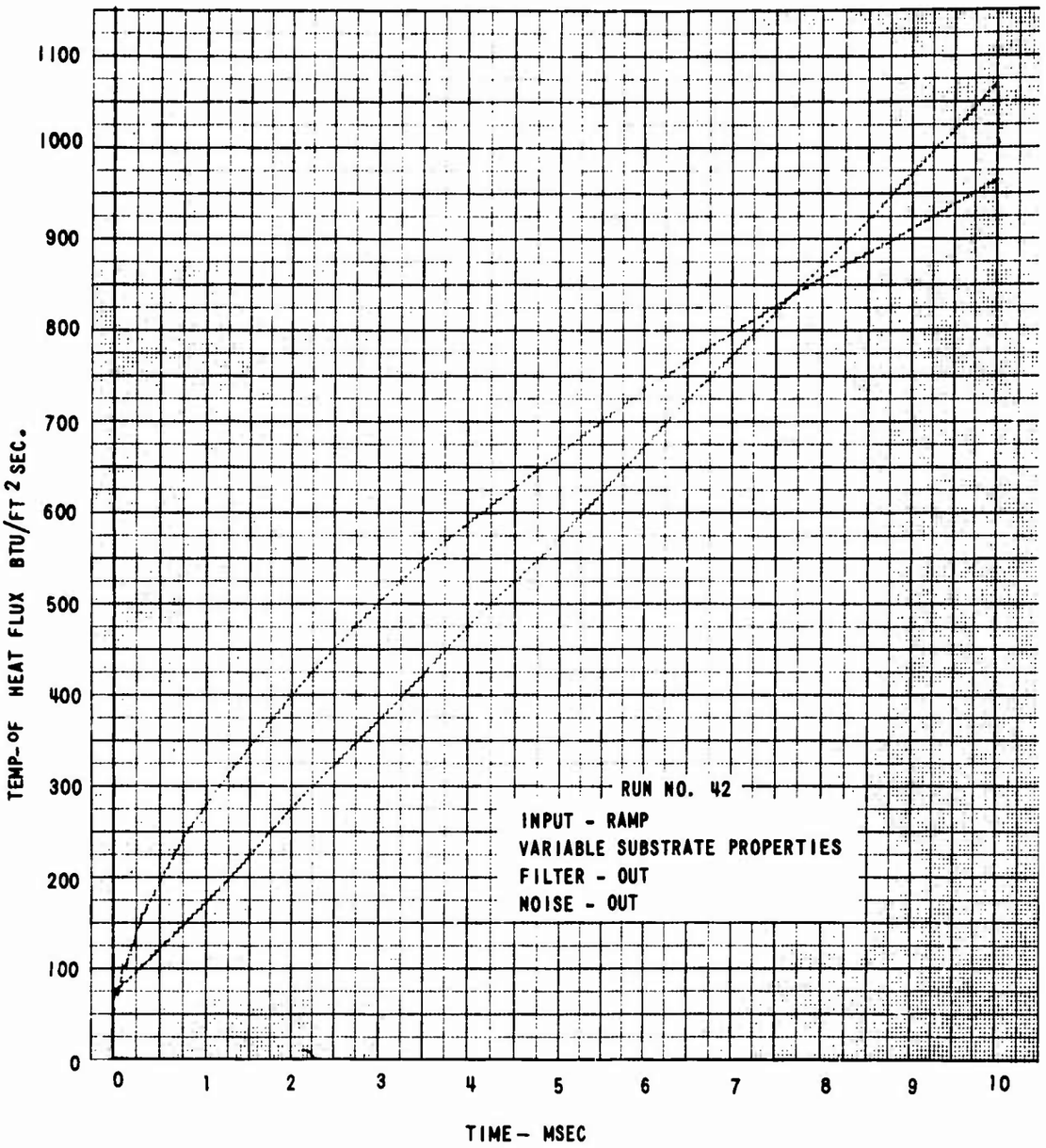
TEMP-°F HEAT FLUX BTU/FT 2 SEC.
1100
1000
900
800
700
600
500
400
300
200
100
0
0
1
2
3
4
5
6
7
8
9
10
TIME— MSEC
RUN NO. 42
INPUT - RAMP
VARIABLE SUBSTRATE PROPERTIES
FILTER - OUT
NOISE - OUT

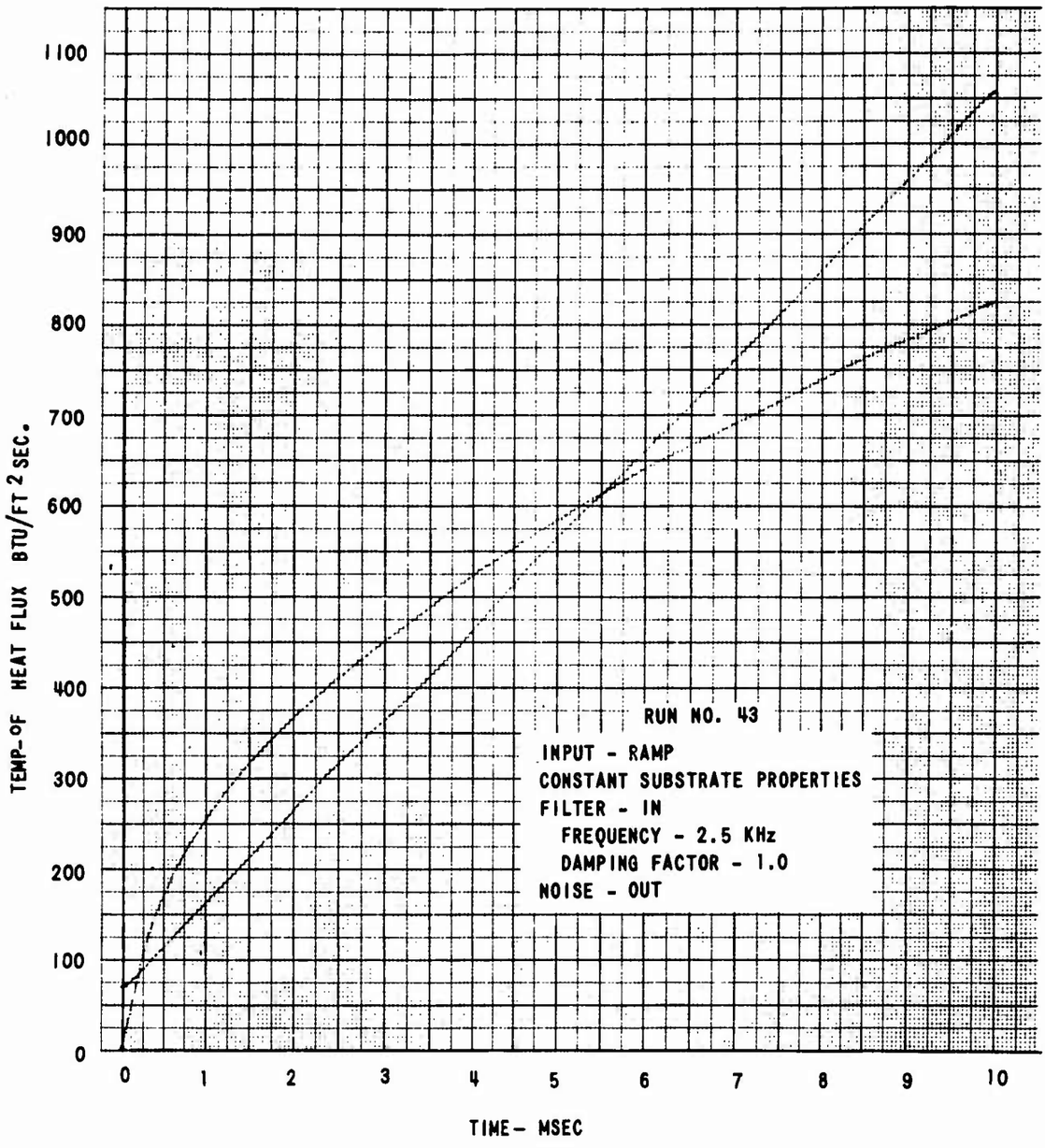
1100
1000
900
800
700
600
500
400
300
200
100
0
TEMP-OF HEAT FLUX BTU/FT 2 SEC.
0
1
2
3
4
5
6
7
8
9
10
TIME- MSEC
RUN NO. 43
INPUT - RAMP
CONSTANT SUBSTRATE PROPERTIES
FILTER - IN
FREQUENCY - 2.5 KHz
DAMPING FACTOR - 1.0
NOISE - OUT

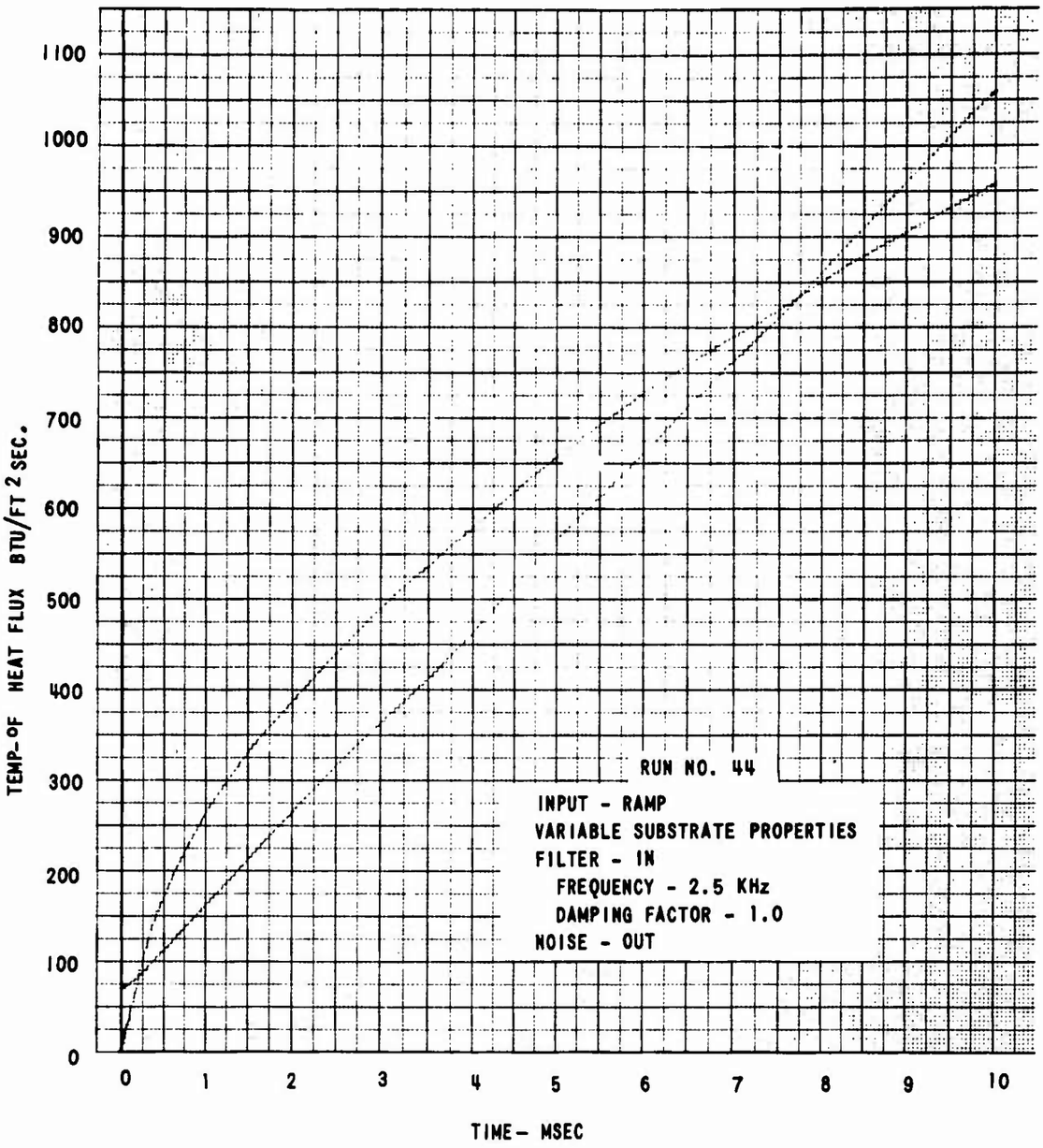
TEMP-OF HEAT FLUX BTU/FT 2 SEC.
1100
1000
900
800
700
600
500
400
300
200
100
0
0
1
2
3
4
5
6
7
8
9
10
TIME- MSEC
RUN NO. 44
INPUT - RAMP
VARIABLE SUBSTRATE PROPERTIES
FILTER - IN
FREQUENCY - 2.5 KHz
DAMPING FACTOR - 1.0
NOISE - OUT

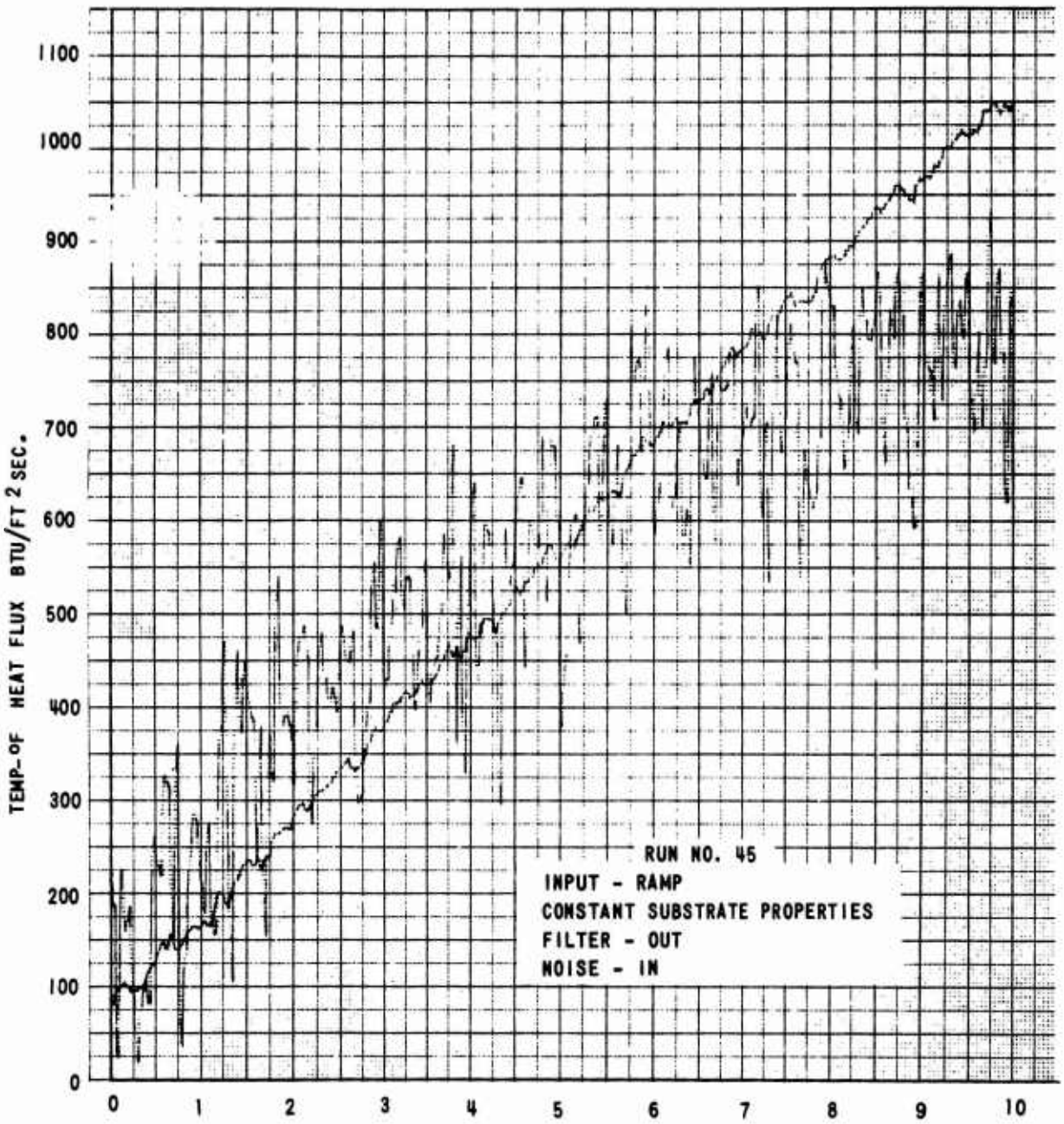
TEMP-OF HEAT FLUX BTU/FT 2 SEC.
1100
1000
900
800
700
600
500
400
300
200
100
0
0
1
2
3
4
5
6
7
8
9
10
TIME- MSEC
RUN NO. 45
INPUT - RAMP
CONSTANT SUBSTRATE PROPERTIES
FILTER - OUT
NOISE - IN

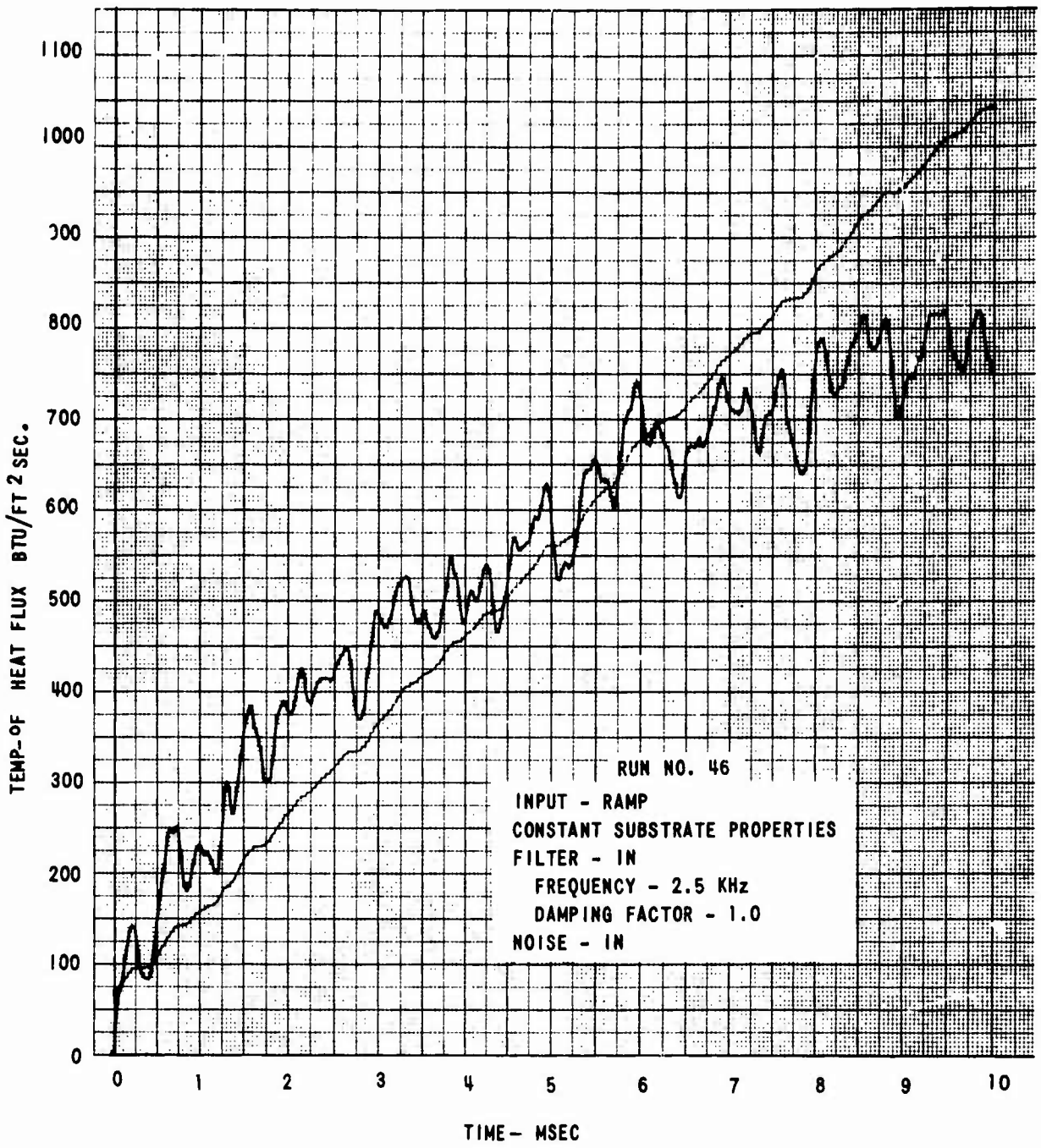
TEMP-OF HEAT FLUX BTU/FT 2 SEC.
1100
1000
900
800
700
600
500
400
300
200
100
0
0
1
2
3
4
5
6
7
8
9
10
TIME- MSEC
RUN NO. 46
INPUT - RAMP
CONSTANT SUBSTRATE PROPERTIES
FILTER - IN
FREQUENCY - 2.5 KHz
DAMPING FACTOR - 1.0
NOISE - IN

APPENDIX B

DIGITAL COMPUTER PROGRAM

W. D. Fryer

The fundamental equation for one-dimensional heat conduction is

$$\frac{\partial T}{\partial t} = \frac{1}{\rho c(T)} \frac{\partial}{\partial x} \left[k(T) \frac{\partial T}{\partial x} \right]$$

With the parameters ρ c(T) and k(T) functions of temperature, the equation is nonlinear.

Represent the solution as T(x, t). The objective is to obtain the solution as a function of time given the following initial conditions

$T(x, 0) = f(x) =$ a constant, $0 \leq x \leq a$

and boundary conditions

$T(0, t) = T(t)$, a prescribed surface temperature history
$T(a, t) =$ a constant end point.

We wish to obtain, $T(x, t)$, $\begin{matrix} 0 \leq x \leq a \\ 0 \leq t < \infty \end{matrix}$

Introduce the variable $\dot{q}$.

$\dot{q} \equiv \dot{q}(x, t) = -k(T) \frac{\partial T}{\partial x}$ (Fortran notation QD $\equiv \dot{q}$)

Substituting into the diffusion equation, we obtain

$\frac{\partial T}{\partial t} = -\frac{1}{\rho c(t)} \frac{\partial \dot{q}}{\partial x}$ (Fortran notation TP $\equiv \frac{\partial T}{\partial t}$)

The temperature T and the heat flow $\dot{q}$ are evaluated at discrete points within the substrate as illustrated below. A total of twenty temperature planes was used (T_o, T_1, ... T_n where n = 19).

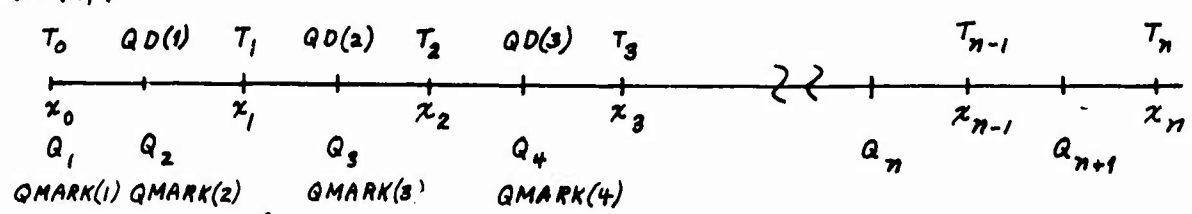

x_i = position of i^{th} temperature plane T(i), i = 0, n (Fortran symbol XMARK)

Q_i = position of i-1 heat flow plane QD(i-1) i = 0, n+1 (Fortran symbol QMARK)

Since the greatest changes in temperature occur near the surface ($x \simeq 0$), the planes are not spaced equally. In this program the plane spacing is defined by a cubic function.

$$p(z) = 5z + \frac{z^2}{2} + \frac{z^3}{3}$$

$$\left.\begin{aligned} x_i &= \text{XMARK (i)} = p(i) \\ Q_{i+1} &= \text{QMARK (i + 1)} = p(i - 1/2) \end{aligned}\right\} \quad \begin{aligned} i &= 1, n \\ Q_1 &= \text{QMARK(1)} = 0 \end{aligned}$$

This transformation in the spatial coordinate provides a close spacing of the planes near the surface.

To calculate the partial derivative with respect to x, the quantity $\partial x / \partial z$ is required.

$$\frac{\partial p(z)}{\partial z} = 5 + z + z^2$$

At the temperature planes

$$\text{DZTT(i)} = 10^{-6} (5 + z + z^2), \; z = i, \; i = 1, \; n.$$

At the heat flow planes

$$\text{DZTQD(i)} = 10^{-6} (5 + z + z^2), \; z = i - 1/2, \; i = 1, n.$$

A factor of 10^{-6} is used to obtain a proper scale factor.

In computing the transient solution it was advantageous to use a change in variable for the time t. This change was of the form $t = \tau^2$ with equal steps of the variable τ used for integration. It was possible by this method to avoid the singularity near t = 0 since the time derivative is infinite at that point for an input function of the form $T = t^{1/2}$.

The substitution $t = \tau (1 - e^{-\beta\tau})$ was made with β a parameter that may be used to control the crossover point (defined as the value of β that makes $\beta\tau = 1$). Thus, $\partial t = \left[1 - e^{-\beta\tau}(1 - \beta\tau)\right] \partial\tau \equiv WF(T)\, \partial\tau$

A simple Runge-Kutta integration scheme is used to advance the temperature history for equal increments of the variable τ. The derivatives are computed from first order differences by the following relation.

$$\dot{q} = \text{QD(I)} = \frac{\text{K*[T(I) - T(I-1)]}}{\text{DZTQD(I)}}, \; \text{I} = 1, \text{N}$$

where K is the value of k(T) evaluated at the temperature

$$T = \frac{\text{T(I)} + \text{T(I-1)}}{2}$$

by the Fortran routine KF(T). This routine fits the experimental data given in Table II for k(T) with two linear equations.

$$k(T) = 2.1765 \times 10^{-4} + 0.111111 \times 10^{7} \; T \; (T \leq 400)$$
$$k(T) = 2.221 \times 10^{-4} - 0.2973 \times 10^{-7} \; (T - 400) \; (T > 400).$$

For the partial derivative of temperature with respect to time,

$$\frac{\partial T}{\partial \tau} = - \frac{1}{\rho c(T)} \frac{\partial \dot{q}}{\partial x} \frac{\partial t}{\partial \tau}$$

$$TP(I) = \frac{-W[QD(I+1) - QD(I)]}{[RHOC*DZTT(I)]} \qquad I = 1, N-1$$

where W is the value of $\partial t/\partial \tau$ evaluated by the Fortran function WF(τ) (WF = $1 - e^{-\beta\tau} + \beta\tau e^{-\beta\tau} = \frac{\partial T}{\partial t}$). And RHOC is the value of $\rho c(T)$ evaluated at the temperature T(I) by the Fortran function RHOCF(T). The data of Table II for $\rho c(T)$ are fitted by two linear functions

RHOCF = 23.7 + 0.02452T, T $\leq$ 420
RHOCF = 34.0 + 0.01155 (T - 420), T > 420

The Runge-Kutta integration routine will produce updated values of T(I), I = 1, N - 1. T(N) is held constant by the boundary condition while T(0) is determined from the function TOF (τ) which is used to generate a parabolic surface temperature history as a trial problem. Setting KONTRL = 1, the substrate properties are held constant at their room temperature values ($k(T) = 2.17 \times 10^{-4}$ and $\rho c(T) = 25.03$). Thus the accuracy of the program may be checked at these specific conditions since the surface heat flux will be constant and of a value calculable exactly from Eq. (3)*. Empirical, or arbitrary, surface temperature data may be introduced by modifying this routine.

True time is obtained from the variable τ by the Fortran function TIMEF(τ) which evaluates the equation $t = \tau\ (1 - e^{-\beta\tau})$. Heat flow at the surface is obtained by linearly extrapolating the values at the first and second heat flow planes. In the program this extrapolation is accomplished in the following manner.

QDS(M, 1) = QD(1) + EXTR[QD(2) - QD(1)]

where EXTR = $\frac{QMARK(2)}{QMARK(2) - QMARK(3)}$

In the present status, the program will accept the following input parameters. If no input parameter isread in, then the default values are automatically supplied.

Fortran Symbol	Definition	Default Value
BETA	β is used in the Fortran function WF(τ)	5000
THICKN	substrate or slab thickness	$\frac{1/16}{12}$
DTAU	$\Delta\tau$ is an equally spaced time interval for the Runge-Kutta integration	5×10^{-6}
KONTRL	equal to 1, ρc and k are kept constant; greater than 1, ρc and k vary with temperature	1
TOAMPL	generates surface temperature input $T_{surface}$ = TOAMPL*$t^{1/2}$ + 70	10,000

*In the main body of the report.

```
CTITLE: MAIN PROGRAM FOR HEAT-FLOW PARTIAL DIFFERENTIAL EQUATION
C           W. FRYER    3/67
C
      COMMON NM,NMP,NMM
      COMMON TAU,DTAU,W,BETA
      COMMON TO,T(30),QD(30),TP(30),XO,XMARK(30),QMARK(30)
      COMMON QDS(201,30),TS(201,30),TIME(201),DAY(2)
      COMMON KONTRL
      COMMON DZTT(30),DZTQD(30)
      REAL KE
      COMMON /LCTO/ TOAMPL
       COMMON/LCTOE/IPRTEM
      NAMELIST/ INPUT/BETA,THICKN,DTAU,KONTRL,TOAMPL,MMAX
C
C     NM  REPRESENTS THE NUMBER OF QD PLANES
C
      NM = 19
      NMP = NM+1
      NMM = NM-1
      XN=NM
C
C
      CALL DVDCHK
      CALL DATE(DAY)
      INB4 = 0
C
C
C    DEFAULT VALUES FOR INPUT DATA
C    THICKN  IS READ IN FEET
        BETA=5000.0
        THICKN=(1.0/16.0)/12.0
        DTAU=.5E-5
        KONTRL=1
        TOAMPL=1.0E+4
        MMAX=200.
C    END OF DEFAULT VALUES FOR INPUT DATA
C
C
C       IPRTEM=INITIAL PRE-RUN TEMPERATURE
        REAL IPRTEM
        IPRTEM=70.0
C
C
C     RKSTEP=NUMBER OF RUNGE-KUTTA INTEGRATION STEPS
        INTEGER RKSTEP
        RKSTEP=2000.
C
C
C       SAVINT=SAVE FOR PRINT INTERVAL DURING R-K. INTEGRATION
C UP TO 200 VALUES OF TIME,QDS,TS,CAN BE SAVED FOR PRINT
        INTEGER SAVINT
        SAVINT=10
C
C
    1 READ (5,INPUT)
        C=(THICKN/(5.*XN+XN**2/2.0+XN**3/3.0) )*1.0E+6
        WRITE(6,3)
    3 FORMAT(1H1)
        WRITE (6,INPUT)
```

```
      IF(KONTRL.GT.0) GO TO 4
      STOP
C
4     CONTINUE
      XO = 0.0
      DO 2  I=1,NM
      Z = I
      XMARK(I)=(5.0*Z+0.5*Z**2+Z**3/3.0)*C
      Z = Z-0.5
    2 QMARK(I+1)=(5.0*Z+0.5*Z**2+Z**3/3.0)*C
      QMARK(1) = C.0
      IF(INB4.GT.0) GO TO 801
      PRINT 800,XO,XO,(XMARK(I),QMARK(I+1),I=1,NM)
  800 FORMAT(1H1 9X 28HPLANE LOCATIONS IN MICROFEET ///
     * 10X 11HTEMPERATURE 13X 4HQDOT // (1X F18.2, F17.2))
      INB4 = 1
      GO TO 802
801   CONTINUE
  802 CONTINUE
C
      TO=IPRTEM
      DO 10  I=1,NM
   10 T(I)=IPRTEM
      DO 18  I=1,NM
      Z = I
      DZTT(I)=C*1.0E-6*(5.0+Z+Z**2)
      Z = Z-0.5
   18 DZTQD(I)=C*1.0E-6*(5.0+Z+Z**2)
      TAU = 0.0
      CALL RNGKT(1,NMM,TAU,DTAU,T,TP)
      EXTR = QMARK(2)/ (QMARK(2)-QMARK(3) )
      J = 0
      M = 0
      DO 100  N=1,RKSTEP
      J = J+1
      CALL RNGKT(2,NMM,TAU,DTAU,T,TP)
   25 IF(J.NE.SAVINT) GO TO 100
      J = 0
      M = M+1
      DO 90  NN=2,NMP
      QDS(M,NN) = QD(NN-1)
   90 TS(M,NN) = T(NN-1)
   95 QDS(M,1) = QD(1) + EXTR*(QD(2)-QD(1))
      TS(M,1) = TO
      TIME(M) = TIMEF(TAU)*1000.0
C
  100 CONTINUE
C
C               CALCULATIONS COMPLETE.
C               GENERATE OUTPUT
110   CONTINUE
      PRINT 120, DAY
120   FORMAT(1H1,23X,36HSURFACE TEMPERATURE AND QDOT HISTORY,10X,2A4/)
      WRITE(6,130)
130   FORMAT(3X,4HTIME,9X,1HT,11X,4HQDOT/2X,6H(MSEC))
      PRINT 140,(TIME(I),TS(I,1),QDS(I,1),I=1,MMAX)
140   FORMAT(1X,F5.2,F11.2,F11.2)
  165 GO TO 1
      END
```

```
CTITLE: SUBROUTINE DAUX FOR HEAT-FLOW EQUATION.  WDF 3/67
      SUBROUTINE DAUX
      COMMON NM,NMP,NMM
      COMMON TAU,DTAU,W,BETA
      COMMON T0,T(30),QD(30),TP(30),X0,XMARK(30),QMARK(30)
      COMMON QDS(201,30),TS(201,30),TIME(201),DAY(2)
      COMMON KONTRL
      COMMON DZTT(30),DZTQD(30)
      REAL K,KF
      T0 = TOF(TAU)
      TMID = (T(1)+T0)/2.0
      K = KF(TMID)
      QD(1) = -K*(T(1)-T0)/DZTQD(1)
      DO 10  I=2,NM
      TMID =(T(I)+T(I-1))/2.0
      K = KF(TMID)
   10 QD(I) = -K*(T(I)-T(I-1))/DZTQD(I)
C
      DO 20  I=1,NMM
      RHOC = RHOCF(T(I))
      W = WF(TAU)
   20 TP(I) = -W*(QD(I+1)-QD(I))/ (RHOC*DZTT(I))
C
      RETURN
      END
```

```
CTITLE: FUNCTION TOF(TAU) - PARABOLA          WDF  3/67
C
      FUNCTION TOF(TAU)
       REAL IPRTEM
      COMMON NM,NMP,NMM
      COMMON DUM,DTAU,W,BETA
      COMMON T0,T(30),QD(30),TP(30),X0,XMARK(30),QMARK(30)
      COMMON QDS(201,30),TS(201,30),TIME(201),DAY(2)
      COMMON /LCTO/ TOAMPL
       COMMON/LCTOF/IPRTEM
      TIM = TIMEF(TAU)
      X = TOAMPL*SQRT(TIM)
      TOFA = (1.0-SQRT(1.0-5.18E-4*X))/2.59E-4
      TOF=TOFA+IPRTEM
      RETURN
      END
```

```
CTITLE: FUNCTION KE(T): CONSTANT                    WDE  3/67
      REAL FUNCTION KE(T)
      COMMON IGNORE(12422)
       COMMON KONTRL
      IF(KONTRL.GT.1) GO TO 20
      KE = 2.17E-4
      RETURN
C
   20 IF(T.GT.400.0) GO TO 30
      KE = 2.1765E-4 + 0.111111E-7*T
      RETURN
   30 KE = 2.221E-4 - 0.2973E-7*(T-400.0)
      RETURN
      END
```

```
CTITLE: RHOCE (CONSTANT)                            WDE  3/67
      FUNCTION RHOCE(T)
      COMMON IGNORE(12422)
      COMMON KONTRL
      IF(KONTRL.GT.1) GO TO 20
      RHOCE = 25.03
      RETURN
C
   20 IF(T.GT.420.0) GO TO 30
      RHOCE = 23.7 + 0.02452*T
      RETURN
   30 RHOCE = 34.0 + 0.01155*(T-420.0)
      RETURN
      END
```

```
CTITLE: FUNCTION TIMEF(TAU)          WDE  3/67
      FUNCTION TIMEF(TAU)
      COMMON NM,NMP,NMM
      COMMON DUM,DTAU,W,BETA
      COMMON T0,T(30),Q0(30),TP(30),X0,XMARK(30),QMARK(30)
      COMMON QDS(201,30),TS(201,30),TIME(201),DAY(2)
   10 ARG = BETA*TAU
      IF(ARG.LT.2.0E-7) GO TO 30
      IF(ARG.GT.20.0) GO TO 40
   20 TIMEF = TAU*(1.0-EXP(-ARG))
      RETURN
   30 TIMEF = TAU*ARG
      RETURN
   40 TIMEF = TAU
      RETURN
      END
```

```
CTITLE: FUNCTION WE(TAU)             WDE  3/67
C
      FUNCTION WE(TAU)
      COMMON NM,NMP,NMM
      COMMON DUM,DTAU,W,BETA
      COMMON T0,T(30),Q0(30),TP(30),X0,XMARK(30),QMARK(30)
      COMMON QDS(201,30),TS(201,30),TIME(201),DAY(2)
C
      ARG = BETA*TAU
      IF(ARG.GT.25.0) GO TO 20
      IF(ARG.LT.1.0E-7) GO TO 30
      E = EXP(-ARG)
      WE = 1.0-E + E*ARG
      RETURN
   20 WE = 1.0
      RETURN
   30 WE = 2.0*ARG
      RETURN
      END
```

```
C IBETC RNGKT                  SINGLE PRECISION RUNGE KUTTA    (IBM 360)
C
C*******************************************************************************
C*                                                                             *
C*                          SUBROUTINE RNGKT                                   *
C*                              CU 0067                                        *
C*                                                                             *
C*     PURPOSE                                                                 *
C*        SINGLE PRECISION RUNGE-KUTTA INTEGRATION (BLUM'S MODIFICAT-          *
C*        ION) FOR N (N=1 TO 30) DIFFERENTIAL EQUATIONS. EACH CALL             *
C*        OF  RNGKT CAUSES INTEGRATION FOR ONE STEP.                           *
C*         NOTE. DOUBLE PRECISION IS USED IN INCREMENTING INDE-                *
C*         PENDENT VARIABLE.                                                   *
C*                                                                             *
C*     USAGE                                                                   *
C*        CALL  RNGKT (INIT,N,X,H,Y,YP)                                        *
C*                                                                             *
C*     DESCRIPTION OF PARAMETERS                                               *
C*        INIT  =1  FOR INITIALIZATION,                                        *
C*              =2 FOR INTEGRATE ONE STEP                                      *
C*        N     NUMBER OF FIRST-ORDER DIFFERENTIAL EQUATIONS                   *
C*        X     INDEPENDENT VARIABLE (SINGLE PRECISION)                        *
C*        H     STEP SIZE (SINGLE PRECISION)                                   *
C*        Y     ARRAY OF DEPENDENT VARIABLES (SINGLE PRECISION)                *
C*        YP    ARRAY OF DERIVATIVES OF Y WRT X (SINGLE PRECISION)             *
C*                                                                             *
C*     REMARKS                                                                 *
C*        USER MUST SUPPLY A SUBROUTINE DAUX, SUCH THAT 'CALL DAUX'            *
C*        (WITHOUT EXPLICIT ARGUMENTS) CAUSES THE YP VALUES TO BE              *
C*        CALCULATED,  USING X AND VALUES FROM THE Y ARRAY.                    *
C*                                                                             *
C*        INITIALIZATION (INIT = 1) IS REQUIRED AFTER USER SETS                *
C*        INITIAL VALUES OF X AND THE Y-ARRAY.  RE-INITIALIZATION              *
C*        IS NOT NECESSARY FOR CHANGES IN STEP SIZE, H.                        *
C*                                                                             *
C*     SUBROUTINES AND FUNCTION SUBPROGRAMS REQUIRED                           *
C*        DAUX     (SEE PREVIOUS REMARKS)                                      *
C*                                                                             *
C*     METHOD                                                                  *
C*        THE E.K. BLUM MODIFICATION OF THE RUNGE-KUTTA FOURTH-                *
C*        ORDER METHOD IS USED. SEE                                            *
C*            'MATHEMATICS OF COMPUTATION', APRIL, 1962  PP 176-187            *
C*                                                                             *
C*     AUTHOR DATE                                                             *
C*        W. FRYER                                                             *
C*        CORNELL AERO. LAB                                                    *
C*        OCTOBER, 1966                                                        *
C*                                                                             *
C*        NOTE. CODING IS ADAPTED FROM SQUARE PARTEE                           *
C*              INTEGRATOR PROGRAMS RINT1 AND RINT.                            *
C*              DECKS CU0053, CU0054.                                          *
C*                                                                             *
C*******************************************************************************
C
      SUBROUTINE  RNGKT (INIT,N,/X/,H,Y,YP)
C
            REAL          X,H,Y(1),YP(1)
      REAL  P(30), Q(30)
      DOUBLE PRECISION X0, HD
```

```
C
      GO TO (4,8), INIT
    4 CALL DAUX
    5 XO = X
      RETURN
C
    8 HO = H
      DO 10 I=1,N
      P(I) = H*YP(I)
      Y(I) = Y(I) + 0.5*P(I)
   10 Q(I) = P(I)
C
      X = XO + 0.500*HO
      CALL DAUX
C
      DO 20 I=1,N
      P(I) = H*YP(I)
      Y(I) = Y(I) + 0.5*(P(I)-Q(I))
   20 Q(I) = Q(I)/6.0
C
      CALL DAUX
C
      DO 30 I = 1,N
      P(I) = H*YP(I) - 0.5*P(I)
      Y(I) = Y(I) + P(I)
   30 Q(I) = Q(I) - P(I)
C
      XO = XO + HO
      X = XO
      CALL DAUX
C
      DO 40 I = 1,N
      P(I) = H*YP(I) + (P(I)+P(I))
   40 Y(I) = Y(I) + (Q(I)+P(I)/6.0)
C
      CALL DAUX
C
      RETURN
      END
```

APPENDIX C

DERIVATION OF CORRECTION FUNCTIONS FOR THE COMPENSATED ANALOG CIRCUIT

S. A. R. Ayyar

This appendix is comprised of three sections. Part I is a summary while Part II discusses the mathematics associated with the correction for the nonlinear resistance-temperature function of the gage resistance element and Part III presents the mathematics underlying the compensation for the variation of substrate thermal properties with temperature.

I. SUMMARY

As the thin-film resistance thermometer is used to measure high heat flux, the surface temperature may be carried into the range where the thermal coefficient of resistivity of the resistance element and the thermal conductivity and diffusivity of the substrate material are affected. Recent research has shown that these temperature sensitive effects can be combined mathematically into a single correction factor and applied as an operation on the gage electrical output. This means, in practice, the gage output voltage is subjected to electrical compensation before it is introduced as the input to a conventional heat transfer analog network to provide a signal proportional to the true heat flux.

The correction factor, which is a curve with voltage output as abscissa and transformed temperature as the ordinate, is the result of two effects. First, we establish the relationship between voltage output and temperature rise of the gage considering the thermal coefficient of resistivity of the resistance element. This relationship for a particular gage under study takes the following form:

$$\theta_w{}^\circ F = 0.386 \times 10^4 - \sqrt{0.149 \times 10^8 - 0.0771 \times 10^8 \frac{\mu_g}{U_{g_o}}} \qquad \text{(C-1)}$$

$\theta_w{}^\circ F$ = temperature rise, °F
μ_g = gage voltage rise
U_{g_o} = initial gage voltage

The derivation of this expression is shown in Part II.

Next, we establish the relationship between temperature rise obtained above and transformed temperature rise which takes into consideration the thermal conductivity and diffusivity effects of the substrate material. This relationship takes the following form:

$$\phi_w^{(o)} = \theta_w \left[1 - \left(\frac{\pi}{16} \alpha \right) \theta_w \right] \qquad \text{(C-2)}$$

$\phi_w^{(o)}$ = transformed temperature rise in °C
θ_w = temperature rise in °C

For the particular gage and substrate thermal properties provided, the following value is obtained for the constant a:

$$a = -.00096/°C \text{ rise}$$

Since we have θ_ω in °F from Eq. (C-1)*, the relationship (C-2) becomes

$$\phi_\omega^{(o)} = \theta_\omega\,(°F)\left[1 + .0001882\left(\frac{5}{9}\right)\theta_\omega\,(°F)\right] \qquad \text{(C-3)}$$

Here,

$\phi_\omega^{(o)}$ = transformed temperature rise in °F

θ_ω = temperature rise in °F.

The derivation of Eq. (C-3) is shown in Part III.

II. EFFECTS OF GAGE NONLINEAR RESISTANCE VARIATION

A. Mathematics

The resistance-temperature function of the thin-film resistance element is defined by the second degree equation.[13]

$$R_{T=T} = a_o + b_o T - c_o T^2$$

$$= a_1 + a_2 (T - 70°) - a_3 (T - 70°)^2 \qquad \text{(C-4)}$$

a_1 = value of gage resistance at T = 70 °F.

Differentiating Eq. (C-4)

$$\frac{dR_T}{dT} = 0 + a_2 - 2a_3 (T - 70°) \qquad \text{(C-5)}$$

The constant a_2 is the value of gage constant k at T = 70 °F, i.e.,

$$a_2 = \frac{dR}{dT}_{T = 70°F} = k_{T = 70°}$$

Substituting into Eq. (C-5) and using experimentally determined values for the coefficients[7], Eq. (C-6) is obtained.

$$\frac{dR}{dT}_{T=T} = \frac{dR}{dT}_{T=70°F}\left[1 - \frac{2a_3}{K_{T=70}}(T-70°)\right] \qquad \text{(C-6)}$$

$$= \frac{dR}{dT}_{T=70°F}\left[1 - 2.59 \times 15^{4}(T-70°)\right]$$

The temperature coefficient of resistance of the gage, β, may be defined as follows.

---

*Eq. (C-2) was derived in the Centigrade unit to afford a direct comparison with information given in the referenced material.

$$\beta = \frac{1}{R_{g_o}} \frac{dR_g}{d\theta}$$

$$\beta_{T=T} = \frac{1}{R_{g_o}} \left(\frac{dR_g}{d\theta}\right)_{T=T}$$

$$\beta_{T=70°F} = \frac{1}{R_{g_o}} \left(\frac{dR_g}{d\theta}\right)_{T=70°F}$$

In Ref. 7 the temperature coefficient of resistance is shown to vary according to the following function

$$\beta(\theta) = \beta_o (1 - \gamma\theta) \tag{C-7}$$

By integration

$$\int_o^{\theta_\omega} (\beta_o - \beta_o \gamma \theta)\, d\theta = \beta_o \left(\theta_\omega - \frac{\gamma}{2} \theta_\omega^2\right)$$

Thus

$$\frac{R_g - R_{g_o}}{R_{g_o}} = \frac{\Delta R}{R_{g_o}} = \beta_o \left(\theta_\omega - \frac{\gamma}{2} \theta_\omega^2\right) \tag{C-8}$$

Rearranging the terms of Eq. (C-8), we obtain

$$\frac{\gamma}{2} \theta_\omega^2 - \theta_\omega + \frac{\Delta R}{R_{g_o} \beta_o} = 0$$

Solving for θ_ω

$$\theta_\omega = \frac{1}{\gamma} - \sqrt{\frac{1}{\gamma^2} - \frac{2\Delta R}{\beta_o \gamma R_{g_o}}} \tag{C-9}$$

Using the data given in Ref. 7, $\gamma = 2.59 \times 10^{-4}$/°F and $\beta_o = 1 \times 10^{-3}$/°F, and substituting into Eq. (C-9)

$$\theta_\omega = \frac{1}{2.59 \times 10^{-4}} - \sqrt{\frac{1}{(2.59 \times 10^{-4})^2} - \frac{2\Delta R}{\frac{1}{R_{g_o}} \frac{dR_g}{d\theta} (2.59 \times 10^{-4}) R_{g_o}}} \tag{C-10}$$

Notation

R	=	resistance
T	=	conditions at temperature T
a_o	=	gage resistance at 0°C
R_{g_o}	=	initial resistance of the thin film
β	=	temperature coefficient of resistance of the thin film
θ	=	temperature rise measured from its initial level
θ_w	=	gage surface temperature rise
γ	=	constant as defined in the equation (6)
ΔR	=	change in resistance of the thin film
u_g	=	voltage rise in the gage
U_{g_o}	=	initial voltage across the gage.

B. Practical Data

By maintaining a constant excitation current through the resistance element of the gage, the following relation will hold

$$\frac{\Delta R}{R_{g_o}} = \frac{u_g}{U_{g_o}}$$

Substituting this relation in Eq. (C-10)

$$\theta_w(°F) = \frac{1}{2.59\times10^{-4}} - \sqrt{\frac{1}{(2.59\times10^{-4})^2} - \frac{2u_g}{\frac{1}{R_{g_o}}\left(\frac{dR_g}{d\theta}\right)_{T=70°F}(2.59\times10^{-4})U_{g_o}}} \quad \text{(C-11)}$$

Equation (C-11) is the general relationship. For circuit design purposes, some typical data were substituted for gage parameters

$$R_{g_o} = 100 \text{ ohms} \qquad \left(\frac{dR_g}{dt}\right)_{T=70°F} = 0.1 \text{ ohm}/°F$$

$$\theta_w(°F) = 0.386\times10^4 - \sqrt{0.149\times10^8 - 0.0771\times10^8\frac{u_g}{U_{g_o}}} \quad \text{(C-12)}$$

III. EFFECTS OF SUBSTRATE PROPERTY VARIATION

A. Mathematics

The derivation of the correction formula, Eq. (C-2), is taken from Ref. 14 except for some changes of notation. The equation governing the thermal diffusion is

$$\rho c(\theta)\frac{\partial\theta}{\partial t} = \frac{\partial}{\partial y}\left[k(\theta)\frac{\partial\theta}{\partial y}\right] \quad \text{(C-13)}$$

Here,

ρ	=	density
c	=	specific heat
θ	=	temperature rise above initial temperature
t	=	time
y	=	distance below surface of slab
k	=	thermal conductivity

We introduce ϕ as the transformed temperature

$$\phi = \frac{1}{k_o} \int_0^\theta k \, d\theta \tag{C-14}$$

Here k_o is the thermal conductivity at the initial temperature. In Ref. 14, a constant b is introduced which reflects a linear relationship between k and k_o. In our case, the k variation with temperature in the range under consideration is such as to make the relationship ϕ versus θ almost equal (see Table II).

Proceeding as per Ref. 14, transformation of Eq. (14) is applied to Eq. (13).

$$\frac{\partial \phi}{\partial t} - K \frac{\partial^2 \phi}{\partial y^2} = 0 \tag{C-15}$$

which is the form in which diffusion equation is customarily given. Equation (C-15) is nonlinear since the diffusivity K is a function of temperature, i. e.,

$$K = K(\phi) \tag{C-16}$$

Hartunian and Varwig[5] applied a perturbation technique to linearize Eq. (C-15). Here we take

$$\begin{aligned} \phi &= \phi^{(0)} + \phi^{(1)} \\ K &= K^{(0)} + K^{(1)} \end{aligned} \tag{C-17}$$

Equation (C-17) is substituted into Eq. (C-15) and terms of like order collected to provide the zeroth order equation

$$\frac{\partial \phi^{(o)}}{\partial t} - K^{(o)} \frac{\partial^2 \phi^{(o)}}{\partial y^2} = 0 \tag{C-18}$$

and the first order equation

$$\frac{\partial \phi^{(1)}}{\partial t} - K^{(o)} \frac{\partial^2 \phi^{(1)}}{\partial y^2} = \frac{K^{(1)}}{K^{(o)}} \frac{\partial \phi^{(o)}}{\partial t} \tag{C-19}$$

The heat flux $\dot{q}$ at the boundary of the semi-infinite body is given by

$$\dot{q} = - k_o \left. \frac{\partial \phi}{\partial y} \right|_w \tag{C-20}$$

where the subscript w refers to the wall surface, y = 0.

The solution to the zeroth order equation is

$$\phi_w^{(o)} = 2 \frac{q_o}{k_o} \sqrt{\frac{K^{(o)} t}{\pi}} \qquad \dot{q} = \dot{q}_o \tag{C-21}$$

The first order solution obtained by Hartunian and Varwig is based on taking $K^{(0)}$ equal to the constant K_o, which is the diffusivity at initial conditions and then further taking $K^{(1)}$ proportional to $\phi^{(0)}$, i. e.,

$$K^{(1)} = a K_o \phi^{(o)} \tag{C-22}$$

With this relation, the first order solution then provides

$$\phi_w^{(1)} = \frac{1}{4} \frac{a K_o}{k_o^2} \dot{q}^2 t \tag{C-23}$$

Using Eq. (C-21)

$$\phi_\omega^{(1)} = \frac{\pi}{16}\, a \left[\phi_\omega^{(0)}\right]^2 \tag{C-24}$$

with which

$$\phi_\omega = \phi_\omega^{(0)} + \frac{\pi}{16}\, a \left[\phi_\omega^{(0)}\right]^2 \tag{C-25}$$

The particular solution required is that for $\phi_\omega{}^{(0)}$. Assuming $\frac{\pi}{16}\, a\, \phi_\omega^{(0)} << 1$, Eq. (C-25) may be inverted without difficulty to yield a polynomial in ϕ_ω.

$$\begin{aligned} \phi_\omega^{(0)} &= \phi_\omega \left[1 - \frac{\pi}{16}\, a\, \phi_\omega + \cdots\right] \\ &= \phi_\omega \left[1 - \frac{\pi}{16}\, a\, \phi_\omega\right] \end{aligned} \tag{C-26}$$

Using the data on substrate properties given in Table II, the diffusivity was approximated by the linear function $K = K_o\,(1 + a\,\phi)$ with "a" evaluated from the slope of K versus ϕ. Substituting the value a = -0.00096/°C into Eq. (C-26) and converting into Fahrenheit, the desired correction function is obtained

$$\phi_\omega(^\circ F_{rise}) = \theta_\omega(^\circ F_{rise})\,[1 + .0001882\,(5/9)\;\theta_\omega(^\circ F_{rise})] \tag{C-27}$$

APPENDIX D

COMPUTER PROGRAM FOR DEFINING COMPONENT VALUES FOR THE ANALOG NETWORK

The program for designing the analog network having a frequency response $k\sqrt{s}$ is written in Fortran and was run on a Quicktran terminal served by an IBM 7044 computer. With minor modifications, it should run on any IBM computer as well as several other machines. Input variables are written into the program since it is not anticipated that several networks would be designed at any one time. These variables specify the lowest frequency at which the response of the network approximates $k\sqrt{s}$ (see Note 1) and the range of frequency coverage, specified as the logarithm of the ratio of the highest usable frequency to the lowest usable frequency (see Note 2). There are eight RC sections in the network. According to Skinner[2], a network of n sections should adequately cover (2n - 1) octaves, i.e., an eight section network is useful over 15 octaves or 4.5 decades.

Output is specified in the form of resistance (ohms) and capacitance (farads) values of the elements of the network. In the program printout, the first value printed is a zero* succeeded by a one ohm terminating resistor, followed by a shunt capacitance, a series resistor, and so on for a total of seventeen elements. The values are scaled to suit the designer by multiplying resistances by a convenient factor and dividing capacitances by the same factor. A listing of the program follows:

```
      LIST
      PROGRAM POLY
      DIMENSION DUP(170),AM(18)
      DIMENSION AR(9,18), ELEMENT(18)
      DIMENSION A(18), D(18), P(*), Z(*)
      INTEGER AO, DO, PO, ZO
      WRITE (6, 92)
   92 FORMAT (8X, 8HSTARTING)
      AO = 0
      PO = 1
      DO = 0
      ZO = 1
      NP = 1
      NZ = 1
      DO 10 J=1, 18
      ELEMNT(J)=0.
      DO 10 I=1, 9
      A(J)=0.
      D(J)=0.
   10 AR(I, J)=0.
      A(1)=1.
      D(1)=1.                    ...(1)
```

*This first value has no significance and should be disregarded.

[1]Lower limit (Hz).

```
      P1=.003
      P1=P1*6.28318                    ...(2)
      AN=4.5
      M=8
      M2=2*M
      RD=M2+1
      DO 1 I=1,M2
      AI I
      RN=AI*AN
      R=RN/RD
    1 AM(I)=10.**R
      DO 2 I=1,M
      L=2*I-1
      Z(I)=P1*AM(L)
    2 P(I)=P1*AM(L+1)
      WRITE (6,99)P                    ...(3)
      WRITE (6,99)Z                    ...(4)
      NP=M
      NZ=M
      AO=1
      DO=1
      I=1
      DO 111 N=1,NZ
      DO 110 IND=1,AO
      I=AO-IND+1
      A(I+1)=A(I+1)*Z(N)+A(I)
  110 CONTINUE
      A(1)=A(1)*Z(N)
      AO=AO+1
  111 CONTINUE
      DO121 N=1,NP
      DO120 IND=1,DO
      I=DO-IND+1
      D(I+1)=D(I+1)*P(N)+D(I)
  120 CONTINUE
      D(1)=D(1)*P(N)
      DO=DO+1
  121 CONTINUE
      WRITE (6,99)A                    ...(5)
      WRITE (6,99)D                    ...(6)
   99 FORMAT(1X,9E12.4)
      DO 131 J=1,AO
      I=AO-J+1
  131 AR(I,1)+D(J)
      DO 132 J=1,DO
      I=DO-J+1
  132 AR(I,2)=A(J)
   91 FORMAT(8X,218)
  130 CONTINUE
      DO 20 J=3,18
      DO 20 I=1,8
      IF(AR(1,J-1))25,25,19
   19 CONTINUE
      AR(I,J)=AR(I+1,J-2)-AR(1,J-2)*
        AR(I+1,J-1)/AR(1,J-1)
   20 CONTINUE
   25 CONTINUE
      DO 30 L=2,18
      IF(AR(1,L))31,31,29
   29 ELEMNT(L)=AR(1,L-1)/AR(1,L)
   30 CONTINUE
   31 CONTINUE
      WRITE (6,90)AR                   ...(7)
   90 FORMAT(1X,9E12.4)
      WRITE (6,90)ELEMNT               ...(8)
      STOP
      END
```

---

[2] Logarithmic range

[3] Poles

[4] Zeros

[5] Polynomial (generated from zeros)

[6] Polynomial (generated from poles)

[7] Array for calculating with Routh's algorithm (Ref. 15)

[8] Element values

Unclassified

Security Classification

DOCUMENT CONTROL DATA - R&D

(Security classification of title, body of abstract and indexing annotation must be entered when the overall report is classified)

1 ORIGINATING ACTIVITY *(Corporate author)*
Cornell Aeronautical Laboratory, Inc.
Buffalo, New York 14221

2a. REPORT SECURITY CLASSIFICATION
Unclassified

2b GROUP
None

3 REPORT TITLE TRANSIENT HEAT TRANSFER MEASUREMENT WITH THIN-FILM RESISTANCE THERMOMETERS--DATA REDUCTION TECHNIQUES

4 DESCRIPTIVE NOTES *(Type of report and inclusive dates)*
Final Report, April 1967 - September 1967

5 AUTHOR(S) *(Last name, first name, initial)*
Bogdan, Leonard

6. REPORT DATE	7a. TOTAL NO. OF PAGES	7b. NO. OF REFS
October 1967	108	15

8a. CONTRACT OR GRANT NO.	9a. ORIGINATOR'S REPORT NUMBER(S)
AF33(615)-67-C-1144	AE-2385-Y-2
b. PROJECT NO. 615E	
c.	9b. OTHER REPORT NO(S) *(Any other numbers that may be assigned this report)* AFAPL-TR-67-141
d.	

10. AVAILABILITY/LIMITATION NOTICES
This document is subject to special export controls and each transmittal to foreign governments or foreign nationals may be made only with prior approval of the Ramjet Engine Div., AF Aero Propulsion Lab., Wright-Patterson AFB, Ohio 45433.

11. SUPPLEMENTARY NOTES	12. SPONSORING MILITARY ACTIVITY
None	Air Force Aero Propulsion Laboratory Research & Technology Div., AF Systems Command, Wright-Patterson AFB, Ohio

13. ABSTRACT

An account is presented of experimental studies of techniques of data reduction required to convert measurements obtained with thin-film resistance thermometers to incident heating rates. Emphasis is on development of practical data reduction techniques accommodating nonspecific gage surface temperature histories as well as temperature excursions sufficiently large to necessitate correction for variable thermal properties of the gage.

Analog computer solutions were obtained for a range of surface temperature functions representative of phenomena observed in actual shock tunnel operations. The mathematical formulation used in the analog studies was adapted to the development of an economical and general digital data reduction program. A description is given of the operation and design details of a compensated analog circuit which operates directly on the electrical output of the thin-film gage to provide an output signal proportional to the true heating rate.

DD FORM 1 JAN 64 1473

Unclassified

Security Classification

Unclassified

Security Classification

14. KEY WORDS	LINK A		LINK B		LINK C	
	ROLE	WT	ROLE	WT	ROLE	WT
Heat transfer Thin-film resistance thermometers Data reduction programs Compensated analog circuit						

INSTRUCTIONS

1. ORIGINATING ACTIVITY: Enter the name and address of the contractor, subcontractor, grantee, Department of Defense activity or other organization *(corporate author)* issuing the report.

2*a*. REPORT SECURITY CLASSIFICATION: Enter the overall security classification of the report. Indicate whether "Restricted Data" is included. Marking is to be in accordance with appropriate security regulations.

2*b*. GROUP: Automatic downgrading is specified in DoD Directive 5200.10 and Armed Forces Industrial Manual. Enter the group number. Also, when applicable, show that optional markings have been used for Group 3 and Group 4 as authorized.

3. REPORT TITLE: Enter the complete report title in all capital letters. Titles in all cases should be unclassified. If a meaningful title cannot be selected without classification, show title classification in all capitals in parenthesis immediately following the title.

4. DESCRIPTIVE NOTES: If appropriate, enter the type of report, e.g., interim, progress, summary, annual, or final. Give the inclusive dates when a specific reporting period is covered.

5. AUTHOR(S): Enter the name(s) of author(s) as shown on or in the report. Enter last name, first name, middle initial. If military, show rank and branch of service. The name of the principal author is an absolute minimum requirement.

6. REPORT DATE: Enter the date of the report as day, month, year, or month, year. If more than one date appears on the report, use date of publication.

7*a*. TOTAL NUMBER OF PAGES: The total page count should follow normal pagination procedures, i.e., enter the number of pages containing information.

7*b*. NUMBER OF REFERENCES: Enter the total number of references cited in the report.

8*a*. CONTRACT OR GRANT NUMBER: If appropriate, enter the applicable number of the contract or grant under which the report was written.

8*b*, 8*c*, & 8*d*. PROJECT NUMBER: Enter the appropriate military department identification, such as project number, subproject number, system numbers, task number, etc.

9*a*. ORIGINATOR'S REPORT NUMBER(S): Enter the official report number by which the document will be identified and controlled by the originating activity. This number must be unique to this report.

9*b*. OTHER REPORT NUMBER(S): If the report has been assigned any other report numbers *(either by the originator or by the sponsor)*, also enter this number(s).

10. AVAILABILITY/LIMITATION NOTICES: Enter any limitations on further dissemination of the report, other than those imposed by security classification, using standard statements such as:

(1) "Qualified requesters may obtain copies of this report from DDC."

(2) "Foreign announcement and dissemination of this report by DDC is not authorized."

(3) "U. S. Government agencies may obtain copies of this report directly from DDC. Other qualified DDC users shall request through _____."

(4) "U. S. military agencies may obtain copies of this report directly from DDC. Other qualified users shall request through _____."

(5) "All distribution of this report is controlled. Qualified DDC users shall request through _____."

If the report has been furnished to the Office of Technical Services, Department of Commerce, for sale to the public, indicate this fact and enter the price, if known.

11. SUPPLEMENTARY NOTES: Use for additional explanatory notes.

12. SPONSORING MILITARY ACTIVITY: Enter the name of the departmental project office or laboratory sponsoring *(paying for)* the research and development. Include address.

13. ABSTRACT: Enter an abstract giving a brief and factual summary of the document indicative of the report, even though it may also appear elsewhere in the body of the technical report. If additional space is required, a continuation sheet shall be attached.

It is highly desirable that the abstract of classified reports be unclassified. Each paragraph of the abstract shall end with an indication of the military security classification of the information in the paragraph, represented as *(TS)*, *(S)*, *(C)*, *or (U)*.

There is no limitation on the length of the abstract. However, the suggested length is from 150 to 225 words.

14. KEY WORDS: Key words are technically meaningful terms or short phrases that characterize a report and may be used as index entries for cataloging the report. Key words must be selected so that no security classification is required. Identifiers, such as equipment model designation, trade name, military project code name, geographic location, may be used as key words but will be followed by an indication of technical context. The assignment of links, roles, and weights is optional.

Unclassified

Security Classification